

AUS Repository

Finite Element-Based Parametric Analysis of Mat Foundations

Item Type	Thesis
Authors	Partazian, Pouya
Download date	2026-03-07 06:27:55
Link to Item	http://hdl.handle.net/11073/8851

FINITE ELEMENT- BASED PARAMETRIC ANALYSIS OF MAT
FOUNDATIONS

by

Pouya Partazian

A Thesis presented to the Faculty of the
American University of Sharjah
College of Engineering
In Partial Fulfillment
of the Requirements
for the Degree of

Master of Science in
Civil Engineering

Sharjah, United Arab Emirates

April 2016

Approval Signatures

We, the undersigned, approve the Master's Thesis of Pouya Partazian

Thesis Title: Finite Element- Based Parametric Analysis of Mat Foundations.

Signature

Date of Signature

(dd/mm/yyyy)

Dr. Magdi El-Emam
Associate Professor, Department of Civil Engineering
Thesis Advisor

Dr. Sami W. Tabsh
Professor, Department of Civil Engineering
Thesis Co-Advisor

Dr. Mousa Attom
Professor, Department of Civil Engineering
Thesis Committee Member

Dr. Samir Emam
Associate Professor, Department of Mechanical Engineering
Thesis Committee Member

Dr. Robert Houghtalen
Head, Department of Civil Engineering

Dr. Mohamed El-Tarhuni
Associate Dean for Graduate Affairs and Research,
College of Engineering

Dr. Richard Schoephoerster
Dean, College of Engineering

Dr. Khaled Assaleh
Interim Vice Provost for Research and Graduate Studies

Acknowledgement

I am thankful to American University of Sharjah and Department of Civil Engineering, for letting me pursue my degree being a student here. I would like to thank the Academic Programs Coordinator, Ms. Salwa Mohamed for all her continues support during this course of time.

I would also like to thank the graduate committee members, Drs. Mousa Attom, and Samir Emam for their time, reviews, and helpful comments.

Most of all, I would like to express my sincere gratitude to my advisors Dr. Magdi El-Emam and Dr. Sami Tabsh for providing knowledge, guidance, support, and motivation throughout my research stages. I am extremely thankful for their time in supporting and steering me through this path on the right direction.

Finally, I must express my very profound gratitude to my parents for providing me with unfailing support and continuous encouragement throughout my study and through the process of researching and writing this thesis. This accomplishment would not have been possible without them. Thank you.

Abstract

Raft or mat foundation is a thick reinforced concrete slab covering the entire contact area of the structure and supporting heavy loads from superstructure to a large area of soil. This type of foundation is employed in scenarios where the column loads are not distributed evenly, level of the structure is lower than the ground water table, and soil is prone to differential settlement. A literature review showed that there is lack of parametric studies on the subject. This study is aimed at using finite element method to investigate the behaviour of mat foundations under gravity loads. The analysis considers mat foundations with different plan dimensions, thicknesses, soil modulus of subgrade reaction, concrete Poisson ratios, modulus of elasticity, panel aspect ratios, number of bays, and load eccentricities. Effect of these design parameters on the maximum and minimum soil bearing pressure below the mat foundation, as well as on the maximum positive and negative bending moment, and shear within the mat will be determined. Result of this study showed that the rigidity of the mat in comparison to the stiffness of the supporting soil is the main parameter that affects the soil bearing pressure and internal forces within the mat. Rigid mats have somewhat uniform soil bearing pressure underneath them, whereas flexible mats have more bearing pressure under the columns than elsewhere. For symmetrically loaded mats subjected to column loads in proportion to their tributary areas, the maximum soil bearing pressure was observed below the corner columns, while the minimum soil pressure occurred within the middle region of central panel. The maximum positive bending moment was found below the interior column closest to the edge, whereas the maximum negative moment was located mid-way between the edge and first interior columns. Location of the maximum shear always happened to be at the face of the edge column nearest to the corner column. Most important parameters that affects the soil bearing pressure, bending moments and shears are mat thickness, soil modulus of subgrade reaction and the distance between columns and eccentricity of the total load with respect to the centroid of the mat.

Keywords: *Mat Foundation, Raft, Soil-Structure Interaction, Soil Bearing Pressure, Bending Moment, Shear force, Finite Element Analysis, Soil Modulus of Subgrade Reaction.*

Table of Contents

Abstract	5
List of Figures	8
List of Tables	11
1. Chapter 1. Introduction.....	12
1.1. Background	12
1.2. Problem Definition.....	16
1.3. Research Objectives	17
1.4. Research Methodology.....	17
1.5. Thesis Organization.....	21
2. Chapter 2. Literature Review.....	22
2.1. Introduction	22
3. Chapter 3. Mat Foundation.....	31
3.1. General	31
3.2. Methods for Mat Foundation Design	31
3.2.1. Conventional rigid method.	31
3.2.2. Mat foundation work-out example.....	34
3.2.3. Approximate flexible method	37
3.2.4. finitedifference method.....	39
3.2.5. Coefficient of subgrade reaction modulus of soil.....	39
4. Chapter 4. Finite Element Analysis	41
4.1. Introduction	41
4.2. History	42
4.3. Advantages of the Method	42
4.4. Steps of the Finite Element Method.....	43
4.5. Finite Element Modeling.....	45
4.6. Finite Element Analysis of Mat Foundations.....	46

4.7.	Modeling with SAFE	46
4.8.	Considered Mat Cases	48
4.9.	Detailed Analysis of the Reference Mat	49
5.	Chapter 5. Parametric Study	55
5.1.	General	55
5.2.	Normalized Results of the Reference Model	56
5.3.	Effect of Mat Thickness	58
5.4.	Effect of Modulus of Sub-grade.....	62
5.5.	Effect of Modulus of Elasticity of Concrete	65
5.6.	Effect of Concrete Poisons Ratio	68
5.7.	Effect of Column Size	70
5.8.	Effect of Change in Length	72
5.9.	Effect of Change in Number of Spans	74
5.10.	Effect of Aspect Ratio	77
5.11.	Effect of Eccentrically Loaded Mat	83
6.	Chapter 6. Summary and Conclusions	87
6.1.	Summary	87
6.2.	Conclusions	87
	References.....	90
	Vita.....	93

List of Figures

Figure 1: Spread footing	12
Figure 2: Combined footing.....	13
Figure 3: Strap beam footings.....	13
Figure 4: Wall footing.....	13
Figure 5: Mat foundation [4].....	14
Figure 6: Examples of deep foundation [1]	14
Figure 7: Example Mat Foundation [5]	15
Figure 8: Effect of the rigidity of the concrete mat on soil pressure distribution [1] ..	16
Figure 9: Effect of soil stiffness on soil pressure distribution [1].....	16
Figure 10 Modeling of a concrete mat on spring supports	19
Figure 11 Finite element model of a mat and corresponding stress contours.....	19
Figure 12 Geometry of the mat to be considered in the analysis.....	20
Figure 13 Various boundary conditions of individual panels within a mat.....	20
Figure 14 Effect of load eccentricity on soil pressure distribution for a rigid mat [2]	21
Figure 15: Coefficients for infinite mat on elastic foundation [10].....	23
Figure 16 Winkler foundation layout [12].....	25
Figure 17: Comparison of edge boundary-condition [20]	26
Figure 18: Boundary condition modeling [20]	26
Figure 19: 15-storied building mat showing locations for study of mat response [21]	27
Figure 20: Variation of mat thickness [21]......	27
Figure 21: Variation of column size [21]......	28
Figure 22: Variation of column spacing [21].....	28
Figure 23: Variation of L/B ratio of the panel. [21]	28
Figure 24: Variation of subgrade reaction in soil [21]......	29
Figure 25 Elastic half space model [24]	30
Figure 26: (a) conventional rigid method; (b) approximate flexible method [15].....	32
Figure 27: Layout of hypothetical mat foundation	34
Figure 28: Layout of strip IJKL	35
Figure 29: Statical system of strip IJKL, and modified ultimate loads notations.....	36
Figure 30: Statical system of strip IJKL, and the modified ultimate loads.....	37
Figure 31: Graphical Data for Finite Element Method [15]	38
Figure 32: Minera Escondida copper mine tunnel and its finite element model [28]..	42
Figure 33: Two different applications of the finite element method [35]......	43

Figure 34: Finite element model of mat foundation in SAFE [40].....	47
Figure 35: Typical Mat Foundation Model Layout	50
Figure 36: Typical Mat Foundation Model Layout	50
Figure 37: Amplified deflection shape of the mat	51
Figure 38: Typical mat foundation - soil bearing pressure result	51
Figure 39: Bending moment results in the reference mat	52
Figure 40: Maximum principal moment at the elements mid-depth.....	52
Figure 41: Minimum principal moment at the elements mid-depth	53
Figure 42: Shear force results in the reference mat	53
Figure 43: Maximum principal shear at the elements mid-depth	54
Figure 44: Nomenclature used on a typical mat foundation	55
Figure 45: Mat considered in parametric study	57
Figure 46: Effect of mat thickness on soil bearing pressure	60
Figure 47: Soil pressure distribution under a mat with different thicknesses.....	60
Figure 48: Effect of mat thickness on maximum bending moment.....	61
Figure 49: Moment diagrams in a panel between columns	61
Figure 50: Effect of mat thickness on maximum shear force	62
Figure 51: Effect of modulus of subgrade reaction on soil bearing pressure	64
Figure 52: Soil pressure distribution under a mat supported by different soils	64
Figure 53: Effect of modulus of subgrade reaction on bending moment	65
Figure 54: Effect of modulus of subgrade reaction on shear	65
Figure 55: Effect of modulus of Elasticity of concrete on soil pressure.....	67
Figure 56: Effect of modulus of elasticity of concrete on shear	67
Figure 57: Effect of modulus of elasticity of concrete on bending moment	68
Figure 58: Effect of Poisson's Ratio on Soil Pressure	69
Figure 59: Effect of Poisson's Ratio on bending moment	69
Figure 60: Effect of Poisson's ratio on shear	70
Figure 61: Effect of column size on soil pressure.....	71
Figure 62: effect of column size on bending moment	71
Figure 63: Effect of column size on shear	72
Figure 64: Effect of span length on soil pressure	73
Figure 65: Effect of span length on bending moment.....	74
Figure 66: Effect of span length of shear	74
Figure 67: Effect of number of span on soil pressure	76

Figure 68: Effect of number of span on bending moment	76
Figure 69: Effect of number of span on shear.....	76
Figure 70: Location of maximum positive and negative moment in mats	77
Figure 71: Definition of panel length and width.....	78
Figure 72: Effect of aspect ratio on maximum soil pressure	80
Figure 73: Effect of aspect ratio on minimum soil pressure	80
Figure 74: Effect of aspect ratio on positive moment along the panel length	81
Figure 75: Effect of aspect ratio on negative moment along panel length	81
Figure 76: Effect of aspect ratio on positive moment along panel width	82
Figure 77: Effect of aspect ratio on negative moment along panel width'	82
Figure 78: Effect of on aspect ratio on max. shear force along panel length	83
Figure 79: Effect of aspect ratio max. shear force along panel width	83
Figure 80: Eccentrically loaded mat	85
Figure 81: Effect of eccentrically loaded mat on soil pressure.....	85
Figure 82: Effect of eccentrically loaded mat on bending moment.....	85
Figure 83: Effect of eccentrically loaded mat on Shear.....	86

List of Tables

Table 1: Column load considered in the work-out-example.....	34
Table 2: Typical values of soil subgrade reaction $k_{0.3}$ [11]	40
Table 3: Typical Mat Specification.....	50
Table 4: Typical Reference Model - Tabulated Results	54
Table 5: Geometry and material properties for the reference mat	57
Table 6: Effect of mat thickness on actual design parameters.....	58
Table 7: Effect of mat thickness on normalized design parameters	59
Table 8: Effect of soil's modulus of subgrade reaction on design parameters	62
Table 9: Effect of Soil Subgrade modulus on normalized design parameters.....	63
Table 10: Effect of concrete modulus of elasticity on design parameters	66
Table 11: Effect of concrete modulus of elasticity on normalized design parameters	66
Table 12: Effect of Poisson's ratio on design parameters.....	68
Table 13: Effect of Poisson's ratio on normalized design parameters.....	69
Table 14: Effect of column size on design parameters	70
Table 15: Effect of column size on normalized design parameters	71
Table 16: Effect of span length on design parameters	72
Table 17: Effect of span length on normalized design parameters.....	73
Table 18: Effect of number of span on design parameters	75
Table 19: Effect of number of span on normalized design parameters	75
Table 20: Effect of aspect ratio on normalized design parameters	79
Table 21: Effect of eccentrically loaded mat on design parameters	84

Chapter 1. Introduction

1.1. Background

A Superstructure is an upward extension of the structure above the ground level and it usually serves the structure's intended purpose. A Substructure is an underlying structure below the ground level. The main part of the substructure is the foundation, which transfers the load from the columns and shear walls to the soil layers' underneath. Therefore, investigations are usually executed to find the geotechnical properties of the construction site for selection of the suitable foundation type to support a given structure. The various types of foundations are classified as either shallow or deep [1]. The selection of suitable type of foundation depends on many factors, such as building loads, allowable settlement for the building, and the construction site soil conditions [2].

Foundations which are constructed on shallow layers of soil closer to the ground surface are called shallow foundations. Types of shallow foundations are spread footings, combined footings, strap beam footings, wall footings, and mats. Figure 1 to Figure 5 show the different types of shallow foundation.

Deep foundations are embedded into the ground such as drilled shafts, caissons, and driven piles. Such elements are used when the shallow soil layers are relatively weak so that it could not support the building loads, and the column loads are relatively high. These foundations transfer loads to a stronger deeper layer of bedrock or hard soil strata bypassing weak upper soil layers using piles, drilled shafts, or caissons [3]. Figure 6 shows two typical pile foundations, one bearing on hard strata and another relying on skin friction.

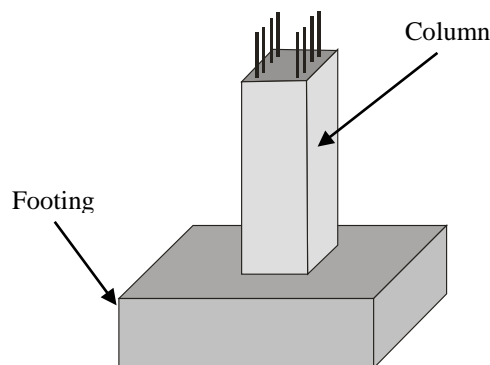


Figure 1: Spread footing

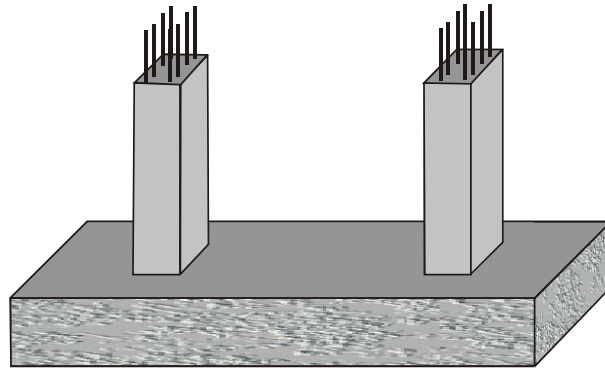


Figure 2: Combined footing

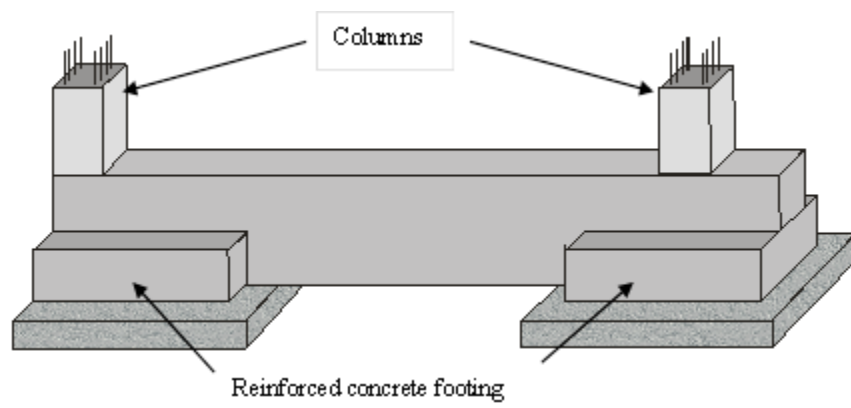


Figure 3: Strap beam footings

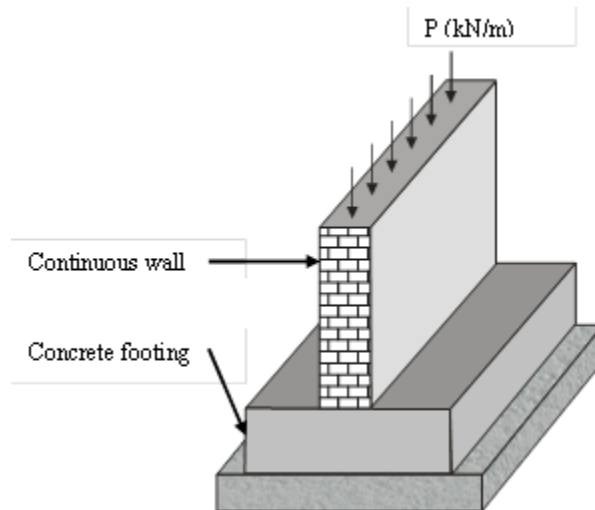


Figure 4: Wall footing

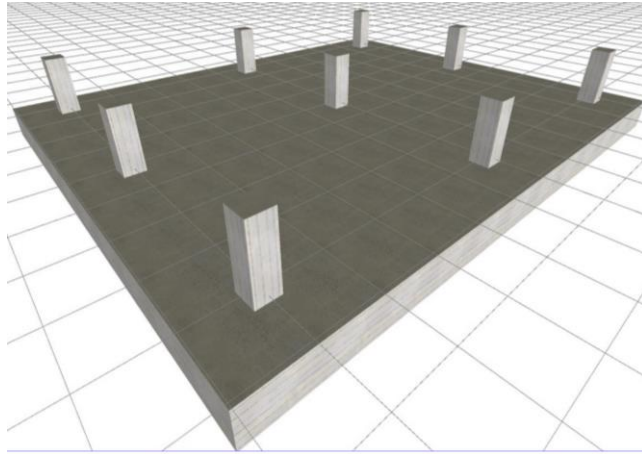


Figure 5: Mat foundation [4]

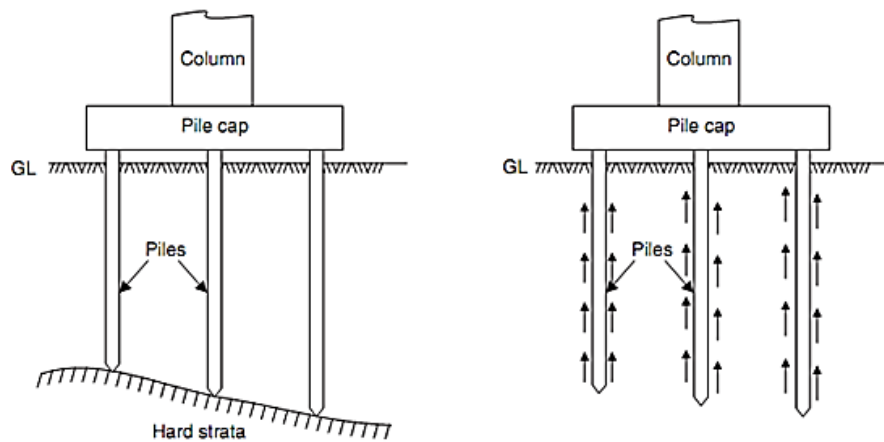


Figure 6: Examples of deep foundation [1]

A mat foundation consists of a flat heavily reinforced concrete slab cast against the soil, as shown in Figure 7. Sometimes the area covered by the mat may be greater than the contact area, depending on the bearing capacity of the soil underneath. It is used to distribute heavy column and wall loads across the entire superstructure area to reduce the magnitude of the contact pressure compared to conventional spread footings. Mat-slab foundations can be constructed near the ground surface, or at the bottom of basements. They are most economical to employ, compared to deep foundation, when the building loads are relatively large, distance between column is small, and the soil type is medium stiff or relatively soft. Practically, mat foundation is preferred whenever single footings would cover more than half of the built area, and/or where differential settlement could be a major problem.

Different methods are used for the structural analysis of mat foundation. Such methods are mainly concerned with determining the minimum plan dimensions based on the soil bearing capacity, minimum mat thickness required for resisting shear, and the amount

of longitudinal reinforcement at the top and bottom in the two directions of the mat to counter resist bending moments.



Figure 7: Example Mat Foundation [5]

Designers usually rely on the strip method, which divides the mat into strips of unit width in the two principal directions of the mat and analyzing the strips as a combined footing on elastic supports. This method is not very accurate and uses many approximations. However, it gives the designer a good idea for initial estimation for further detailed analysis, quick validation of computer results, and for cost estimation purposes.

Another method is to treat the mat under the applied loads as an infinitely rigid pad; thus, resulting in a linear pressure distribution under mat. In this method, the mat is assumed more rigid than the surrounding soil, so flexure of the mat does not affect the distribution of the soil bearing pressure under the mat. The magnitude and distribution of the bearing pressure depends only on the applied loads and weight of the mat, and is either uniform or varies linearly within the mat. If the applied load is symmetrical on the mat, then the soil pressure would be uniform. This method is not appropriate, especially when the spacing between columns and walls is large, because portions of the mat below the columns or load bearing walls deflect more than other portions of the mat subjected. This increases the bearing pressure beneath the heavily-loaded zones, especially for rafts on stiff soils and rock; thus, reduces the bending moment in the mat. Figure 8 shows how the soil pressure distribution is affected by the

rigidity of the mat, while Figure 9 demonstrates the consequences of the stiffness of the soil.

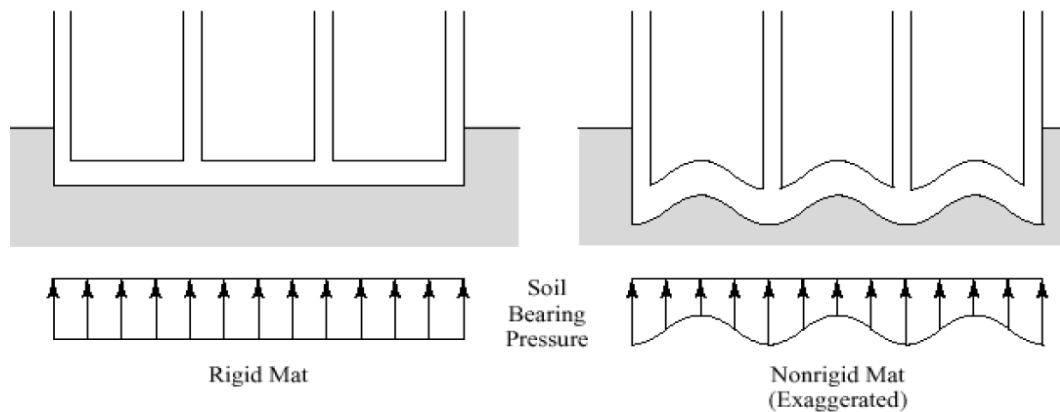


Figure 8: Effect of the rigidity of the concrete mat on soil pressure distribution [1]

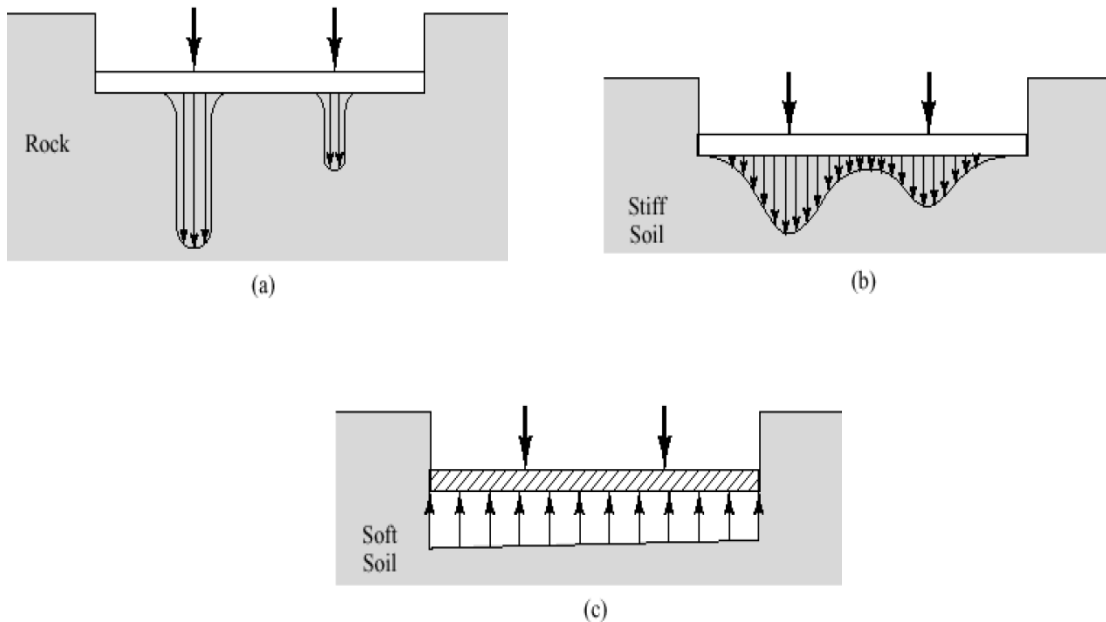


Figure 9: Effect of soil stiffness on soil pressure distribution [1]

1.2. Problem Definition

Mat foundations are continuous concrete slabs that are used to spread heavy gravity and lateral loads from a superstructure over a large area of soil. They are often utilized when the soil is prone to large differential settlement, column loads are unevenly distributed, and the structure is located below the ground water table. A literature review, included in the next chapter, shows that there is lack of parametric studies on mat foundations that consider the most important design parameters on the structural behavior. Most of the cited research on the subject is based on the assumption

that the mat is infinitely rigid plate, resulting in linearly distributed soil pressure. Despite the simplicity of this approach, it often results in over-estimation of the internal forces in the mat and under-estimation of the soil bearing pressure beneath the mat. On the contrary, consideration of the elastic characteristics of the soil beneath a mat and flexibility of the foundation could give relatively more accurate results; however, such an approach is tedious, time-consuming and requires sophisticated software. Therefore, there is a need to develop a simple and practical approach to determine the load effect in mats foundation having different geometrical dimensions and subjected to various types of loads with consideration of a range of soil stiffness. The effect of mat thickness, soil elastic properties, and load eccentricity on the soil pressure under the concrete mat and internal forces (both shear and bending moment) within the mat will be investigated. Moreover, the accuracy of currently used methods for mat foundations needs to be validated.

1.3. Research Objectives

The main objectives of this research project are to:

- (1) study the behavior of mat foundations subjected to various types of loads received from the superstructure.
- (2) determine the effect of the mat geometry on the soil bearing pressure under the mat and the internal load effects (shear and bending moment) within the mat. Specifically, the considered parameters here are the mat thickness, panel length and width, panel aspect ratio, and number of bays in each direction.
- (3) evaluate the impact of soil's modulus of subgrade reaction, concrete modulus of elasticity and concrete Poisson ratio on the soil bearing pressure, maximum shear, and maximum bending moment in the mat.
- (4) assess the influence of the eccentricity of the loads from the columns with respect to the centroid of the mat on the geotechnical and structural response.

The analysis will involve the use of commercially available finite element software.

1.4. Research Methodology

To accomplish the stated objectives, a large number of mats with different geometries, load distribution, soil types, and concrete properties will be investigated using a finite element analysis. The methodology is divided into six tasks with details of each task are as per followings:

Task 1 – Problem Comprehension

A thorough understanding of the problem of soil-structure interaction is required, as well as consideration of the different aspects of the problem and its significance.

Task 2 – Literature Review

Review the available literature and research work completed to date on the subject. The aim of the review is to consolidate the previous efforts and to compare, wherever possible, the findings of this study to their results.

Task 3 – Finite Element Modeling

Develop a finite element model using the SAFE program from CSI [6] to simulate the subject problem and develop the reference models.

Task 4 – Parametric Analysis

A parametric study is conducted in order to find the effect of the change in one variable on the behavior in terms of soil bearing pressure and internal forces of the considered mats. Different parameters are used to model and analyze the typical mat foundation in SAFE. Of interest are the maximum positive/negative moments, maximum shear, and minimum/maximum soil pressure under the mat.

Task 5 – Conclusions and Recommendations

The results of the above study will be used to develop practical recommendations on soil bearing stress under the mate, as well as bending moment and shear within the mate.

1.5 Scope of Study

The SAFE software that will be used in this study for the analysis of the considered mat foundation models the concrete mat by shell elements, the soil by elastic springs, and columns by solid elements [7]. Figure 10 presents a schematic finite element model of a mat in SAFE.

Figure 11 shows an example of a finite element model of a mat foundation and the resulting stress contours in the mat, produced by the SAFE software.

The variables that will be considered in the analysis are the soil properties (modulus of subgrade reaction), mat geometry, panel boundary conditions, length-to-width ratio of the panels, and eccentricity of the column loads with respect to the centroid of the mat.

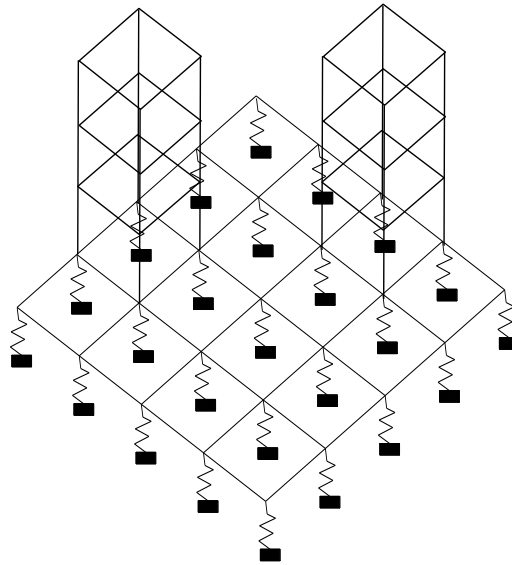


Figure 10 Modeling of a concrete mat on spring supports

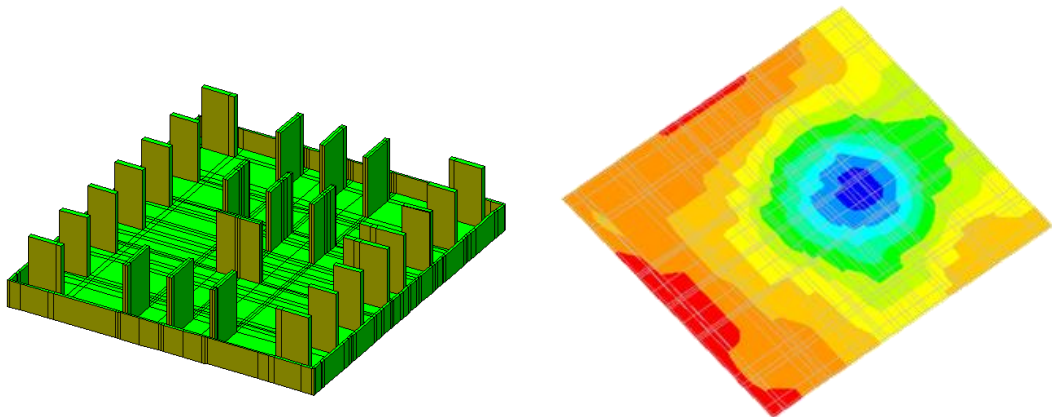


Figure 11 Finite element model of a mat and corresponding stress contours

With regards to the modulus of subgrade reaction, a wide range varying between 10 and 130 MN/m³ will be considered. The lower limit represents medium dense sand and medium stiff clay; whereas the higher limit refers to dense sand and stiff clay. The approach that will be followed to address the mat geometry, boundary conditions, and aspect ratio of the individual panels within the mat will involve a basic model consisting of a rectangular prismatic mat supporting 16 columns, and composed of 9 panels, as shown in Figure 12. Such an approach results in different boundary conditions for the panels between the columns (namely interior, edge/side and corner), as presented in Figure 13. Varying the panel width W and panel length L will change the aspect ratio of the individual panels (in this study, $L/W=1$ to 2); thus, covering a wide range of cases.

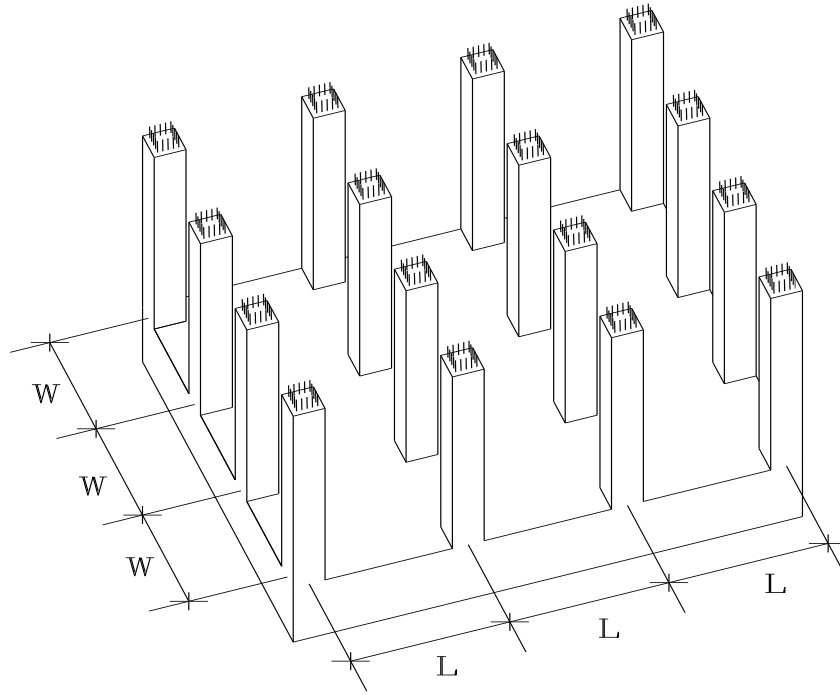


Figure 12 Geometry of the mat to be considered in the analysis

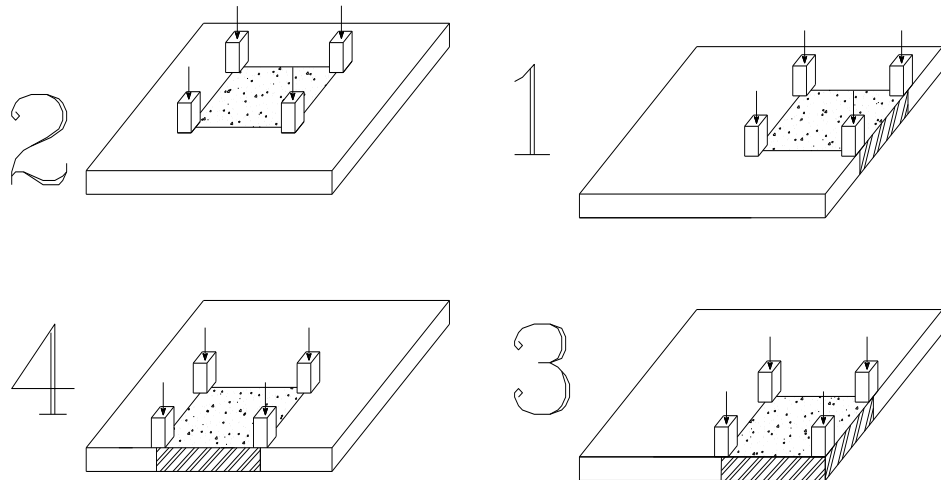


Figure 13 Various boundary conditions of individual panels within a mat

As a part of the scope of this research, the analysis will consider the effect of the eccentricity of the column loads relative to the centroid of the mat. The possible variables that will be affected by the load eccentricity are the soil pressure distribution, magnitude of the minimum and maximum soil pressure, and their effect on the internal forces within the concrete mat. Figure 14 shows the effect of the load eccentricity on the soil pressure distribution under infinitely rigid mat.

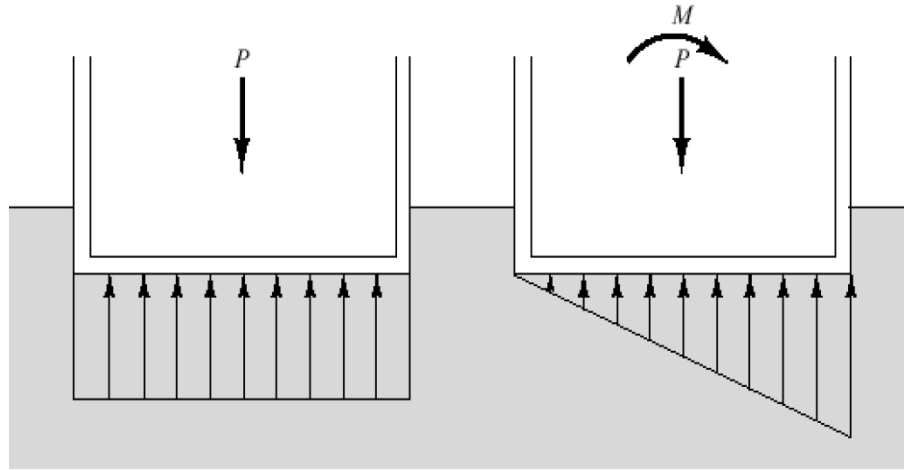


Figure 14 Effect of load eccentricity on soil pressure distribution for a rigid mat [2]

1.5. Thesis Organization

The thesis is comprised of six chapters. First chapter (Chapter 1) provides an introduction to the subject of research followed by problem statement, objectives, scope of study, and methodology of the research.

Chapter 2 summarizes the available literature related to research on structural analysis of mat foundation.

Chapter 3 introduces background on mat foundation. It includes details on the behavior of mat foundation, methods of analysis, design procedure, soil-structure interaction.

Chapter 4 discusses the finite element method of analysis which is used in this study. It also includes detailed input and output parameters of the base mat model in SAFE.

Chapter 5 includes a parametric study which considers the effect of mat thickness, soil subgrade modulus, concrete modulus of elasticity, Poisson ratio, panel aspect ratio, and load eccentricity.

The last chapter, Chapter 6, summarizes the important findings and provides final conclusions and recommendations. Potential future studies on the subject are also included.

Chapter 2. Literature Review

2.1. Introduction

In 1977, Wood developed an approximate procedure that utilizes a simplified soil model for estimating the settlement and internal bending moment in mat foundations. When compared to more accurate methods developed by others, Wood's method yielded satisfactory agreement over a wide range of soil properties [8]. Three years later, Mehrotra et al. [9] approximate method of stiffness analysis was presented for mat foundation considering a building as a multi-panel framed. The maximum bending moment intensity was obtained and it resulted in 25% reduction in the raft comparing with the conventional rigid method. Next, Shukla [10] computations of modulus of subgrade reaction was advanced in a simpler form to design mat foundations on elastic soil mediums. This method was used to obtain the shear forces, deflection of subgrade reaction and moments on the mat using the chart in Figure 15. Bowles in 1986 [11], reviewed the available methods for mat foundations which could be done by computer to understand the advantages of finite grid method, finite difference and finite element as the most three common discrete element methods. Furthermore, the disadvantages of each method were surveyed and overall the effect of modulus of subgrade reaction of the soil and the coupling between substructure and superstructure were highlighted as the critical parameters. Later on, Liou and Lai [12], developed a simplified structural analysis model for mat foundations upon their study on the treatment of grid floor beams as stiffeners. The model considered the subgrade modulus for the soil and utilized the yield-line theory in the analysis of the stiffened mat. Comparisons with the results by a sophisticated finite-element model were made in order to demonstrate the accuracy of the model. In 2002, Meyerhof [13] reviewed the design and performance of rafts resting on sand and gravel in relation to the settlement and allowable bearing pressures, and found out that the bearing capacity in some cases could be increased by 50% if the allowable settlement is increased to 2 times the observed value. Tabsh and Al-Shawa [3] used the finite element approach to investigate the flexibility of shallow foundations and their effect on the soil pressure distribution, shear and moment within the foundation. The study showed that maximum shear forces within a spread footing are less sensitive to changes in the stiffness of a footing than bending moments. A rigidity factor that governs the structural behavior of the foundation was also developed. Recently, Thangaraj and Ilamparuthi [14] performed an interaction analysis of space

frame-raft-soil system under static load to study the influence of stiffness of raft on space frame. These analyses were carried out for both linear and nonlinear conditions of soil. The influence of interaction between a space frame, raft and soil was considered in terms of relative stiffness of superstructure and relative stiffness of raft.

According to Das [15], mats may be supported by piles if a structure is built on a highly compressible soil in order to reduce the settlement. In addition, regularly the mats are placed over piles to control buoyancy in places with high water table. Moreover, in cases where the spread footing covers more than half of the building area, a mat foundation may be more economical option.

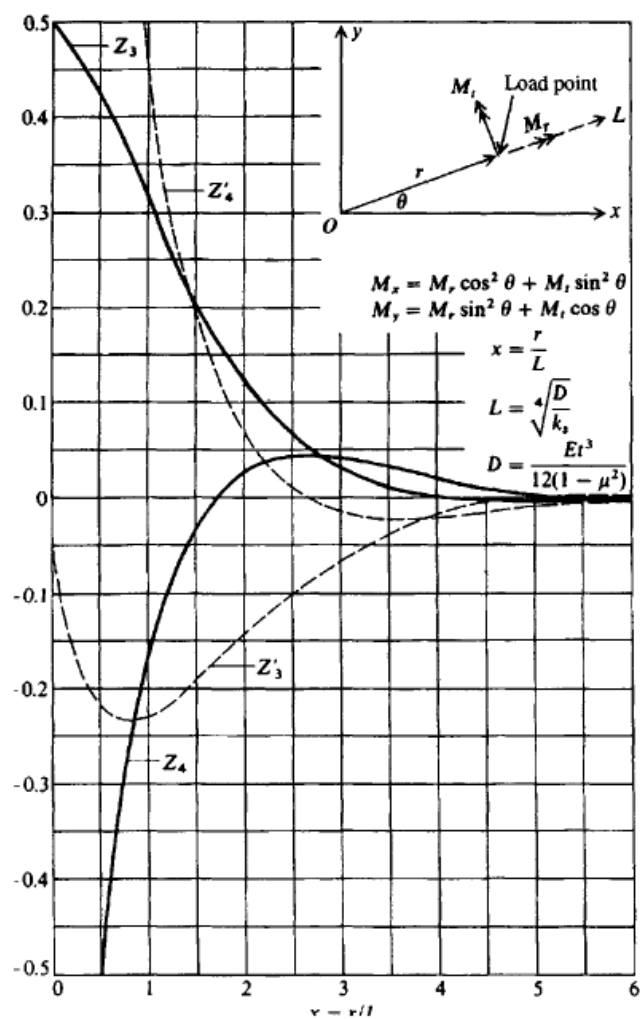


Figure 15: Coefficients for infinite mat on elastic foundation [10]

Current approaches for structural design of mats assume the foundation to be infinitely rigid. Preliminary studies by the authors show that this approach often overestimates the critical shear and moment in the mat, but under-estimates the maximum soil pressure beneath the mat. This could lead to a mat thickness larger than required

and an amount of steel reinforcement more than needed; thus, resulting in an unnecessary cost increase in the foundation. Underestimation of the soil pressure can also result in a lower factor of safety against bearing capacity failure and may cause excessive settlement of the structure beyond the allowable limits.

Coduto [16] explained how a mat foundation can be analyzed and designed using the finite element method (FEM). He stated that the mat can be subdivided into a large number of discrete elements with defined dimensions and sizes, a specified stiffness and strength with connectivity to the ground with springs defined as a function of the coefficient of the subgrade modulus reaction of the soil. Loads on the mat include applied column loads, applied wall loads, applied area loads, and the own weight of the mat itself. All these loads force the mat downwards and to be resisted by the soil “springs”. In advance, this method can be modified and expanded to include the stiffness of the superstructure, the mat, and soil in a single three-dimensional finite element model. This makes the design more complex how gives a more economical structure. Thought it is rarely performed, because it is time-consuming and difficult to establish accurate soil properties.

Furthermore, Cemica [17] highlighted the definition of mat foundation as an elevated slab made up of a series of spread or individual footings. The wide area of the mat foundation is beneficial as it increases the allowable bearing capacity of the soil. Settlements, especially the differential settlements are the most important and critical concern for the structural engineers since it is a sophisticated phenomenon and controlled directly by the variation of soil properties within the construction land. Cemica suggested several ways by which settlement is reduces such as improving the soil stratum supporting the mat and increasing the area of the foundation over the soil.

Also, Liou and Lai [12] inspected a basic structural analysis model for mat foundations with beam grid floors as stiffeners. Assuming the Winkler type of subgrade reaction for the entire area under the mat foundation as per Figure 16 and the yield-line theory of slab, the authors lumped the Winkler springs under the slabs to match locations under the adjacent floor beams of the slabs in the model. This resulted in having each floor beam supported by springs having a segmentally linearly varied spring constant. Therefore, the complete analysis model was simplified being subjected to loadings from the columns as having a grid beam system on an elastic foundation that is segmentally linearly varied spring constant. Finally, Numerical comparisons

were employed using a finite-element model to show the effectiveness of the analyzed model.

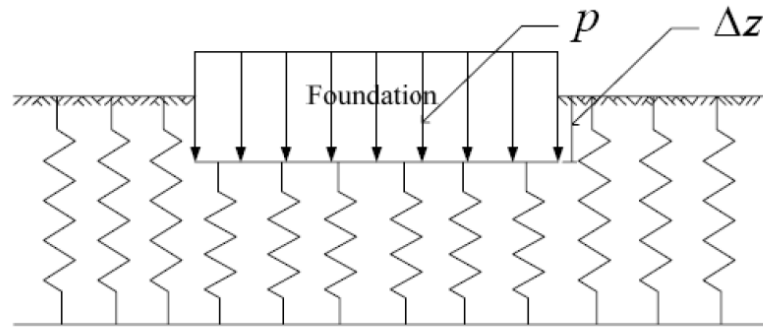


Figure 16 Winkler foundation layout [12]

In addition, in the article titled effect of spread footings flexibility on structure response [3], Tabsh and Al Shawa investigated a new relative stiffness factor, k which indicates the rigidity of the footing for the structural design. This study is a modification of Meyerhof's in 1953, taking in consideration the size of the columns on the footings. The footing models were square and rectangular thick plate elements and they were subjected to eccentric and concentric loads by finite elements, elastic springs were used for the soil. With a reasonable accuracy, the studied that footings with relative factors greater than zero considered rigid footings, taking in account soil pressure, vertical displacements, shear force and bending moments.

According to Braja [15], mats may be supported by piles in a structure is built on a highly compressible soil in order to reduce the settlement. Also, regularly the mats are placed over piles to control buoyancy in places with high water table. Also, in cases there are spread footing covers more than half of the building area, a mat foundation may be more economical option.

Furthermore, Peck Ralph [18] stated that if the center of gravity of the loads on a mat foundation coincides with the centroid of the mat itself, then the soil pressure below the foundation is assumed uniform. In that case, the total pressure is equal to the sum of the downward loads divided by mat's area. The authors suggested that the column loads are not uniformly located on the mat, or if large differential settlements are expected to happen, then it must be reinforced with stiffed partitions such as rigid frames, beams and girders.

In 2009, Wang et al. [19] studied further design of raft foundation by performing analysis using finite element method as a practical approach. The result of the

calculation between the soil conditions and structure stiffness resulted in uniform base reaction and lower reaction. Therefore, the foundation reinforcement can be minimized and save cost and time while the safety of the foundation will remain the same. More recently, research on the subject of modulus of subgrade for soil structure reaction have been carried out by Colasanti and Horvath [20]. It is emphasized that significant role in foundation practice and research is played by the subgrade models for calculation of actual load displacement and actions. As Winkler's theory is not using connection between adjacent subgrade springs or coupling the actual subgrade behavior will not be accurate and reliable. Therefore, Colasanti and Horvath developed a subgrade model (Figure 17 and Figure 18) with spring coupling to be used with commercially available platforms in structural analysis to overcome this approximation [20].

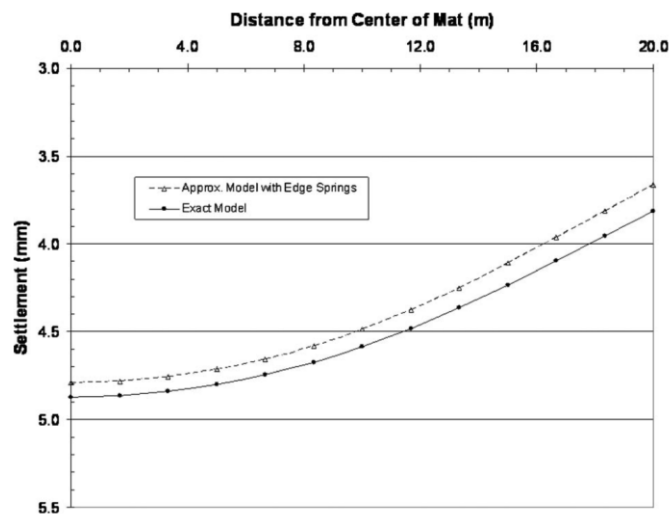


Figure 17: Comparison of edge boundary-condition [20]

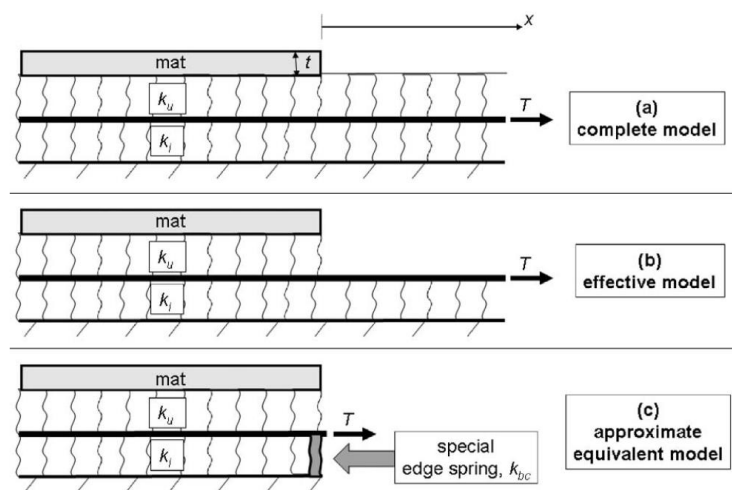


Figure 18: Boundary condition modeling [20]

In 2011, Imam [21], performed a study on deflection of mat foundation behavior as per Figure 19 with different parameters of soil and structure. It was intended to provide results and analysis for effect of the considered parameters in to design more economical and safe mat foundation. Finite element method was used with SAFE program on rigid frame structure using lateral and gravity loads.

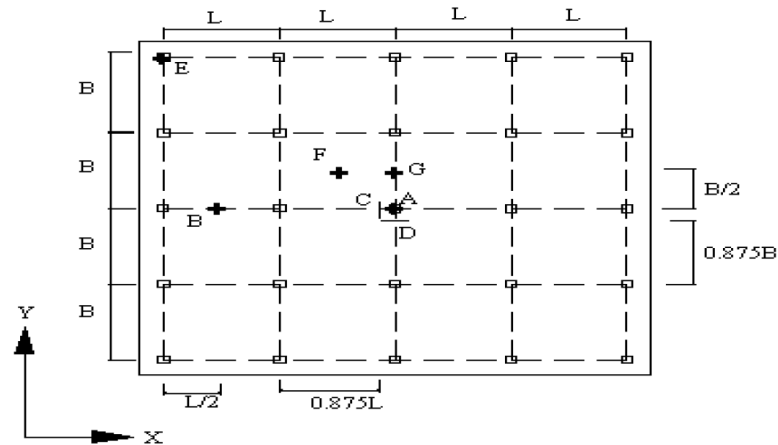


Figure 19: 15-storied building mat showing locations for study of mat response [21]

The parameters considered in this study were mat thickness, column spacing and size, overhanging portion of mat and span –width ratio of panel which resulted in different deflection behaviors as per Figure 20 to Figure 24.

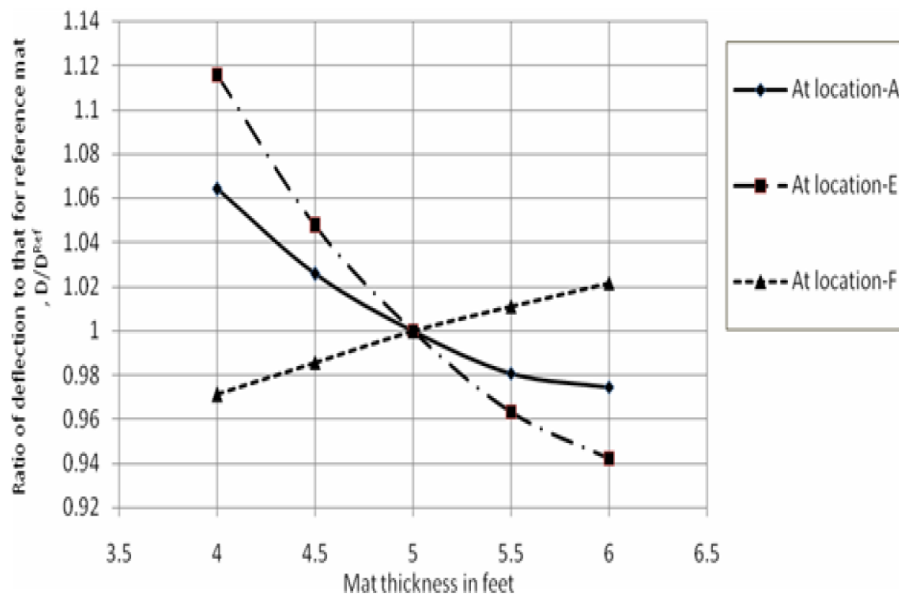


Figure 20: Variation of mat thickness [21].

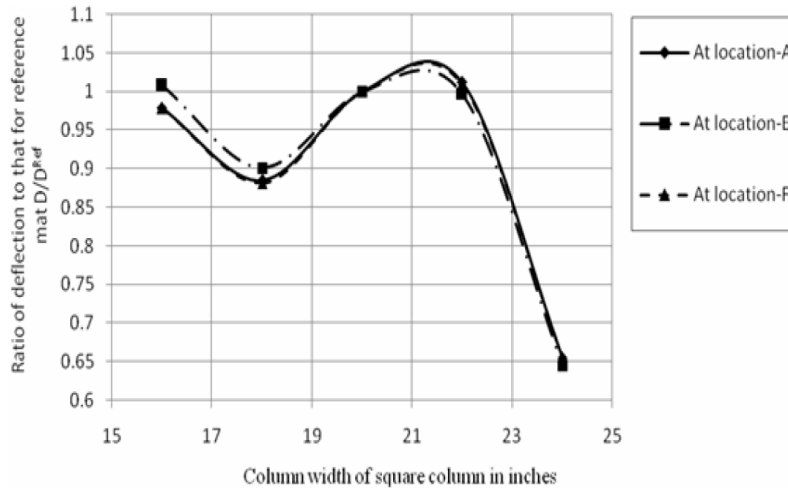


Figure 21: Variation of column size [21].

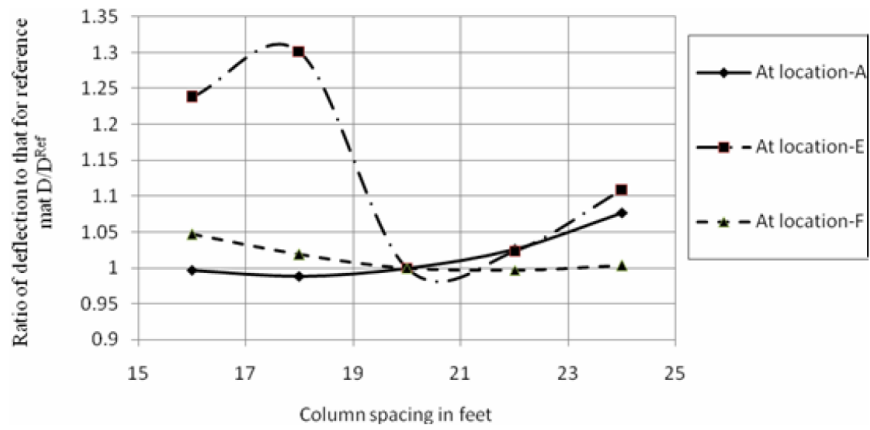


Figure 22: Variation of column spacing [21]

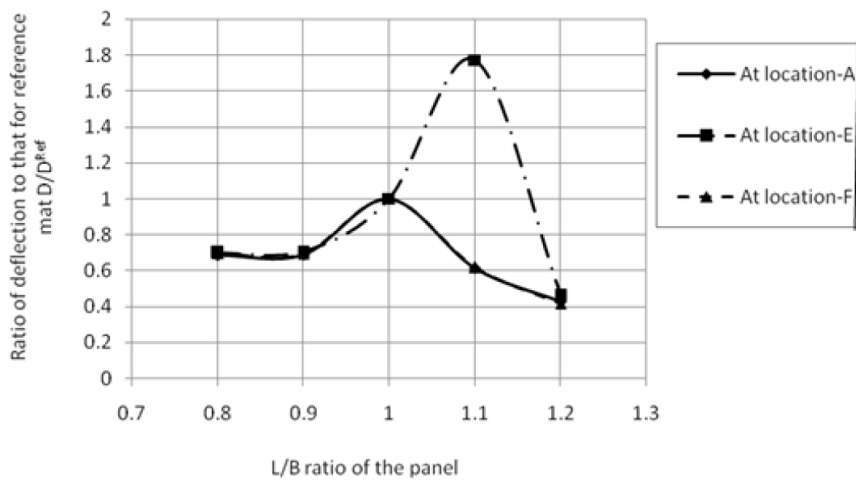


Figure 23: Variation of L/B ratio of the panel. [21]

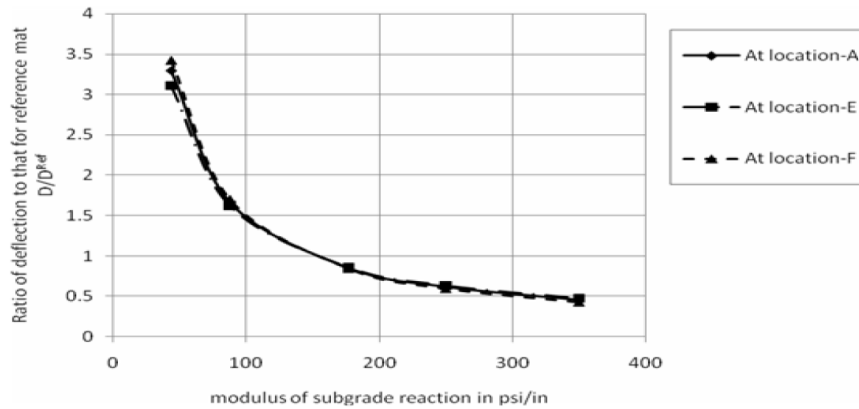


Figure 24: Variation of subgrade reaction in soil [21].

Imam [21] concluded that, as the mat thickness and sub-grade reaction increases the deflection decreases. On the other hand, the increase of column size and changing the span to width ratio will show fluctuated results in the mat deflection behavior. Finally, as the column spacing decrease the mat deflection will increase in the center of the mat.

As per a research done in 2015, behavior of raft foundation was studied by experiment on the geotechnical parameters which may affect. Accordingly, a design is done by considering the local shear failure of the soil [22]. In addition, effect of soil-structure interaction was studied by Kumar et al. [23], which highlights the effects of mat foundation parameters on the supporting soil as the analysis of the interaction between structural foundation and supporting soil on certain type of structures as well as dynamic loads. Finite element method was utilized on this study to compare the effect of different loading on the mat foundation and its responses. It is noticed that there are displacements when soil-structure interaction effect is taken into consideration. Based on the above, there is a need to investigate the accuracy of currently used procedures and propose a method for sizing mat foundations for a given set of loads, soil type and material properties.

Recently, previous studies on soil-structure interaction considering different parameters were tabulated and investigated to overcome the existing issues. These parameters are divided into type of foundation, geometry of superstructure, domain and forms of structure. In this study, it is concluded that consideration of static loading and dynamic loading is critical as it affects the soil structure interaction. Furthermore, the effect of soil structure is determined to be significant in determination of superstructure forces. In relation to settlement, load redistribution is affecting the behavior of the

settlement in nonlinear analysis. As per tabulated information from previous investigations, it is considered that finite element method is a useful approach to understand the soil structure interaction. Finally, it is understood that the seismic base shear will be affected significantly by soil structure interaction specially on low rise building resting on isolated footings [24].

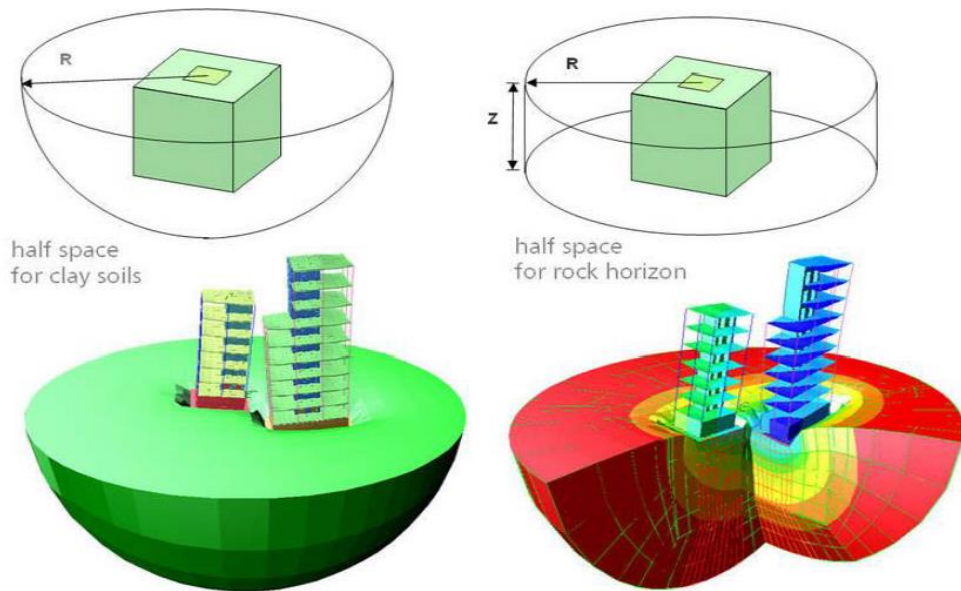


Figure 25 Elastic half space model [24]

Chapter 3. Mat Foundation

3.1. General

Mat foundation is a large concrete slab founded to interface columns, walls, or both in several lines, with the base soil Bowels [11]. It is used wherever the soil on the site is weak so or the column load is so large that the areas of the individual footing exceed 50% of the structure built area. This is practically occurred when the building number of floors is 6 and more, and the soil under the building is medium stiff to soft soil. Mat foundations are very beneficial for deep basements to spread the pressure underneath the mat linearly on a wider area of soil and to provide perfect flat area for the basement that can be utilized for different purposes. Moreover, mat foundations might be used at the level of ground water, where they act as water barriers. In cases of high ground water levels, piles may be used to support the mat against buoyancy and the uplift forces. Nowadays, mat foundations are one of the most popular foundations and used under various tower structures and high-rise buildings.

3.2. Methods for Mat Foundation Design

The analysis and design of mate foundation could be conducted using different analytical methods such as conventional rigid method or approximate flexible method. In addition, numerical methods such as Finite Difference and Finite Elements methods could be used whenever a powerful computational tool are available [11]. This section provides a detailed description of the two analytical methods commonly used in practice, which are the conventional rigid method and the approximate flexible method. Finally, detailed work out example using the conventional rigid method is presented for understanding the research topic.

3.2.1. Conventional rigid method. In the conventional rigid design method, the mat is assumed to be infinitely rigid, which results in a non-uniform linear distribution of the pressure over the soil underneath. In addition, the centroid of the soil pressure is coincident with the line of action of the resultant column loads. Figure 26a) shows the force equilibrium of a typical mat used for conventional rigid method. For infinitely rigid mat, it could be assumed that the flexural deflection does not affect the pressure distribution under the mat. Hetenyi [25] checked the relative rigidity of the mat using the characteristic coefficient (λ), which is defined by,

$$\lambda = \sqrt{\frac{Bk_s}{4EI}} \quad (1)$$

Where, k_s is the coefficient of subgrade reaction, B is the strip width, E is the modulus of elasticity of the mat material (i.e. concrete in this case), and I is the moment of inertia of a strip width B .

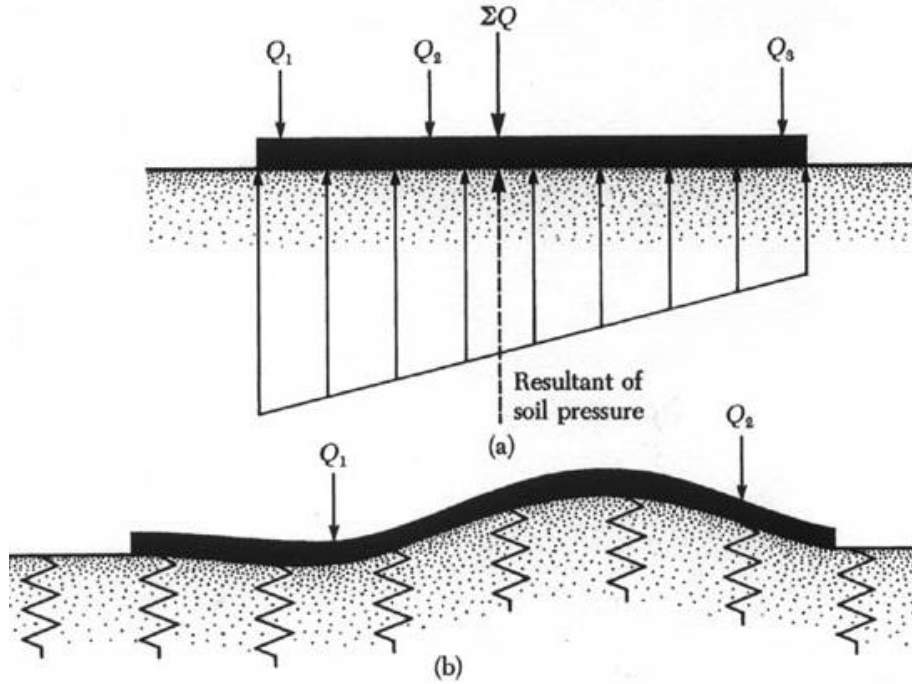


Figure 26: (a) conventional rigid method; (b) approximate flexible method [15]

The procedure for the conventional rigid method will be explained step-by-step in this section with reference to Figure 27 as follows:

1. Determine the line of action of all loads acting on the raft as shown in Figure 27 neglecting the self-weight of raft, as it is taken directly by the soil. It should be noted that Q_i in this case is the summation of the column DL and the column live load LL .

$$R = Q_1 + Q_2 + \dots + Q_8 = \sum Q_i \quad (2)$$

2. The eccentricities e_x and e_y are found by summing moment about any selected locations, for example the axis x' and y' .
3. Determine the pressure distribution q_o on the soil below the mat at its corner points and/or any critical points the designer selected. Soil pressure due to the working loads (i.e. $DL + LL$) is calculated as:

$$q_o = \frac{\sum Q_i}{A} + \frac{M_x}{I_x} y + \frac{M_y}{I_y} x \quad (3)$$

Where, A is the mat base area (BL), I_x is the moment of inertia about x axis ($I_x = BL^3/12$), I_y is the moment of inertia about y axis ($I_y = LB^3/12$), M_x is the moment of the column loads about x axis ($M_x = e_y \cdot \sum Q_i$), and M_y is the moment of the column loads about y axis ($M_y = e_x \cdot \sum Q_i$).

4. Values of q_o calculated using Equation 3 at mat corners should be less than the allowable bearing capacity of the soil, q_{all} .
5. For the limit state design of the mat foundation, Equation 3 should be re-written to include the ultimate column loads Q_{ui} instead of column working loads Q_i . The ultimate load $Q_{ui} = 1.2 DL_i + 1.6 LL_i$, according to the ACI code of practice [26]. The new equation is taking the form:

$$q_{ou} = \frac{\sum Q_{ui}}{A} + \frac{e_x \sum Q_{ui}}{I_x} y + \frac{e_y \sum Q_{ui}}{I_y} x \quad (4)$$

6. Values of q_{ou} calculated using Equation 4 at mat corners should be less than the ultimate bearing capacity of the soil, q_u .
7. Divide the mat into several strips in the two principal directions. Each strip is assumed to act as independent beam subjected to the contact pressure and the columns loads.
8. Determine the modified column load and average soil pressure for each strip as explained below for one strip as an example. To plot shear force and bending moment diagrams for each strip, a statical system is needed. However, it is generally found that each strip is not satisfying the static equilibrium required to apply load and moment equilibrium. This means that the resultant of column loads and the resultant of contact pressure are not equal because of ignoring the shear transfer between adjacent strips.

Considering the strip carrying column loads Q_2 , Q_5 and Q_6 as seen in Figure 27, let B_i be the width of the strip and let the average soil pressure on the strip q_{avg} and let L the length of the strip. The load acting on the specified strip is assigned, and adjusted to reach static equilibrium. Then the static system of the strip is plotted with the real dimensions, and shear forces and bending moment diagrams are plotted accordingly. These steps are systematically repeated for each strip until internal forces diagrams (i.e. shear and bending moment diagrams) are plotted for all strips in longitudinal and transvers directions.

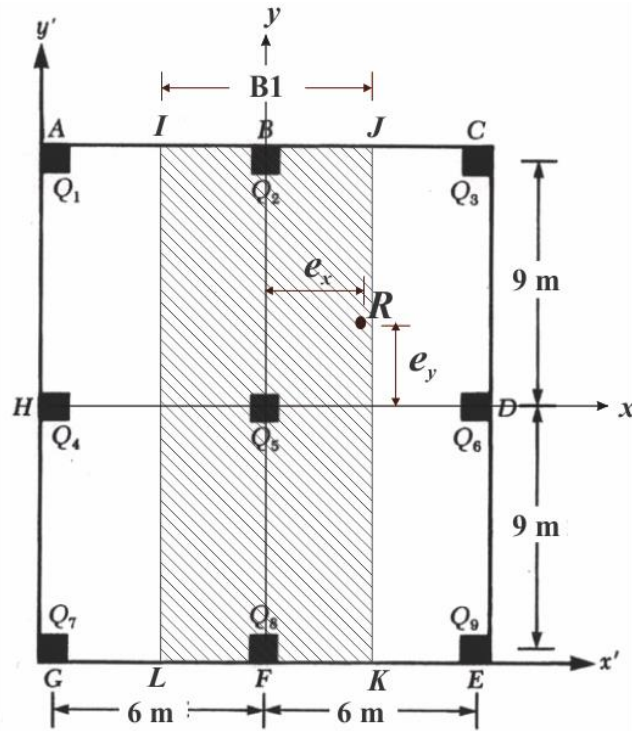


Figure 27: Layout of hypothetical mat foundation

3.2.2. Mat foundation work-out example. In this section, a hypothetical mat foundation is selected to be worked out as an application of the conventional rigid design method outlined in Section 3.2.1. The mat dimensions, and columns locations are shown in Figure 27. All column dimensions are assumed to be equal with square cross section of side $C = 0.5$ m. Column loads are given in Table 1 for both dead loads ($D.L$), and live loads ($L.L$).

Table 1: Column load considered in the work-out-example

Column No.	$D.L$ (kN)	$L.L$ (kN)	Q_i (kN)	Q_u (kN)	X_i (m)	Y_i (m)	$M_{x'}$ (kN.m)	$M_{y'}$ (kN.m)
Q1	600	300	900	1200	0.25	18.25	225	16425
Q2	1200	600	1800	2400	6.25	18.25	11250	32850
Q3	700	350	1050	1400	12.25	18.25	12862.5	19162.5
Q4	1000	500	1500	2000	0.25	9.25	375	13875
Q5	1500	750	2250	3000	6.25	9.25	14062.5	20812.5
Q6	1200	600	1800	2400	12.25	9.25	22050	16650
Q7	500	250	750	1000	0.25	0.25	187.5	187.5
Q8	1000	500	1500	2000	6.25	0.25	9375	375
Q9	600	300	900	1200	12.25	0.25	11025	225
Sum			12450	16600			81412.5	120562.5

From Table 1 the following design parameters can be extracted or calculated:

Summation of Column service loads = $\sum Q_i = 12450$ kN.

Ultimate (factored) load $Q_u = 1.2 D.L + 1.6 L.L$

Summation of Column ultimate loads = $\sum Q_u = 16600$ kN.

Location of the resultant (e_x and e_y) can be calculated as follows:

$$\bar{X} = \frac{\sum Q_i X_i}{\sum Q_i} = \frac{814125}{12450} = 6.54m$$

$$\bar{Y} = \frac{\sum Q_i Y_i}{\sum Q_i} = \frac{1205625}{12450} = 9.68m$$

$$e_x = 6.54 - 6.25 = 0.29 \text{ m}$$

$$e_y = 9.68 - 9.25 = 0.43 \text{ m}$$

Applied ultimate stress over the soil can be calculated from Equation 4 after calculating the moment of inertia of the mat area.

$$I_x = BL^3/12 = 12.5 \times (18.5)^3/12 = 6595 \text{ m}^4$$

$$I_y = LB^3/12 = 18.5 \times (12.5)^3/12 = 3011 \text{ m}^4$$

Then the ultimate stress q_{ou} is equal to:

$$q_{ou} = \frac{\sum Q_{ui}}{A} + \frac{e_x \sum Q_{ui}}{I_x} y + \frac{e_y \sum Q_{ui}}{I_y} x$$

$$q_{ou} = \frac{16600}{12.5 * 18.5} + \frac{0.43 * 16600}{6595} y + \frac{0.29 * 16600}{3011} x$$

$$q_{ou} = 71.8 + 1.6 x + 1.08 y \quad (5)$$

This is the equation that is used to calculate soil reaction pressure on each strip on the mat as shown by q_{ou-F} and q_{ou-B} for the strip in Figure 28.

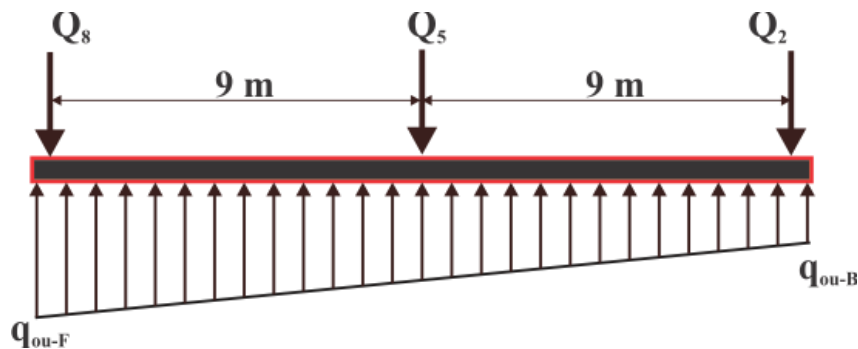


Figure 28: Layout of strip IJKL

Equation 5 is used to calculate the ultimate stress under the strip *IJKL*, specifically under points *B* and *F* which represents the average stress at the 4 corners of the strip under consideration.

$$q_{ou-B} = 71.8 + 1.6*(0) + 1.08 (9.25) = 81.8 \text{ kPa}$$

$$q_{ou-F} = 71.8 + 1.6*(0) + 1.08 (-9.25) = 61.8 \text{ kPa}$$

So, the average uniform soil pressure can be calculated as $q_{avg.} = (q_{ou-B} + q_{ou-F})/2$

$$q_{avg.} = (81.8 + 61.8)/2 = 71.8 \text{ kPa}$$

Summation column load on the strip = 7400 kN

$$\text{Soil Reaction} = q_{avg.} * A_{strip} = 71.8 * 18.5 * 6 = 7969.8 \text{ kN}$$

It could be noticed that the summation of column loads acting on the strip (downwards) is less than the soil reaction (upwards), therefore, the strip theoretically is not statically under equilibrium. So, the following steps are to modify the strip to be under statically force equilibrium, however, the moment still could result in some offset (Figure 29).

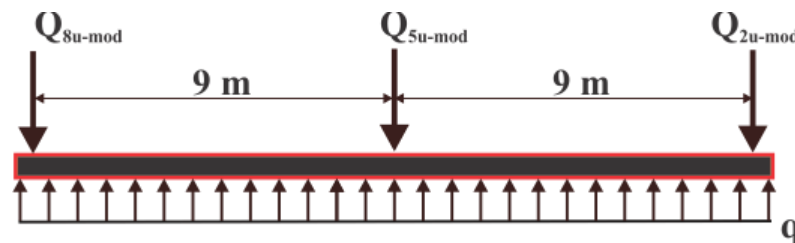


Figure 29: Statical system of strip IJKL, and modified ultimate loads notations

Average load on strip = (sum. Column load + soil reaction)/2 = (7400 + 7970)/2 = 7685 kN

$$\text{Modified average soil pressure, } q_{u-avg-mod} = \frac{\text{average load}}{A_{strip}} = 7685/(6*18.5) = 69.2 \text{ kPa}$$

Uniform distributed load over the strip $q = q_{u-avg-mod} * B_1 = 69.2 * 6 = 415.2 \text{ kN/m}$

$$\text{Column load multiplying factor } F = \frac{\text{average load}}{Q_{2u} + Q_{5u} + Q_{8u}} = 7685/7400 = 1.039$$

Then the modified column loads are as follows:

$$Q_{2u-mod} = 1.039 * 2400 = 2494 \text{ kN}$$

$$Q_{5u-mod} = 1.039 * 3000 = 3117 \text{ kN}$$

$$Q_{8u-mod} = 1.039 * 2000 = 2078 \text{ kN}$$

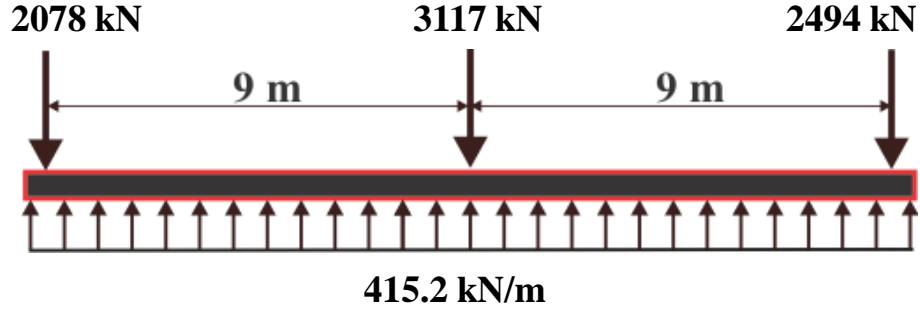


Figure 30: Statical system of strip IJKL, and the modified ultimate loads

Figure 30 can be used to extract the moment and shear numerical values and to construct shear force and the bending moment diagrams for the strip.

3.2.3. Approximate flexible method. In the previous design method, the mat is assumed to be infinitely rigid, and the soil pressure is linearly distributed. In the approximate flexible method, the soil is represented by infinite number of elastic springs as shown in Figure 26b. These springs are represented by their elastic constants which is called coefficient of subgrade reaction, k_s . The method is described by ACI Committee 336 [26], and described step-by-step in Das [15]. The method is outlined briefly as follow:

1. Determine the thickness of the raft by checking for diagonal tension shear near various columns.
2. Estimate the radius of effective stiffness as,

$$L' = \sqrt[4]{\frac{E_c t^3}{12k_s(1-\mu_c^2)}} \quad (6)$$

Where; E_c and μ_c are modulus of elasticity and Poisson's ratio of concrete respectively, t is mat thickness, and k_s is the soil modulus of subgrade reaction. The influence zone of any column load will be on the range of 3 to 4 L' .

3. At any point in the range of the column load, the radial and tangent moments (in polar coordinates) caused by this column can be calculated as:

$$M_r = -\frac{Q}{4} \left[A_1 - \frac{(1-\mu_c)A_2}{\frac{r}{L'}} \right] \quad (7)$$

$$M_t = -\frac{Q}{4} \left[\mu_c A_1 + \frac{(1-\mu_c)A_2}{\frac{r}{L'}} \right] \quad (8)$$

Where; r is the radial distance from the column load to the point, Q is column load, and A_1 and A_2 are function of r/L' and obtained from Figure 31b. To convert the tangent and radial moments to moments in Cartesian coordinate system the following equations [15] can be used, Figure 31a:

$$M_x = M_t \sin^2 \alpha + M_r \cos^2 \alpha \quad (9)$$

$$M_y = M_t \cos^2 \alpha + M_r \sin^2 \alpha \quad (10)$$

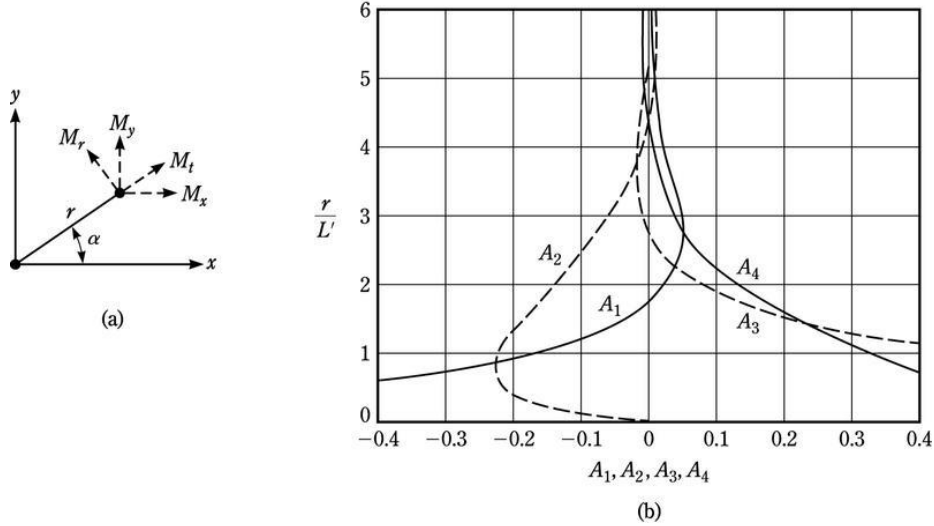


Figure 31: Graphical Data for Finite Element Method [15]

4. For the unit width of the mat, the shear force V caused by the column load Q can be calculated as:

$$V = \frac{Q}{4L'} A_3 \quad (11)$$

Where, the constant A_3 is related to r/L' and obtained from Figure 31b.

5. The deflection at and point of the mat can be calculated as:

$$\delta = \frac{QL'}{4R} A_4 \quad (12)$$

where, the constant A_4 is related to r/L' and obtained from Figure 31b.

At a specific point of the mat, moment shear and deflection from all columns which the point is located within their ranges of influence L' are required to be calculated. The rule of superposition is applied to calculate the total moment, shear and deflection at the point. In conclusion, the conventional rigid analysis method usually gives relatively more conservative design of the raft against bending moment resulting in much bigger section, and area of steel. Hence, flexible design is preferable from the economy of structure point of view. Analysis using flexible design approach is usually looked at as a Soil Structure Interaction problem.

3.2.4. finitedifference method. The finite difference method is based on the fourth-order differential equation obtained for plates and shells that can be found in any textbook, see for example Bowels [11]. This equation can be simplified and transferred to a finite difference equation. The advantages of using the difference method are the following;

1. It has been widely used as a research tool, however, for practical purpose, it could be used as a check on alternate design method.
2. It is rapid compared to the other discrete methods since the input data are minimal. This because the computations to build the global stiffness matrix is not extensive as it is with the other numerical methods such as Finite elements.
3. It is more reliable for the structural engineers if the mat could be modeled using the finite difference method.

However, the finite difference method has number of disadvantages such as;

1. It is extremely difficult to establish boundary conditions of column fixity
2. It is not easy to include notches, holes, or reentrant corners in the finite difference model.
3. It is difficult to apply a concentrated moment since this method uses moment per unit length.

The finite element technique that is explained in more details in Chapter 4 replaced this method as *FE* is powerful and capable to model sophisticated structures.

3.2.5. Coefficient of subgrade reaction modulus of soil. To perform complete design of mat foundation using flexible approach, the modulus of subgrade reaction of soil is required. According to Bowels [11], the modulus of subgrade reaction can be determined by different methods and tests like:

- a) Plate load test,
- b) Special tables of correlations with typical values, or
- c) Direct calculating the settlement of the foundation.

The plate load test is one of the oldest methods of computing the modulus of subgrade reaction by means of load tests performed on a 1 ft (30 cm) square plate. The weakness of this method is that it is limited to a small soil thickness compared to the soil stratum loaded by the raft. Therefore, the value of the subgrade modulus should be corrected for this shortcoming according to the following equation:

$$k = k_{0.3} \left(\frac{B + 0.3}{2B} \right) \quad \text{for sandy soil} \quad (13)$$

$$k = k_{0.3} \left(\frac{0.3}{B} \right) \quad \text{for clay soil} \quad (14)$$

Where $k_{0.3}$ and k are coefficient of subgrade reactions measured for 0.3m x 0.3m and B (m) x B (m), respectively. Units should be in kN/m^2 and m. Table 2 gives typical values of subgrade reaction modulus for different soil measured using plate loading tests.

Table 2: Typical values of soil subgrade reaction $k_{0.3}$ [11]

Soil Type	$k_{0.3}$ (kN/m^3)
Dry or moist sand	
Loose	8,000 – 25,000
Medium	25,000 – 125,000
Dense	125,000 – 375,000
Saturated Sand	
Loose	10,000 – 15,000
Medium	35,000 – 40,000
Dense	130,000 – 150,000
Clay	
Stiff	10,000 – 25,000
Very Stiff	25,000 – 50,000
Hard	Larger than 50,000

Chapter 4. Finite Element Analysis

4.1. Introduction

In civil engineering applications, most of structural and geotechnical encountered problems in practice involve complicated geometries, nonlinear material properties and difficult load combinations. According to Logan [27], these problematic cases cannot be solved using the common analytical solutions that are usually used to solve simple analytical tasks. For this reason, the finite element method can be the most feasible approach to solve these problems.

The finite element method is a numerical method for solving problems of engineering and mathematical physics. Specifically, it can be used to solve problems in mechanics, heat transfer, mass transportation, fluid flow, electromagnetic potential, and many others. One of the typical areas of interest that are covered by the finite element method is structural analysis. Analytical solutions generally involve solving ordinary or differential equations, which because of the complicated geometry, material properties, and loads are not usually reachable. Hence, numerical methods are the preferred technique to solve simultaneous algebraic equations and generate approximate values of the unknowns at discrete number of points in the continuum. Mainly, this process involves subdividing the object or the body into an equivalent system of elements (finite elements) [27]. Instead of solving the entire body in one equation, the finite element method allows us to come up with equations for each element and then combine them to come up with the solution of the whole body. In general, the solution for structural problems refers to determining the displacement and at each node in the element and the stress within each element throughout the structure that experiences the applied loads. Figure 32 shows the Minera Escondida copper mine tunnel together with its finite element model. The tunnel is basically a cut-and-cover bridge that carries a haul road over the mine's conveyor system. The model was developed to check distress in the tunnel structure and its foundation due to differential settlement.

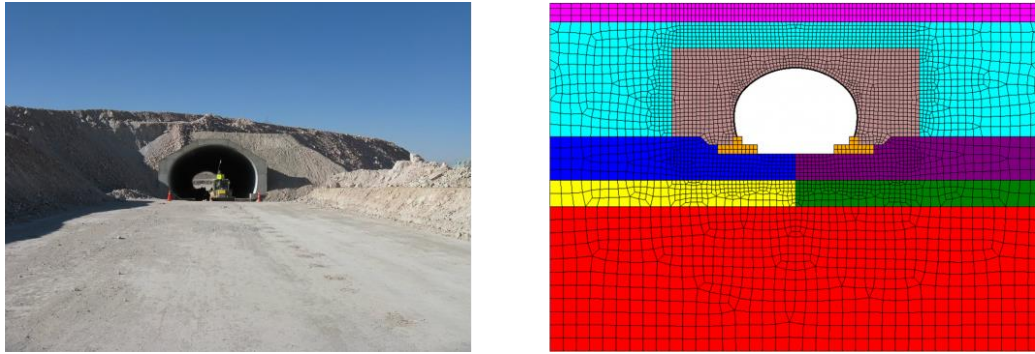


Figure 32: Minera Escondida copper mine tunnel and its finite element model [28]

4.2. History

The progress of Finite element method started in 1941 by Herznikoff [29], where continuous solids were solved with usage of one dimensional elements. Thereafter, a combination of variational form analysis and Ritz method were utilized by Courant [30] to provide a solution for displacements and stresses in vibration problems. Later, Turner et al. [31] introduced a method to calculate the stiffness of the structure by utilizing either one or two dimensional elements. This method was introduced as the direct stiffness method which was used for obtaining the deflection and stiffness of structures. Three dimensional elements were introduced later in 1960s for complex computations for deflections and internal stresses; however, their practical use was limited to large industries due to high computational costs [32].

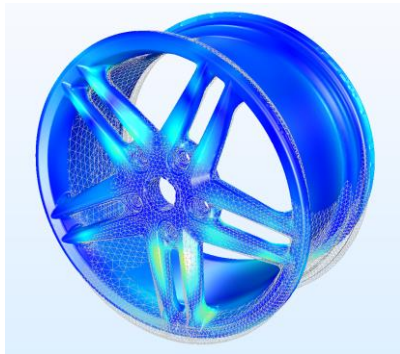
Finite element Method is vital when there is complexity in calculations of a structural scheme and the accuracy will be more reliable than manual calculations or other methods of analysis such as approximations. This method uses discrete finite elements to study the internal stresses and deformations of the structure by dividing the scheme into multiple elements which are joined at nodes. Accuracy of the results obtained from the finite element method depends on the mesh size, boundary conditions and selected elements [33].

4.3. Advantages of the Method

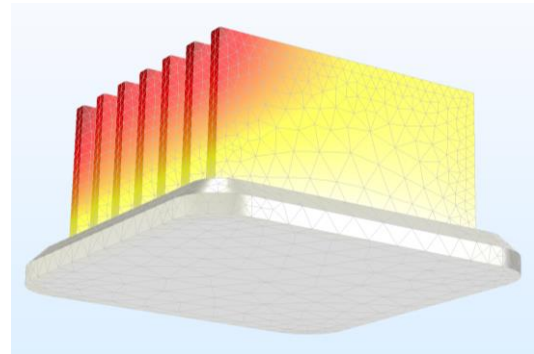
Over the past 40-50 years, the finite element method has established itself as the most powerful method to solve complex structural and geotechnical problems. This is because of the many advantages that the method provides over other techniques. These advantages include its ability to model irregular shapes without difficulty. It can also handle any type of loading easily and model structures involving several different

material properties. It has the capability of solving static and dynamic problems, with linear or nonlinear behavior. For nonlinear problems, the method can account for material nonlinearity or large displacements. The method can account for any boundary conditions. It can consider the temperature effect on the structure. Applications of the finite element method have been summarized by Clough [34]. Figure 33 shows two different applications of the finite element method, one structural and another heat transfer.

Once developed, the model of the structure can be changed and modified easily and economically. The size of the elements can be reduced within the model in order to account for stress concentration over a small area. Because of the several stated advantages of the finite element method compared to other methods and the availability of a commercial finite element program that is costume-made for reinforced concrete plates that can rest on soil, i.e. SAFE [6], the study will utilize such an approach for the analysis of the considered mat foundation.



(a) Stresses, and deformations of a wheel rim



(b) Temperature field in the heat sink

Figure 33: Two different applications of the finite element method [35]

4.4. Steps of the Finite Element Method

While it is not possible to establish a set of standard procedures for all the computations involved in the solution of all engineering problems by the finite element method, this section summarizes the general guidelines. There are generally eight steps in a finite element analysis [36].

1. Discretization of real continuum or structure. This step essentially is about selecting the element types and establishing the finite element mesh. There are variety of elements to choose from, including bar elements for 1-D, triangular and quadrilateral elements for 2-D plane and axisymmetric structures, and tetrahedron and hexahedron elements for 3-D media. This step includes

assignment of element and nodal numbers, entering nodal coordinates and element descriptions, providing nodal actions and constraints, and meshing.

2. Identify primary unknown quantity. This step depends on the type of problem being solved. It involves element displacements for stress analysis, or element temperature for heat conduction analysis, or element velocities for fluid dynamic analysis.
3. Interpolation functions and their derivation. This is crucial step in any finite element analysis because while the primary unknown quantities in method are for those within the elements, the solution provides values at the nodes. Since the elements are interconnected at nodes, it is important to establish relationship for the quantities in the elements with those at the associated nodes.
4. Derivation of element equations. There are generally two methods to derive the element stiffness equations: (a) Rayleigh-Ritz method for stress analysis of solid structure using the potential energy approach, and (b) Galerkin method for heat conduction analysis and fluid dynamic analysis.
5. Derive overall stiffness equations. In assembly of the total stiffness matrix from the element stiffness matrices, the nodes entries that are shared by more than one element should be added algebraically.
6. Solve for primary unknowns from overall stiffness equations. In solid mechanic's problems, the primary unknowns are often the displacements and the known values are the applied loads.
7. Solve for secondary unknowns. The secondary unknown quantities in the analysis can be obtained after getting the primary unknown quantities in the previous step. In stress analysis of solid structures, the strains in the elements can be related to the element displacements and the stresses by the element strains through Hooke's law.
8. Interpretation of the results. Here, the von-Mises stress in the output of stress analysis of solid structures, which represents the stress in elements with multi-axial stresses, needs to be kept below the yield stress. Also, the nodal displacements due to the deformation of the structure should be kept below the allowable value set by the design requirement.

4.5. Finite Element Modeling

For the finite element method to be a useful tool in the analysis of reinforced concrete mats, accurate modeling of the structure and boundary conditions is necessary. Modeling involves understanding the significant relations between the physical world and the analytical model. The finite element method is not an exact approach; hence, the obtained results from using the method must be judgmentally assessed before approval.

First, the number of elements used in the model can seriously affect the accuracy of the solution. Generally, as the fineness of the mesh is increased, the accuracy of the results increases also. However, there comes a point beyond which a finer mesh may not significantly impact the results. It should be noted that displacements will generally converge faster than stresses.

Second, the element type can also greatly affect the correctness of the results because different finite elements are derived from different assumptions and shape functions. For example, elements with higher order shape functions are more accurate than those with lower, and elements with mid-side nodes are generally more reliable than those without. The main difference between thin and thick shell formulation is the presence of transverse shear deformation in the plate-bending performance. Thin-plate formulation tracks a Kirchhoff application [37], which disregards transverse shear deformation. On the other hand, thick-plate formulation follows Mindlin-Reissner [38] [39], which accounts for shear behavior [6]. Note that shear deformation tends to be important when span-to-thickness is less than 5 to 10. Hence, thick-plate formulation is generally recommended for mat foundations because it is more accurate, while slightly stiffer.

Finally, once the specific elements and mesh size have been chosen and the numerical solution has converged, several other checks are needed to make sure results of the analysis are reasonable. The total reactions of the model in a given direction should be verified with hand calculations as equal to the net applied forces in the same direction. Also, the displacements should be checked and verified to be small with respect to the geometry of the structure. Once these checks have been implemented, it is important to validate if the results roughly follow the expected outcome. The deflected shape of the structure should approximately correspond to the applied forces. Symmetric results must be obtained for a structure having symmetric geometry and

loading. Any nonconformity between the likely and computed findings must be examined.

4.6. Finite Element Analysis of Mat Foundations

The finite element analysis of reinforced concrete flat plates, such as mat foundations, requires many assumptions. As the type of analysis used in this study is a linearly elastic, it assumes the gross section is resisting the applied loads and the stress-strain relation for the material is perfectly linear, even at high levels of compressive and tensile strains. Another assumption in the analysis is that the material is isotropic and homogeneous, although the presence of reinforcing bars disrupts the isotropy of the concrete. A third important assumption is that generally both Kirchoff and Mindlin plate bending elements are derived based on the assumptions of small displacements and rotations, which ignores geometric nonlinearity. This assumption is valid if the deflections of the structure are small when compared to its thickness.

The importance of accurately modeling the structure and boundary conditions should be emphasized in the analysis of rafts, which involve reinforced concrete flat plates resting on soil. Great efforts shall be exercised to validate that the model has converged and that the specific elements used are appropriate to the expected behavior.

Element stress resultants are defined as the calculated stress components per unit width at a node of a finite element. For a plate bending analysis, the main element stress resultants are the bending stress resultants and the shear stress resultants. Element stresses can be computed in many locations throughout the element. While stresses computed at the integration points are thought to be the most precise, such results are of little use to engineers because the positions of the Gauss points are unknown to the user. A common solution to this problem is to extrapolate the stresses to the nodes. Element stresses can also be computed directly at the nodes by evaluating the strain-displacement relation at the nodes, and then applying the material constitutive relationship.

4.7. Modeling with SAFE

In this study, the commercial software SAFE from Computers and Structures, Inc., will be utilized for analyzing reinforced concrete mats under gravity loading [6]. This software is a means for designing concrete floors and foundation systems. Using this computer package, laying out models is fast and effective, especially by importing

data from CAD, spreadsheet, or database programs. The software has capability of incorporating beams into the mat, and can account for presence of piles. Foundations can be of any geometry and can include edges shaped with curves.

The finite element model in SAFE requires subdividing the mat into small rectangular or square elements resting on soil. Each of the plate elements has four nodes, and each node has 3 degrees of freedom (two rotational and one translational). The soil is represented in the finite-element model by linearly elastic springs. The finite-element mesh of the analyzed mats is based on the maximum acceptable element size, with finer mesh introduced at the regions near the columns. The spring supports are applied at the nodes, and their stiffness is based on the tributary area associated with each node. SAFE uses an iterative procedure to produce a support condition that does not allow tensile resistance by the soil. Each element of the concrete mat is assumed to be an isotropic, thick plate bending element. The thick plate element is a four-node element and considers bending and the effect of shear deformations. Membrane stresses for such an element in the plane of the mat are ignored in the model. Mat element moments and shears are calculated at the mesh nodal points of the element. The loading on the mat structure is applied as point loads located at the nodes. Following the ACI 318 code approach [26], the shear and moment results are reported after dividing the mat into strips along two mutually perpendicular directions by references to the finite-element mesh. The total integrated cross-sectional shears and moments for a strip are provided by the software.

Figure 34 shows a summary of the finite element mode of the mat foundation in SAFE.

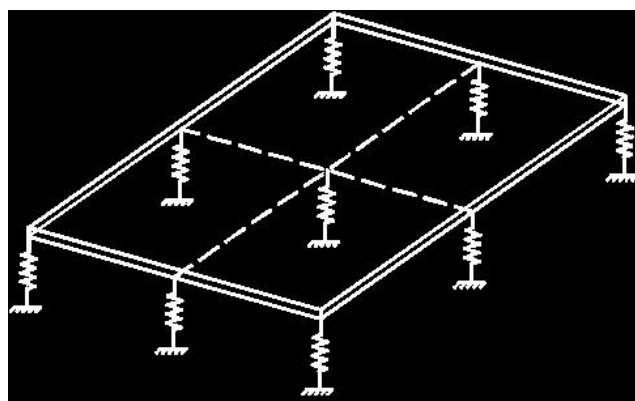


Figure 34: Finite element model of mat foundation in SAFE [40]

4.8. Considered Mat Cases

The design variables that will be considered later in Chapter 5 are the mat thickness, modulus of subgrade reaction of the soil, the modulus of elasticity of the concrete, the Poisson ratio of the concrete, the plan geometry of the mat, and the eccentricity of the applied column loads on the mat with respect to the centroid of the mat.

With regards to the mat thickness, t , all mats are assumed to have a constant thickness. This is a reasonable assumption, although a few mats in practice may have some part of the mat thicker or thinner than the rest. The mat thickness will have a value of 0.5, 1.0, 1.5, 2 and 10 meters. Of course, the 10 m thickness is not realistic, but included in the study to judge the infinitely rigid mat assumption which commonly employed in practice.

As for the modulus of sub-grade reaction, k_s , it will also be assumed constant for the soil under the entire mat. Again, this is an acceptable assumption because rarely, if ever, the soil properties under a shallow foundation would significantly change. The coefficient of subgrade reaction is related to the flexibility of the supporting soil. It is a measure of how the soil responds elastically to a given load over a given area. It depends on several factors such as the length, width, and depth at which the foundation is embedded. It has the units of MN/m per m² of area, leading to a combined unit of MN/m³. In this study, the variable k_s takes the values of 25, 50, 75, 100, 200 and 400 MN/m³ in order to cover different soil rigidities.

The modulus of elasticity of concrete, E_c , measures how elastic the concrete is under elastic loading condition. It is similar to the modulus of subgrade reaction of the soil. It depends mainly on the compressive strength of concrete and is affected by moisture, the water/cement ratio, temperature, humidity and the age of the concrete at the time of loading. The considered values of E_c in the study are 20, 25, 30 and 40 GPa is covered for normal concrete to high strength concrete.

The Poisson ratio for concrete is related to its ability to expand laterally under compressive loads. It varies over a narrow range and is often taken as 0.20 for uncracked concrete. For full cracked concrete, the Poisson ratio is taken zero. For the study purpose, a range between 0 and 0.3 is considered in the parametric study. When the concrete Poisson ratio is not part of the parametric study, it is take equal to 0.2.

The loads will be applied on the considered mats will be a function of the tributary areas of the columns that are supporting the floors above. The interior columns are assumed to carry the largest loads; the corner columns one-fourth of the load carried by the interior columns and the edge columns carry one-half the load applied on the interior columns. In the analysis of typical mat supporting 16 columns, the 4 interior columns will be assumed to carry a load of 400 kN, the 4 corner columns are assumed to be subjected to a load of 200 kN, while the remaining 8 edge columns will take a load of 100 kN. Since the results of soil bearing pressure, internal bending moments and shears are going to be normalized and the analysis is linearly elastic, the final results will be independent of the actual values of the applied loads.

The reference mat is symmetrical and consists of 3 bays along the two principal directions. This means that the mat is carrying 16 columns. In the reference mat, the center-to-center spacing between the columns along the x and y directions is equal to 6 m, i.e. $L = W = 6$ m. This value will be changed in the parametric study as follows: 3 m, 6 m, 8 m, and 10 m. Mats having nonuniform column spacing will also be considered.

A typical column size of 0.3 m by 0.3 m is used in the majority of the analyses. Typically, the size of the columns has little effect, if any, on the soil bearing pressure, bending moments and shear forces. For the reference mat, the effect of varying the column size on the results is carried out by considering 0.1 m x 0.1 m, 0.3m x 0.3 m and 0.5 m x 0.5 m square columns.

A panel is the region within the mat that is enclosed by 4 columns. In the study, the length-to-width ratio of the panel, often referred to as the aspect ratio, is varied between 0.5 to 1.0. This variation will cover one-way and two-way bending conditions within the mat.

4.9. Detailed Analysis of the Reference Mat

In this section, the mat shown in Figure 35 is considered with the geometric parameters and material properties presented in Table 3. It is analyzed with the help of the SAFE software [6]. The soil bearing pressure, bending moment, and shear force results are reported. The symmetrical mat supports 16 columns at a 6 m spacing. The applied load on each column is proportional to its tributary area.

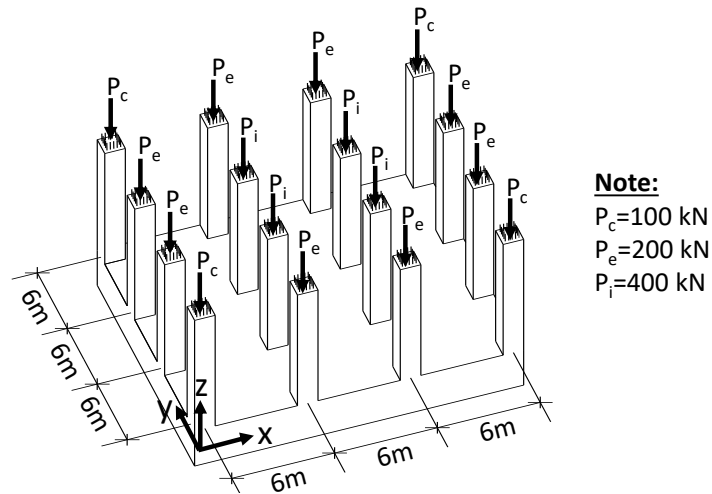


Figure 35: Typical Mat Foundation Model Layout

Table 3: Typical Mat Specification

Design Parameter	Magnitude
Concrete modulus of elasticity, E_c (GPa)	25
Modulus of subgrade reaction, k_s (MN/m ³)	50
Concrete Poisson's Ratio, μ_c	0.2
Center-to-center span length along x-axis, L (m)	6
Center-to-center span length along y-axis, W (m)	6
Mat thickness, t (m)	1

The finite element model consists of 0.5 m x 0.5 m plate elements on spring supports. The optimum mesh size of the mat was reached after considering several element sizes and comparing the results to each other. The finite element model, together with the applied loading on the mat, from SAFE is presented in Figure 36. The amplified deflected shape of the mat due to the applied load is presented in Figure 37 where, the maximum deflection is 0.47 mm and minimum deflection is 0.16 mm.

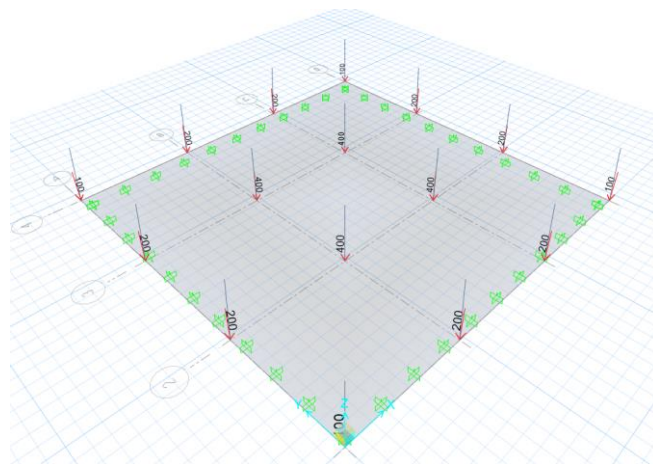


Figure 36: Typical Mat Foundation Model Layout

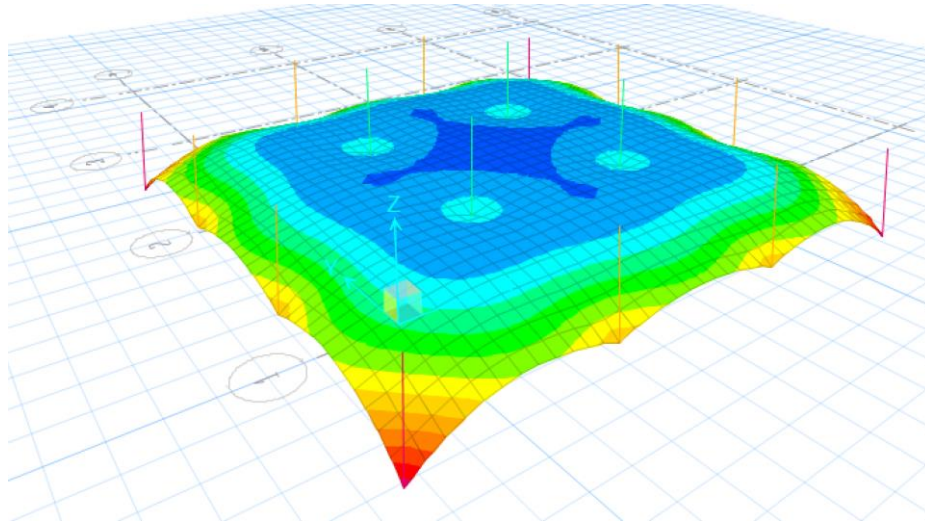


Figure 37: Amplified deflection shape of the mat

Findings of the finite element analysis are shown in the Figure 38 to Figure 45. In all cases, the symmetrical results validate the accuracy of the model. Figure 38 shows stress contours for the soil bearing pressure under the mat. The results showed that the entire mat was under compression and no region experienced uplift. Maximum compression was found at the 4 corners of the mat, whereas minimum compression was observed at the center of the mat. The entire perimeter of the mat experienced high compressive stresses, although the columns located at the boundary of the mat are not subjected to the largest loads. The large nonuniformity in the soil pressure confirms that the mat does not behave as rigid but rather as flexible plate.

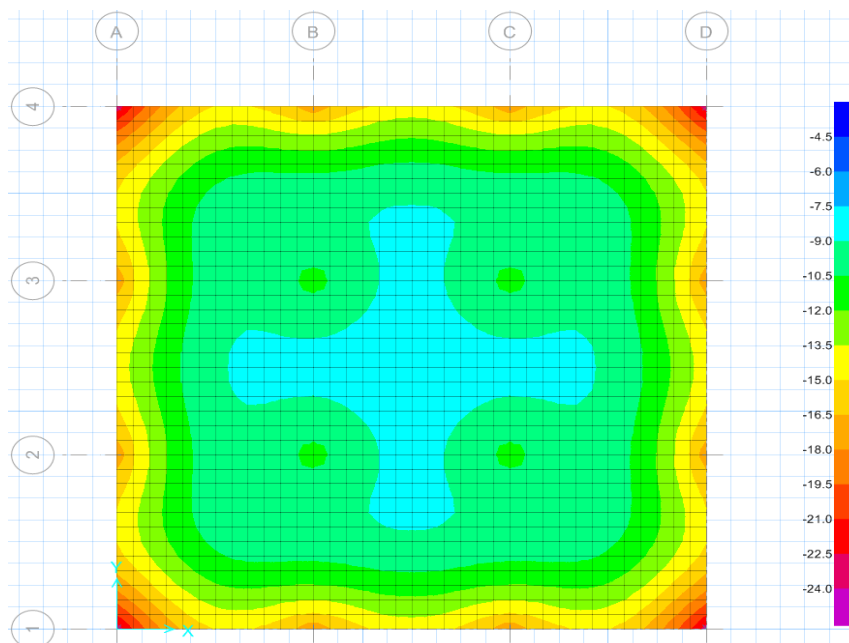


Figure 38: Typical mat foundation - soil bearing pressure result

Figure 39 shows the bending moment about the y-axis in strips taken along the x-direction along the columns and mid-way between the columns. The reported values are in the units of kN-m per m-strip. Due to symmetry, the bending moment about the x-axis in strips taken along the y-direction will show the exact same behavior; hence, they are not presented. As expected, the results show positive bending moments in the mat (compression at top) at the location of the columns, and negative bending moment (compression at bottom) at locations between the columns. Both the maximum positive and maximum negative bending moments occurred in the interior strips along gridlines 2, 3, B and C, in reference to Figure 39. Along those strips, the positive moment was about 20% larger than the negative moment. Figure 40 and Figure 41 respectively shows graphical results of the maximum and minimum principal moments per unit length acting at the mid-surface of the elements. Note that the principal moments are oriented such that the associated twisting moments per unit length is zero [6].

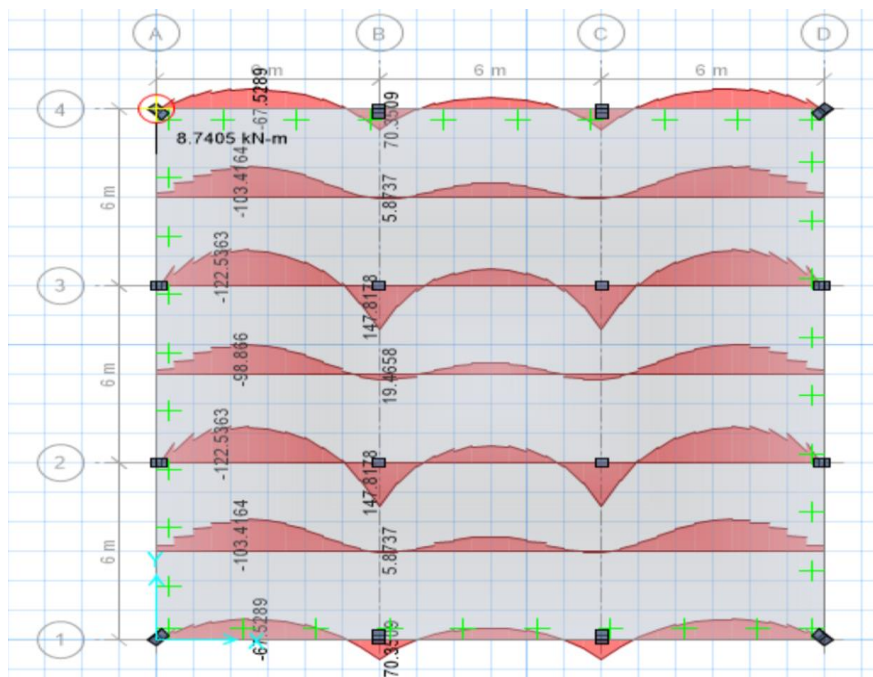


Figure 39: Bending moment results in the reference mat

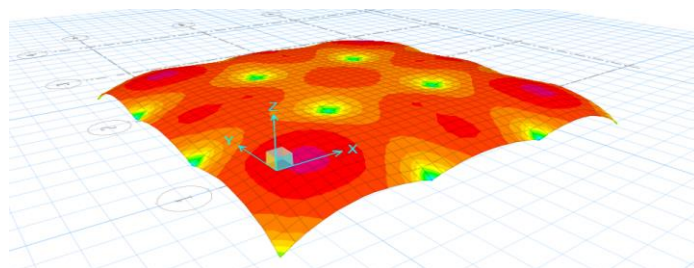


Figure 40: Maximum principal moment at the elements mid-depth

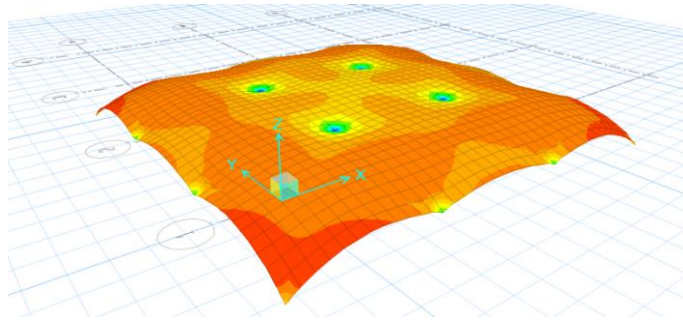


Figure 41: Minimum principal moment at the elements mid-depth

Figure 42 shows the shear forces along the vertical z-axis in strips taken along the x-direction along the columns and mid-way between the columns. The reported values are in the units of kN per m-strip. Due to symmetry, the shear forces along the z-axis in strips taken along the y-direction will be the same. For the column strips, the results show that the location of maximum shear is consistently at the columns and zero shear midway between the columns. As in the case of bending moment, the maximum critical shear occurred in the interior strips along gridlines 2, 3, B and C, in reference to Figure 39. The maximum principal stress per unit length acting at the mid-depth of the element is presented in Figure 43. Note that these shear forces are oriented on faces of the elements such that the associated shears unit length on perpendicular faces are zero [6].

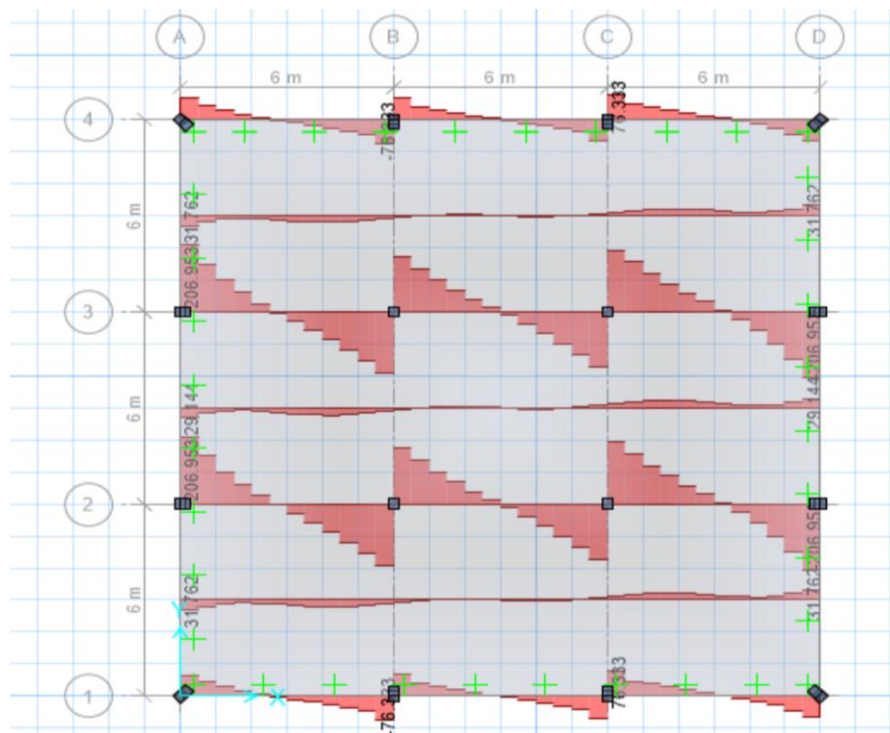


Figure 42: Shear force results in the reference mat

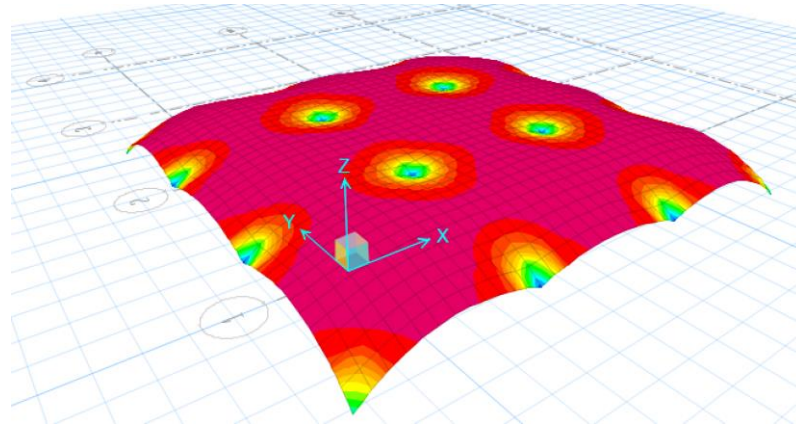


Figure 43: Maximum principal shear at the elements mid-depth

The magnitude of the maximum soil pressure, minimum soil pressure, maximum positive moment, maximum negative moment, and maximum shear force in the reference mat are included in Table 4.

Table 4: Typical Reference Model - Tabulated Results

Critical Values	Magnitude
Maximum Deflection (m)	0.00047
Minimum Deflection (m)	0.00016
Maximum Soil Pressure (kPa)	23.4
Minimum Soil Pressure (kPa)	8.22
Maximum Positive Moment (kN-m per m-strip)	148
Maximum Negative Moment (kN-m per m-strip)	123
Maximum Shear (kN per m-strip)	207

Chapter 5. Parametric Study

5.1. General

The finite element software SAFE [6] is used to determine the effect of different design parameters on the response of the mat foundation. Specifically, the soil bearing pressure and the critical positive and negative bending moments in the two principal directions, as well as the maximum shear within the mat are considered. In order to generalize the obtained results, present them in an objective manner, and allow for a fair comparison between different mats, the considered values are normalized with respect to the applied load and the mat's plan geometry. The normalization scheme is explained below in reference to Figure 44. Note that in all the analyzed mats in this chapter, the column loads are selected such that they are proportional to the tributary area they serve. For example, the corner column load P_c is assigned a value of one-quarter the load on the interior column (i.e. $P_c=P_i/4$) and one-half the assigned value to the edge column load P_e (i.e. $P_c=P_e/2$). In reality, column loads may not follow this assumption, but in this study, this is used for lack of any other reasonable approach.

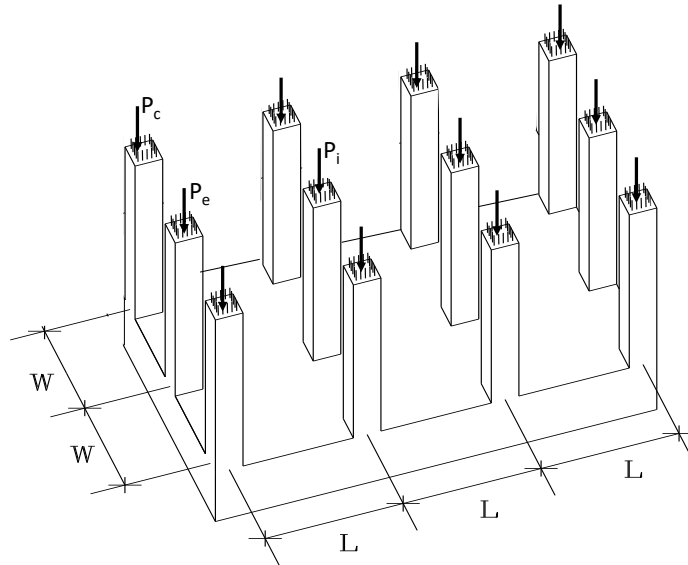


Figure 44: Nomenclature used on a typical mat foundation

For example, the normalized maximum and minimum soil pressure under a mat are presented as follows:

$$(q_{Max})_{Nor} = q_{Max} / q_{avg} \quad (15)$$

$$(q_{Min})_{Nor} = q_{Min} / q_{avg} \quad (16)$$

where $(q_{Max})_{Nor}$ and $(q_{Min})_{Nor}$ are the maximum and minimum normalized soil bearing pressure, respectively, and q_{avg} is the average soil pressure under the mat, given by:

$$q_{avg} = \Sigma P / A \quad (17)$$

in which ΣP is the total load from the columns and A is total mat area ($\Sigma L \cdot \Sigma W$).

The normalized maximum positive and maximum negative bending moment along the length direction within the raft are defined by:

$$(M^+{}_L)_{Nor} = M^+{}_L / (q_{avg} L^2) \quad (18)$$

$$(M^-{}_L)_{Nor} = M^-{}_L / (q_{avg} L^2) \quad (19)$$

Note that the bending moment shown above are presented for a strip of unit width (units = force-length/length)

Similarly, the normalized maximum positive and maximum negative bending moment along the width direction within the raft are defined by:

$$(M^+{}_W)_{Nor} = M^+{}_W / (q_{avg} L^2) \quad (20)$$

$$(M^-{}_W)_{Nor} = M^-{}_W / (q_{avg} L^2) \quad (21)$$

The normalized maximum shear forces per unit width within the raft along the length and width are defined respectively by:

$$(V_L)_{Nor} = V_L / (q_{avg} L) \quad (22)$$

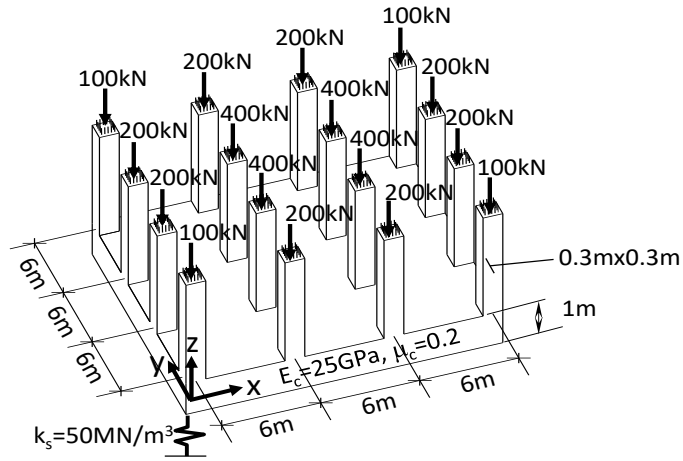
$$(V_W)_{Nor} = V_W / (q_{avg} W) \quad (23)$$

Note that in practice the absolute maximum shear within the raft is of interest to the structural engineer since it is used to check the adequacy of the mat thickness against shear. Hence, the largest value obtained from Equations 22 and 23 is considered in the analysis.

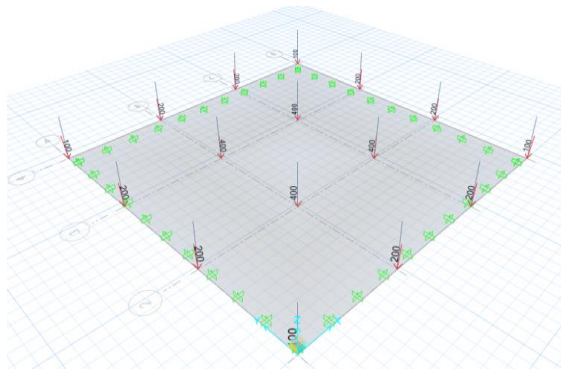
5.2. Normalized Results of the Reference Model

In this section, the normalization scheme discussed earlier is demonstrated on the results of analysis of the mat with 3 bays of 6 m in each direction considered in the previous chapter and shown in Figure 45. For simplicity, the self-weight and direct superimposed dead and live load pressures applied on the mat are not considered. This is not a concern because any uniform self-weight and additional uniform pressure will only affect the bearing soil pressure, but not the bending moments and shears within the mat. The effect of the mat weight and any additional direct load on the mat will cause the soil pressure to increase by the same amount.

A summary of the geometry and material properties for the reference mat is presented in Table 5.



(a) Reference Mat



(b) SAFE Model

Figure 45: Mat considered in parametric study

Table 5: Geometry and material properties for the reference mat

Design Parameter	Value
Concrete Modulus of Elasticity (kN/m ²)	25x10 ⁶
Modulus of Subgrade reaction, K (kN/m ³)	50,000
Concrete Poisson's Ratio	0.20
Center-to-Center Span, L & W (m)	6
Mat Thickness, t (m)	1
Column size (mxm)	0.3x0.3

The average soil pressure is calculated from Equation 17 as follow:

$$q_{avg} = \Sigma P / A = 3600 \text{ kN} / 324 \text{ m}^2 = 11.11 \text{ kN/m}^2$$

where ΣP = Summation of all Loads = 3600 kN, and $A = (6 \times 3) \times (6 \times 3) = 324 \text{ m}^2$

Then the normalized maximum soil pressure is calculated from Equation 15 as:

$$(q_{Max})_{Nor} = q_{Max} / q_{avg} = 23.39 \text{ kN/m}^2 / 11.11 \text{ kN/m}^2 = 2.10$$

The above value represents the maximum soil pressure for the given (flexible) mat with reference to corresponding mat having infinite rigidity.

The normalized maximum bending moment within the mat can be obtained from Equation 18:

$$(M^+_L)_{\text{Nor}} = (M^+_w)_{\text{Nor}} = M^+_L / (q_{\text{avg}} L^2) = (123 \text{ kN-m/m}) / [11.11 \text{ kN/m}^2 \times (6 \text{ m})^2] = 0.31$$

The normalized maximum shear within the mat can be obtained from Equation 22 (or 23, due to symmetry of mat and loading):

$$(V_L)_{\text{Nor}} = V_L / (q_{\text{avg}} L) = (207 \text{ kN/m}) / (11.11 \text{ kN/m}^2 \times 6 \text{ m}) = 3.10$$

In the following sections, the effect of all the involved design parameters in a mat foundation on the structural (and geotechnical) behavior will be investigated for a range of values.

5.3. Effect of Mat Thickness

In this section, the effect of changing the thickness of the reference mat provided in Figure 45 on the maximum and minimum soil pressure, maximum positive and negative bending moments, and maximum shears, while keeping all other variables constants is determined. The mat thickness is considered for a range of values between 0.5 m and 10 m. Note that while the mat thickness of 10 m is unrealistic, this case is included in the analysis in order to show the response of infinitely rigid mat, a case which is commonly assumed in practice for design purposes. Table 6 shows the results of finite element analysis using SAFE for the reference mat with different thicknesses.

Table 6: Effect of mat thickness on actual design parameters

Mat Thickness (m)	Max Soil Pressure (kPa)	Min Soil Pressure (kPa)	Positive Moment (kN-m/m)	Negative Moment (kN-m/m)	Shear (kN/m)
0.5	48.8	2.45	150	91.3	195
1	23.4	8.22	148	123	207
1.5	17.6	8.89	122	132	209
2	14.9	9.67	101	140	210
10	11.3	11.1	66.7	158	211

The corresponding normalized results of the values in Table 6 based on the approach in Section 5.1 are shown in Table 7.

Table 7: Effect of mat thickness on normalized design parameters

Mat Thickness (m)	Max Soil Pressure	Min Soil Pressure	Positive Moment	Negative Moment	Shear
0.5	4.39	0.22	0.39	0.23	2.93
1	2.11	0.74	0.37	0.31	3.10
1.5	1.58	0.80	0.31	0.33	3.14
2	1.34	0.87	0.25	0.35	3.15
10	1.01	1.00	0.17	0.39	3.16

The results with regards to the effect of the mat thickness are presented in Figure 46. They indicate that the concrete mat thickness has significant effect on the soil pressure distribution and magnitude. As expected, an increase in the slab thickness makes the raft more rigid; therefore, the mat deforms less, which leads to a near uniform bearing pressure on soil, as shown in Figure 47. For the case of infinitely rigid mat ($t = 10\text{m}$), the maximum and minimum bearing pressure values approach the average pressure, which is equal 11.11 kPa. However, the results show that the effect of the raft thickness on the soil pressure distribution diminishes after a threshold value, in this case of 2 m. It is interesting to note that the maximum soil pressure is not necessarily located under the columns that are subjected to the largest loads. Instead, it was found below the corner columns due to the discontinuity of the raft at that location, which results in more deflection under the column. The minimum soil pressure for the considered mat was observed at the center of the interior panel. This is due to the fact that the columns along the raft perimeter experienced much more deflection compared to the interior columns, leading to upward bulging between the four central interior columns.

The effect of the thickness on the maximum positive and negative bending within the mat is shown in Figure 48. The results indicate that the concrete mat thickness has great effect on the bending moment. Note that negative moment (tension on top) occurs between the columns, whereas positive moment (tension at bottom) in regions located near the columns.

In general, an increase in the mat thickness causes the positive moment to decrease and the negative moment to increase. For relatively thin mats, $(t)_{Nor} < 0.2$, the positive bending moment is less sensitive to the change in thickness than the negative moment. The opposite is true for relatively thick mats, $(t)_{Nor} > 0.2$. As the slab thickness

increases, it makes the raft more rigid; therefore, it curves less leading to near-uniform soil bearing pressure within the whole raft panel.

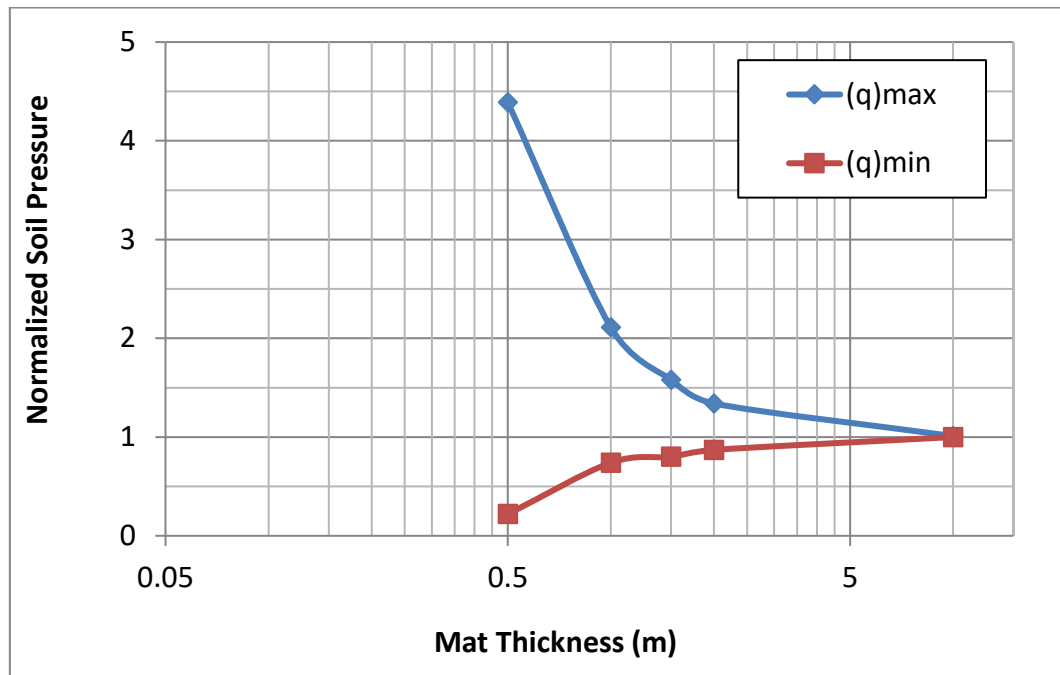


Figure 46: Effect of mat thickness on soil bearing pressure

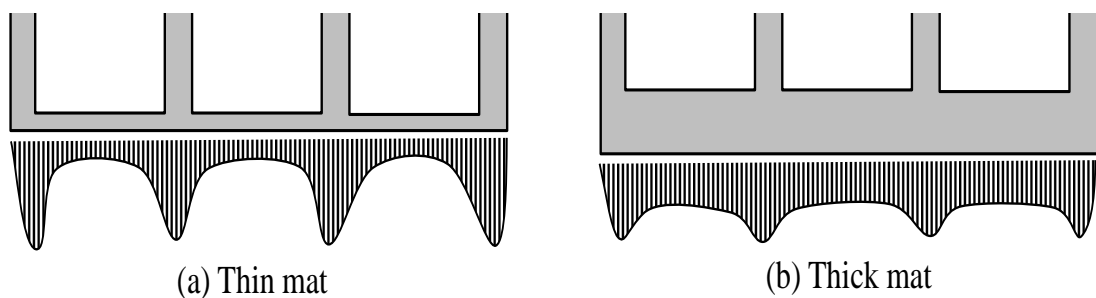


Figure 47: Soil pressure distribution under a mat with different thicknesses

Note that within a panel, the negative moment and positive moment regions are somewhat equal to each other for thin mats. This is shown in Figure 49a, in which the deflection points in the bending moment diagram are relatively far away from the columns. For thick mats, the points of contra-flexure are closer to the columns, as presented in Figure 49b. The variation in bending moment with changes in mat thickness is mainly due to the change in soil bearing pressure distribution. In the case of thin mats, the soil pressure under the columns is very large (Figure 47a), whereas in the case of thick mats the pressure is nearly uniform when subjected to the same loading (Figure 47b). The findings can be explained by pointing out that large soil pressure under the columns (accompanied with small soil pressure near midspan) has little effect

on the negative moment in regions midway between the columns. Alternatively, small soil pressure under the columns (accompanied with large soil pressure near midspan) has significant effect on the negative moment in regions midway between the columns.

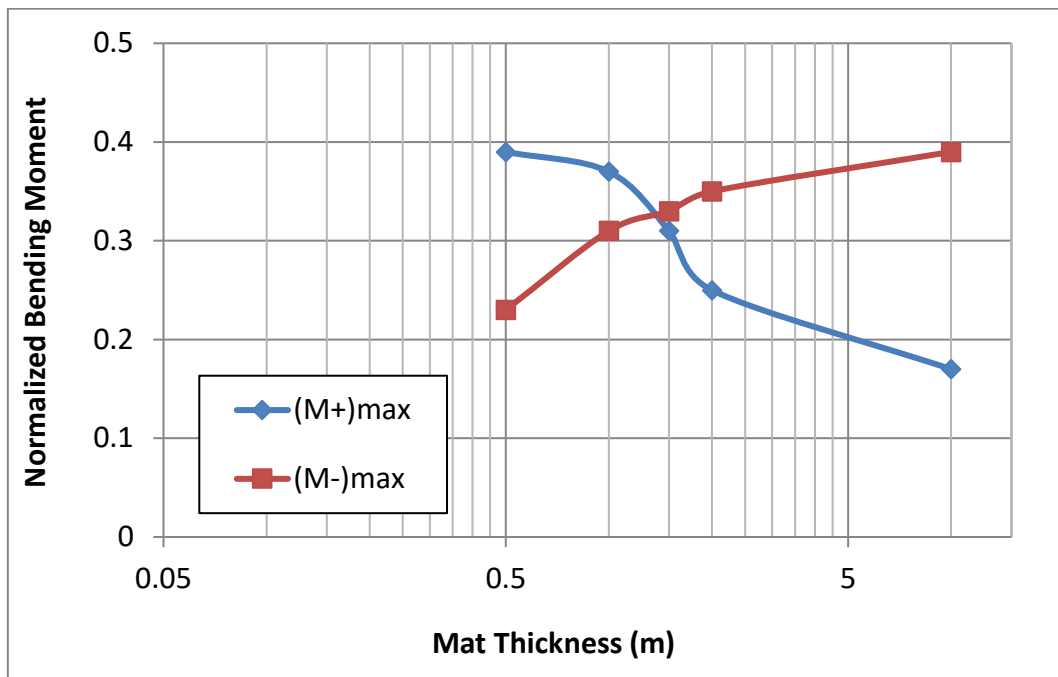


Figure 48: Effect of mat thickness on maximum bending moment

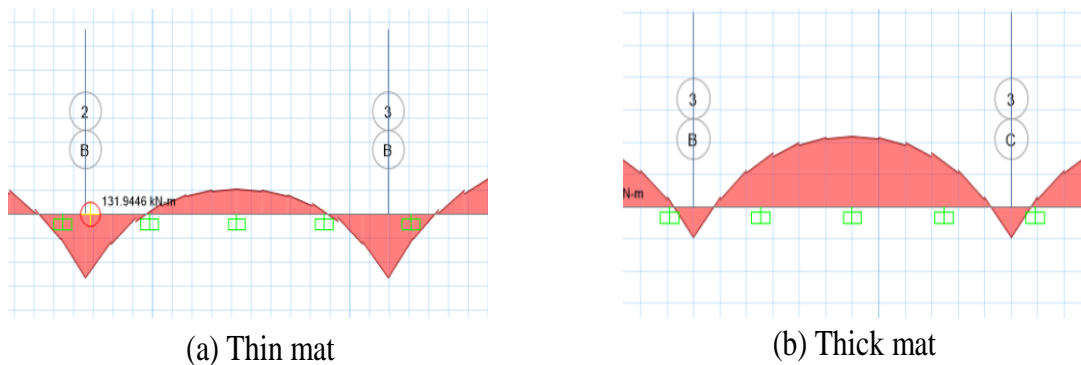


Figure 49: Moment diagrams in a panel between columns

The effect of the mat thickness on the shear force in the reference mat is included in Figure 50. The results show that this effect on the maximum shear within the mat is minimal. This is mainly due to the fact that both the mat and the loading are symmetrical; thus, the critical shear at the face of the columns is affected by the volume under the soil pressure under the mat, which is independent of the distribution of the soil pressure (since the loading is unchanged).

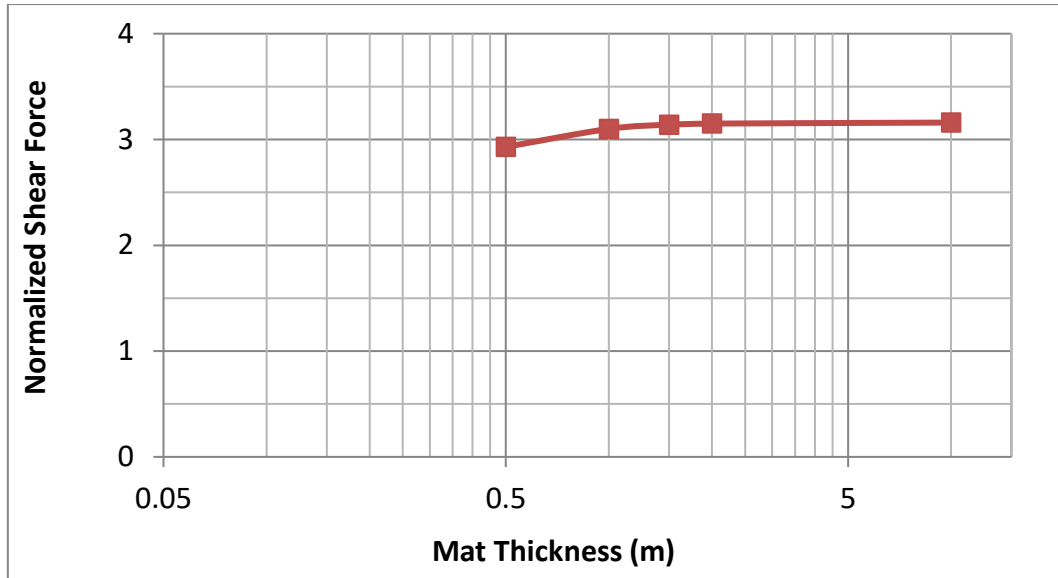


Figure 50: Effect of mat thickness on maximum shear force

5.4. Effect of Modulus of Sub-grade

In this section, the effect of the soil's modulus of subgrade reaction, k_s , on the design parameters of a mat foundation is considered. Note that the modulus of subgrade reaction is a conceptual relationship between soil pressure and deflection that is extensively used in the structural analysis of foundations. The reference mat considered in the previous section is now analyzed with different modulus of subgrade reaction, ranging from 25 MN/m³ to 400 MN/m³. The lower value of k_s represents soil condition composed of soft clay or loose sand, while the high value represents well graded clean sand-gravel mixture. Table 8 shows the results of the analysis.

Table 8: Effect of soil's modulus of subgrade reaction on design parameters

Modulus of Subgrade Reaction (MN/m ³)	Max Soil Pressure (kPa)	Min Soil Pressure (kPa)	Positive Moment (kN-m/m)	Negative Moment (kN-m/m)	Shear (kN/m)
25	19.3	8.53	135	126	208
50	23.4	8.22	148	123	207
75	26.7	8.14	153	118	206
100	29.8	7.94	155	115	205
200	40.7	6.53	157	104	201
400	57.9	2.01	154	93	195

The corresponding normalized results of the values in Table 8 based on the approach in Section 5.1 are shown in Table 9.

Table 9: Effect of Soil Subgrade modulus on normalized design parameters

Modulus of Subgrade Reaction (MN/m³)	Max Soil Pressure	Min Soil Pressure	Positive Moment	Negative Moment	Shear
25	1.73	0.77	0.34	0.31	3.13
50	2.11	0.74	0.37	0.31	3.10
75	2.41	0.73	0.38	0.30	3.09
100	2.68	0.71	0.39	0.29	3.07
200	3.66	0.59	0.39	0.26	3.01
400	5.21	0.18	0.39	0.23	2.92

The impact of the modulus of subgrade reaction of the soil on the bearing soil pressure is presented in Figure 51. The results indicate that as k_s increases, the maximum soil pressure occurring under the columns greatly increases. This is accompanied by a very small decrease in the minimum pressure, which takes place in the central region of the panels between the columns. This can be explained with reference to Figure 52, which shows the soil pressure distribution for two mats, one supported by soil having small k_s and another carried by soil having high k_s . For mats supported on stiff soil (Figure 52a), there is concentration of high soil pressure just under the columns, while for mats on soft soil the pressure is more evenly distributed under the mat. This means that for the case of high k_s , the raft under the columns deflect more for the case of low k_s . However, regions of the mat located at the center of the panels (which represent minimum soil pressure) experience the same minimum soil bearing pressure, irrespective of k_s . In all cases, the integration of the soil pressure over the underside area of the mat, which denotes the total applied load through the columns, is the same.

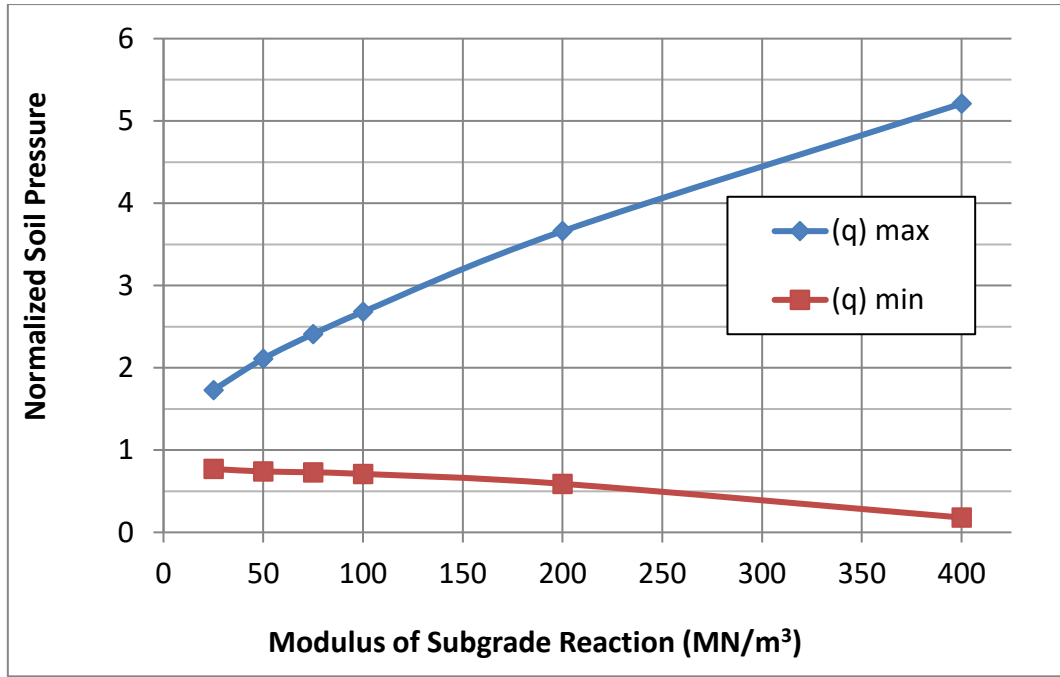


Figure 51: Effect of modulus of subgrade reaction on soil bearing pressure

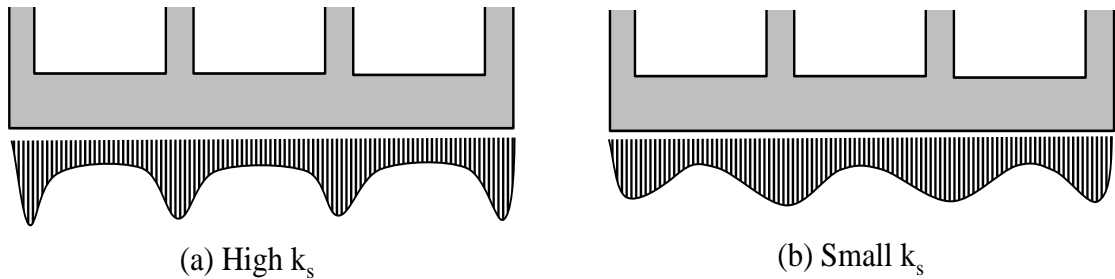


Figure 52: Soil pressure distribution under a mat supported by different soils

The effect of the modulus of subgrade reaction on the maximum positive and negative bending within the mat is shown in Figure 53. The results indicate that k_s has slightly more effect on the positive moment (under the columns) than on the negative moment (away from the columns). This can be attributed to the change in the soil pressure distribution due to the soil stiffness, as shown in Figure 52. While the minimum soil pressure remains the same in both cases, as shown in Figure 51, the maximum soil is a little lower when k_s is small compared to when k_s is large, although the length over which the maximum pressure is applied is different in the two cases. Since the soil pressure between the columns, which is independent of k_s , is responsible for the negative moment, the change in k_s does not significantly affect that moment. The increase in the positive moment with increase in k_s is due to the increase in the soil pressure in that region.

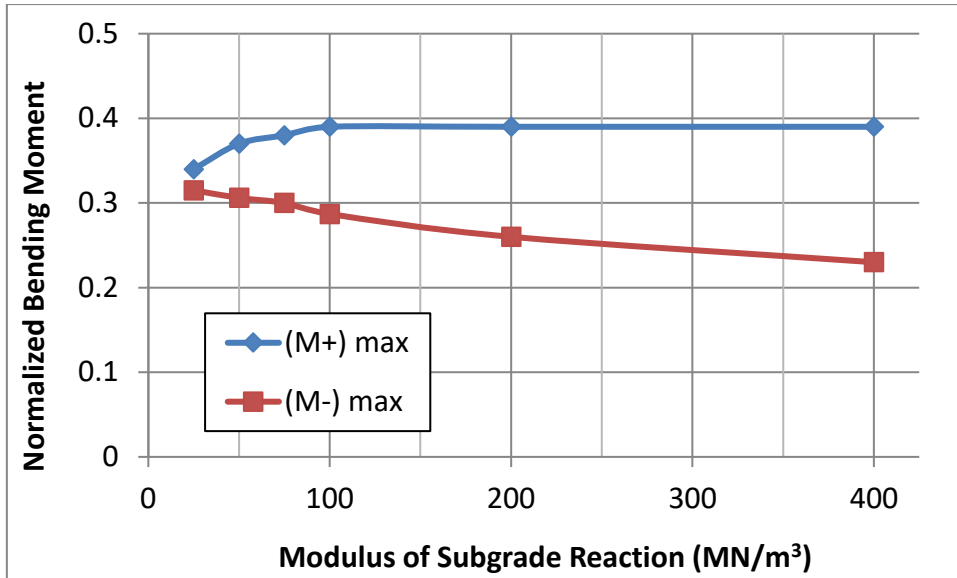


Figure 53: Effect of modulus of subgrade reaction on bending moment

The effect of the soil’s modulus of subgrade reaction on the maximum shear in the mat is presented in Figure 54. The results show that this effect on the maximum shear within the mat is negligibility small. As explained in the previous section, this is mainly due to the fact that the critical shear in symmetrical mats is related to the total applied load on the mat, which is the same in all the analyzed mats in this section, and is independent of the distribution of the soil pressure.

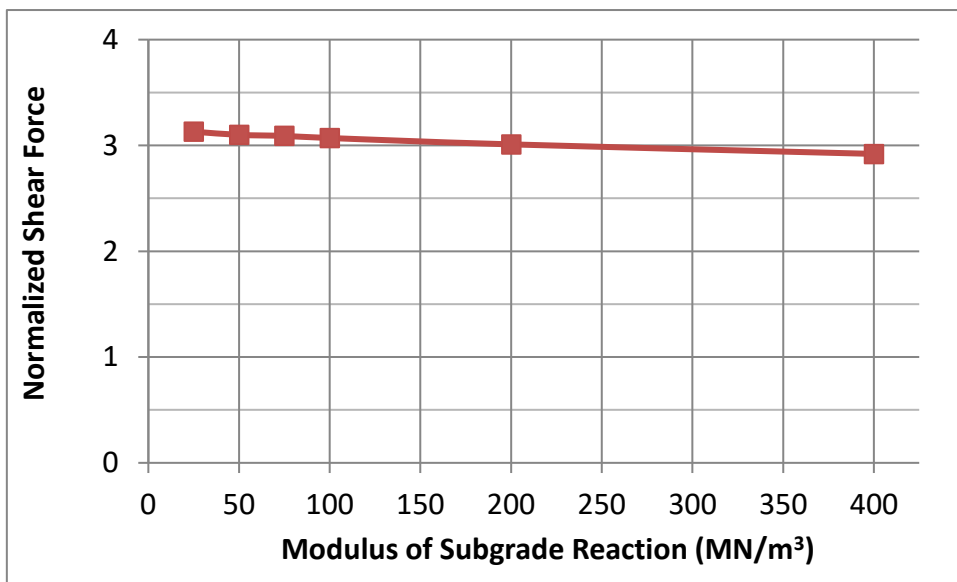


Figure 54: Effect of modulus of subgrade reaction on shear

5.5. Effect of Modulus of Elasticity of Concrete

In this section, the effect of the modulus of elasticity of the concrete of which the foundation is made from on soil bearing pressure, bending moments, and shears, is

investigated. Past studies show that this parameter is a function of the compressive strength and density of the concrete (ACI 318) [26]. Although the compressive strength of commonly used concrete can vary over a wide range, between 20 and 50 MPa, the corresponding modulus of elasticity varies over a narrower range, between 21 and 35 GPa, because its correlated with the square-root of the compressive strength. The values of the modulus of elasticity that are considered in the study are 20, 25, 30 and 40 GPa. Table 10 shows the change in the design parameters with a change in the modulus of elasticity of concrete.

Table 10: Effect of concrete modulus of elasticity on design parameters

Modulus of Elasticity of Concrete (GPa)	Max Soil Pressure (kPa)	Min Soil Pressure (kPa)	Positive Moment (kN-m/m)	Negative Moment (kN-m/m)	Shear (kN/m)
20	25.2	8.17	151	120	206
25	23.4	8.22	148	123	207
30	21.6	8.27	145	120	207
40	20.4	8.40	140	128	208

The corresponding normalized results of the values in Table 10 based on the approach in Section 5.1 are shown in Table 11.

Table 11: Effect of concrete modulus of elasticity on normalized design parameters

Modulus of Elasticity of Concrete (GPa)	Max Soil Pressure	Min Soil Pressure	Positive Moment	Negative Moment	Shear
20	2.26	0.74	0.38	0.30	3.10
25	2.11	0.74	0.37	0.31	3.10
30	1.94	0.74	0.36	0.30	3.11
40	1.84	0.76	0.35	0.32	3.12

Figure 55 shows that concrete modulus of elasticity versus the soil bearing pressure. While the results indicate no change in the minimum soil bearing pressure with a change in the concrete modulus of elasticity, there is some effect on the maximum soil pressure, especially for low concrete modulus of elasticity.

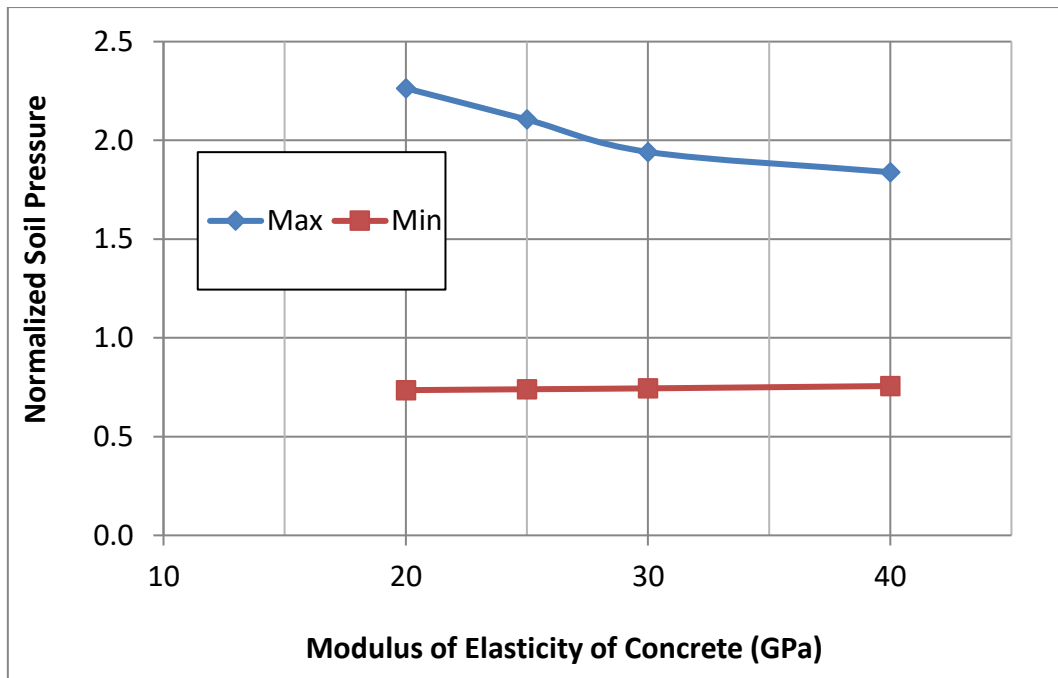


Figure 55: Effect of modulus of Elasticity of concrete on soil pressure

As the modulus of elasticity increases, the maximum soil pressure under the column decreases due to the increased rigidity of the mat, which results in better distribution of the soil pressure underneath it. The corresponding results for bending moment and shear are depicted in

Figure 56 and Figure 57. They indicate minimal effect on the bending moment and almost no effect on the shear. For the case of moment, as the modulus of elasticity increases, the maximum negative and positive moments approach each other.

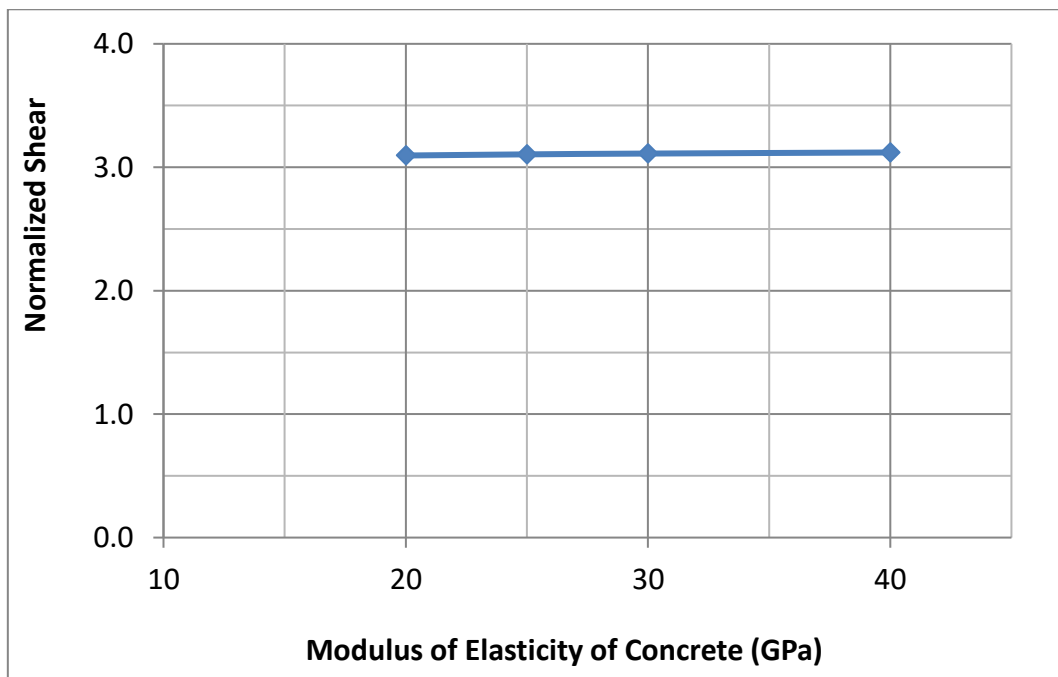


Figure 56: Effect of modulus of elasticity of concrete on shear

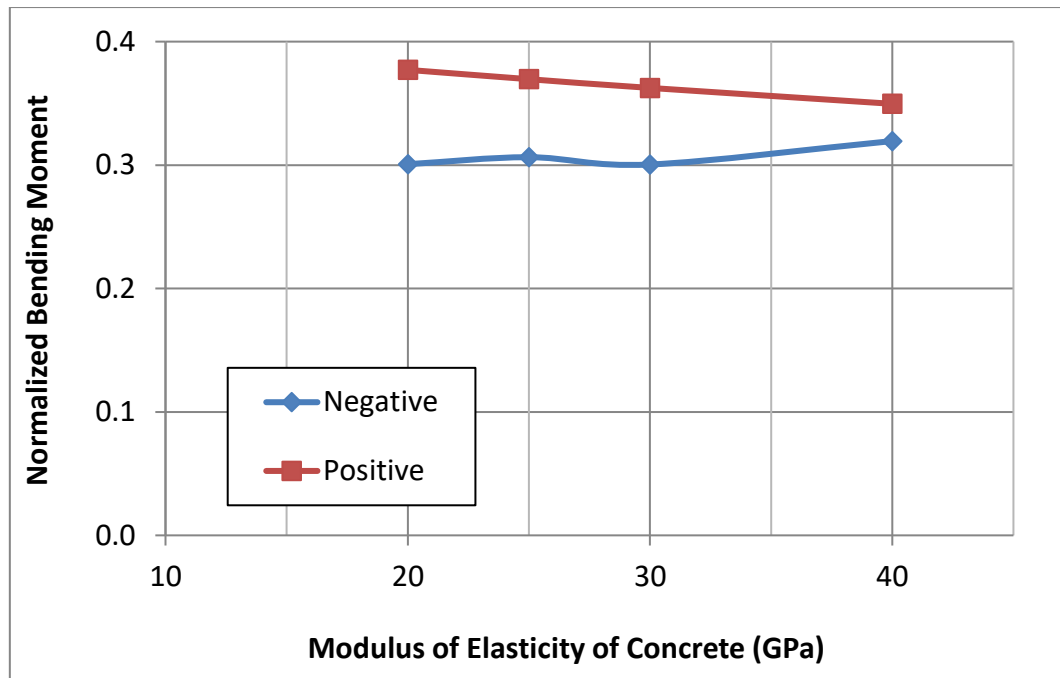


Figure 57: Effect of modulus of elasticity of concrete on bending moment

5.6. Effect of Concrete Poisons Ratio

The effect of changing the Poisson's ratio of the concrete in the mat is on the structural behavior is investigated. This ratio represents the extent of transverse expansion due to axial compression. Concrete has a Poisson ratio equal to about 0.2 when uncracked and zero when cracked. In this section, a range of Poisson ratio between zero and 0.3 is considered. Table 12 and Table 13 respectively show the effect of the concrete Poisson ratio on the actual and normalized design parameters. Presentation of the results in a graphical form is presented in Figure 58 to Figure 60. Overall, findings of the analysis show that the bearing soil pressure, bending moments and shear are insensitive to changes in the concrete Poisson ratio.

Table 12: Effect of Poisson's ratio on design parameters

Poisson's Ratio	Max Soil Pressure (kPa)	Min Soil Pressure (kPa)	Positive Moment (kN-m/m)	Negative Moment (kN-m/m)	Shear (kN/m)
0.0	24.3	8.10	140	126	203
0.1	23.9	8.16	144	125	205
0.2	23.4	8.22	148	123	207
0.3	22.8	8.29	151	119	209

Table 13: Effect of Poisson's ratio on normalized design parameters

Poisson's Ratio	Max Soil Pressure	Min Soil Pressure	Positive Moment	Negative Moment	Shear
0.0	2.18	0.73	0.35	0.32	3.05
0.1	2.15	0.73	0.36	0.31	3.08
0.2	2.11	0.74	0.37	0.31	3.10
0.3	2.05	0.74	0.38	0.30	3.12

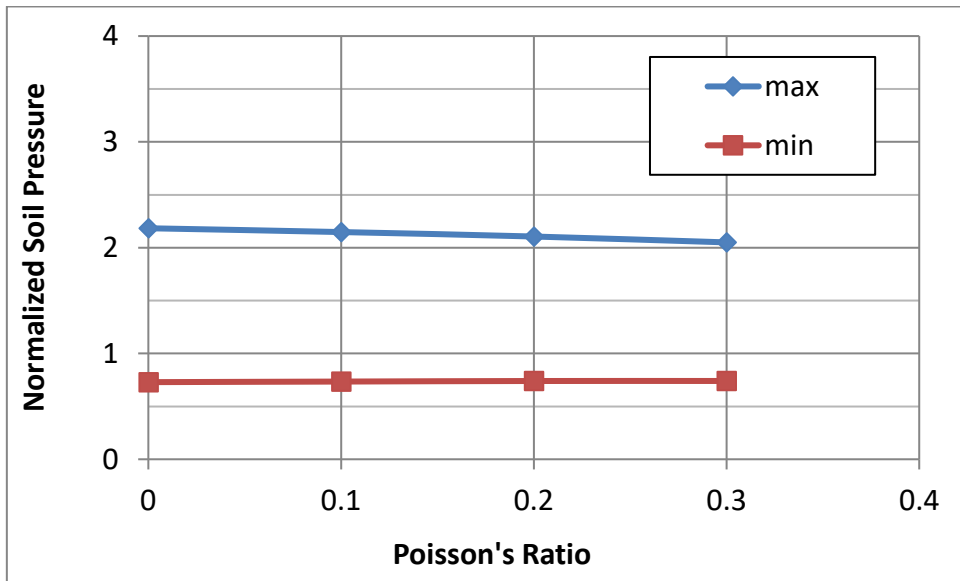


Figure 58: Effect of Poisson's Ratio on Soil Pressure

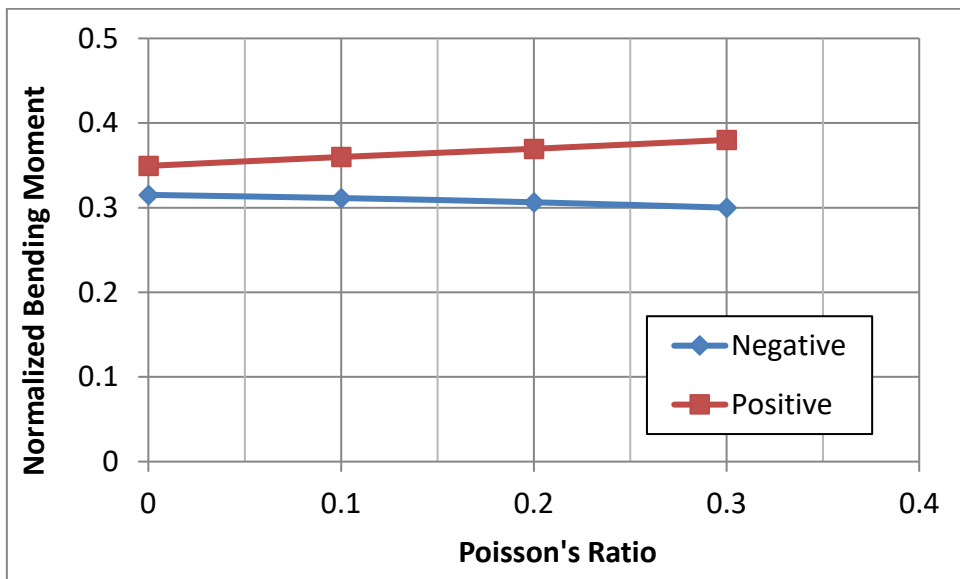


Figure 59: Effect of Poisson's Ratio on bending moment

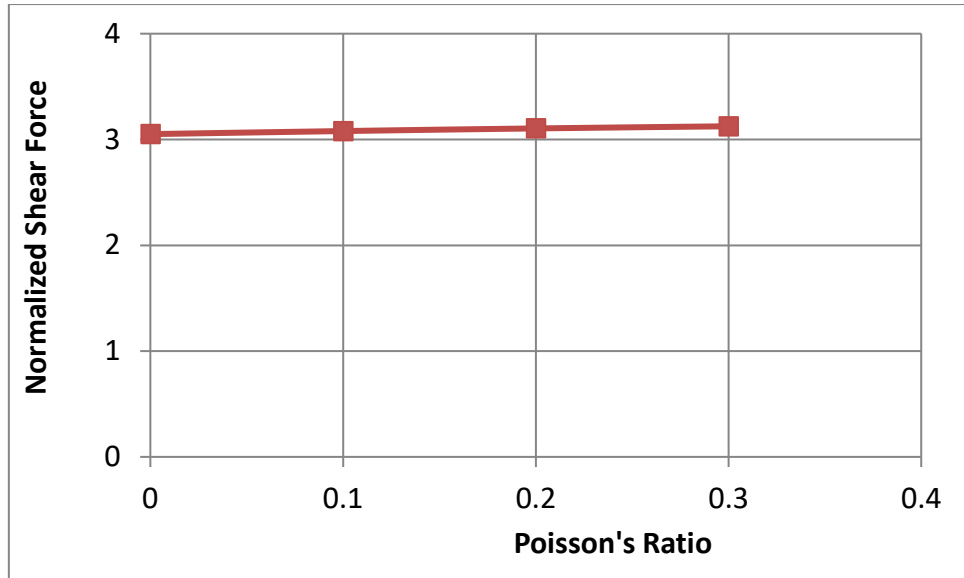


Figure 60: Effect of Poisson's ratio on shear

5.7. Effect of Column Size

In order to complete the analysis, the impact of the size of the square columns supported by the reference mat on the design parameters has been checked. Of course, the size of the column is a function of the magnitude of the applied load, which is often related to the number of supported floors. Note that an increase in the size of the column slightly increases the area over which the column load is applied, as well as the stiffness of the mat at that location. Three different sizes are used; namely, 0.1 m x 0.1 m, 0.3 m x 0.3 m, and 0.5 m x 0.5 m. The numerical results are presented in Table 14 and Table 15, whereas the graphical ones are shown in Figure 61 to Figure 63. The obtained results confirm that the cross-section size of the columns has no effect on the bearing soil pressure, bending moments and shear.

Table 14: Effect of column size on design parameters

Column Size (m)	Max Soil Pressure (kPa)	Min Soil Pressure (kPa)	Positive Moment (kN-m/m)	Negative Moment (kN-m/m)	Shear (kN/m)
0.1x0.1	23.51	8.20	147.72	123.08	207.15
0.3x0.3	23.4	8.22	148	123	207
0.5x0.5	23.39	8.22	147.82	122.54	206.95

Table 15: Effect of column size on normalized design parameters

Column Size (m)	Max Soil Pressure	Min Soil Pressure	Positive Moment	Negative Moment	Shear
0.1x0.1	2.12	0.74	0.37	0.31	3.11
0.3x0.3	2.11	0.74	0.37	0.31	3.10
0.5x0.5	2.11	0.74	0.37	0.31	3.10

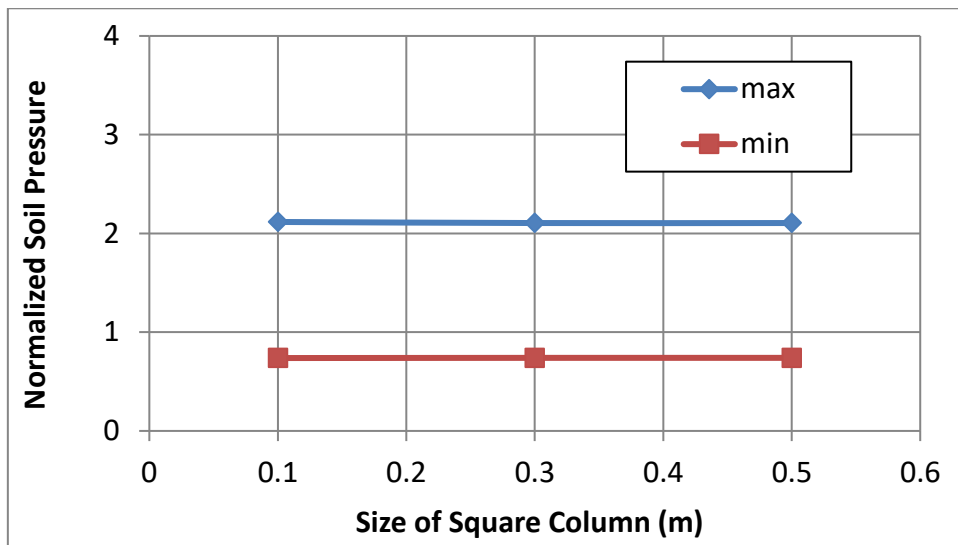


Figure 61: Effect of column size on soil pressure

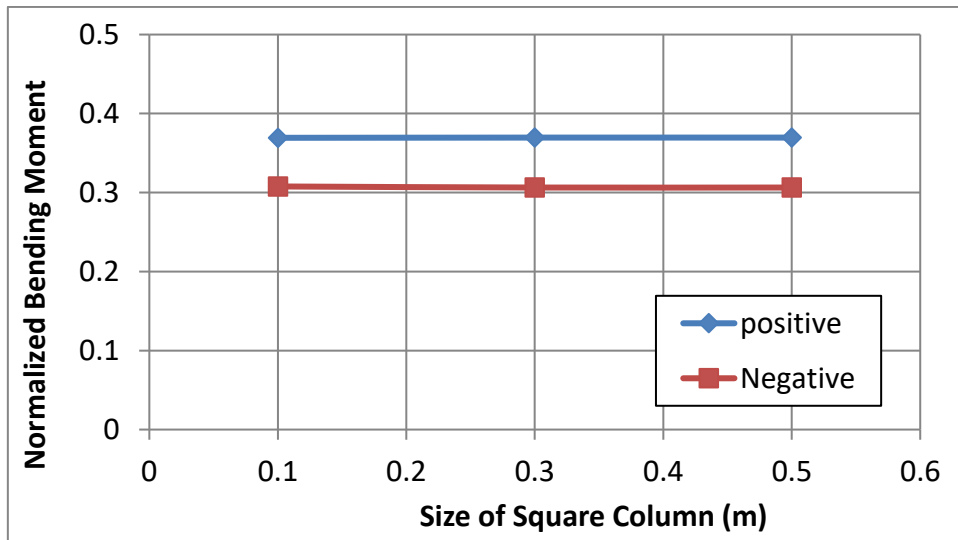


Figure 62: effect of column size on bending moment

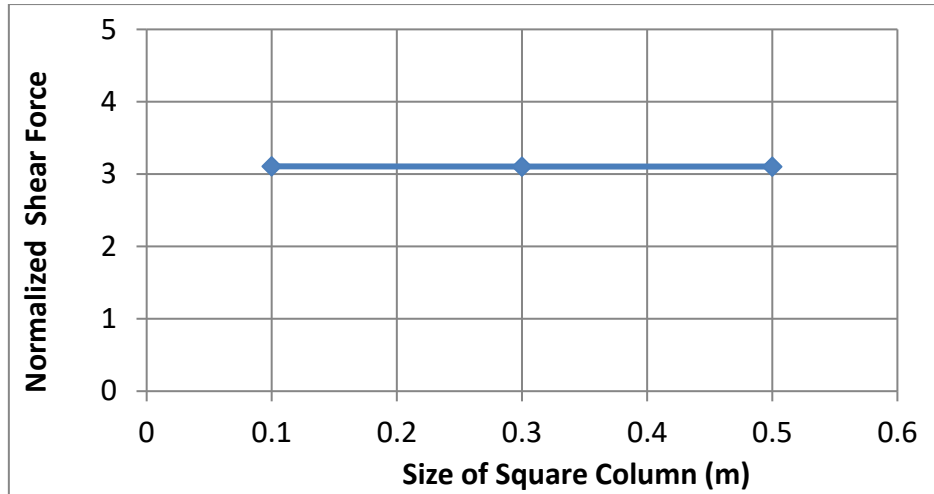


Figure 63: Effect of column size on shear

5.8. Effect of Change in Length

The effect of changing the length of the panels within the mat on the soil pressure, bending moment, and shear is determined. The analysis considers 3 m x 3 m, 6 m x 6 m, 8 m x 8 m and 10 m x 10 m square panels. Larger panel dimensions are not considered because a mat would not be a feasible economic option in that case. The results are presented in Table 16 and Table 17, and graphed in Figure 64 to Figure 66. Although the results are normalized, the analysis showed that the mat response greatly varies with the modification in the span length. This is not surprising because the distance between the supported columns significantly changes the behavior of the mat from rigid to flexible as the span increases. For a mat consisting of 3mx3m panels, the close spacing of the columns stiffens the mat and makes it hard to bend. The opposite happens for a mat comprising of 10mx10m panels, if the cross-section of the columns stays constant. Table 16 and Table 17 show the results of the analysis in actual quantities and in normalized form, respectively.

Table 16: Effect of span length on design parameters

Span Length (m)	Max Soil Pressure (kPa)	Min Soil Pressure (kPa)	Positive Moment (kN-m/m)	Negative Moment (kN-m/m)	Shear (kN/m)
3	13.1	10.26	11.4	18.5	46.6
6	23.4	8.22	148	123	207
8	35.2	6.51	376	254	375
10	53.0	2.27	730	424	588

Table 17: Effect of span length on normalized design parameters

Span Length (m)	Max Soil Pressure	Min Soil Pressure	Positive Moment	Negative Moment	Shear
3	1.18	0.77	0.11	0.19	1.40
6	2.11	0.74	0.37	0.31	3.10
8	3.16	0.59	0.53	0.36	4.21
10	4.77	0.20	0.66	0.38	5.29

Figure 64 shows the maximum and minimum soil pressures under the considered mats. As expected, the results indicate as the panel dimensions increase, a sharp increase in the maximum pressure and moderate decrease in the minimum pressure take place, especially for panel larger than 6 m x 6 m. For maximum bending moments, shown in Figure 65, both negative and positive moments increase with the panel dimension; however, the effect of the size of the panel on the positive moment under the columns is more pronounced. It is interesting to note that for small panels (less than 4.5 m x 4.5 m), the negative moment exceeds the positive, while the opposite is true for large panels. The results also reveal that the maximum shear in the mat is very sensitive to variations in the panel dimensions, as presented in Figure 66. Moreover, the normalized shear force is linearly related to the panel length.

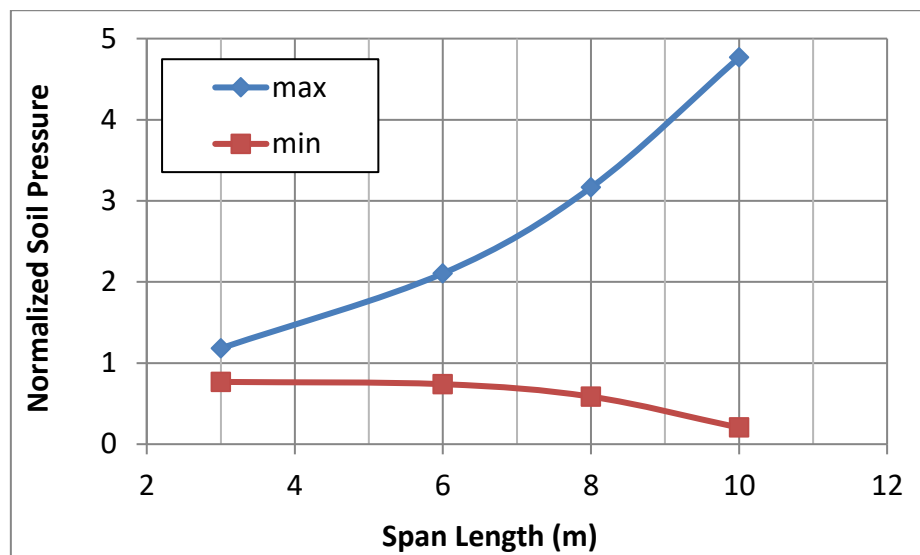


Figure 64: Effect of span length on soil pressure

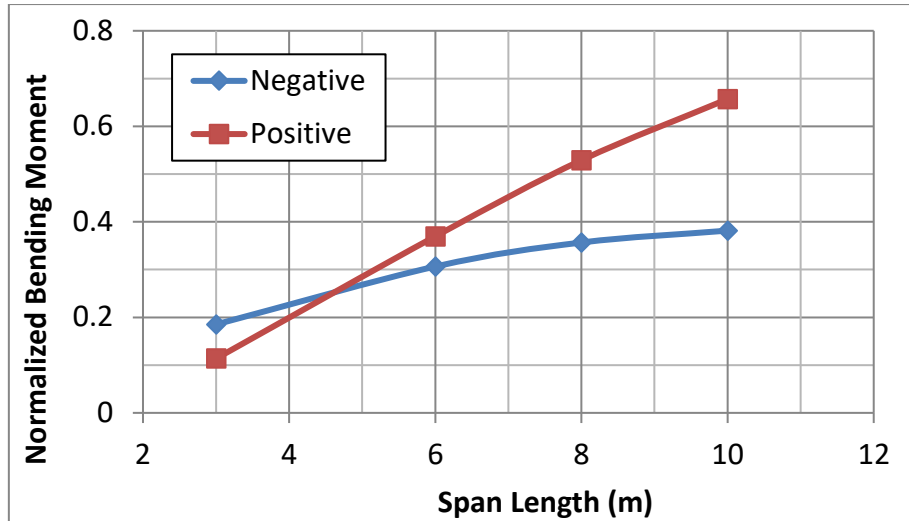


Figure 65: Effect of span length on bending moment

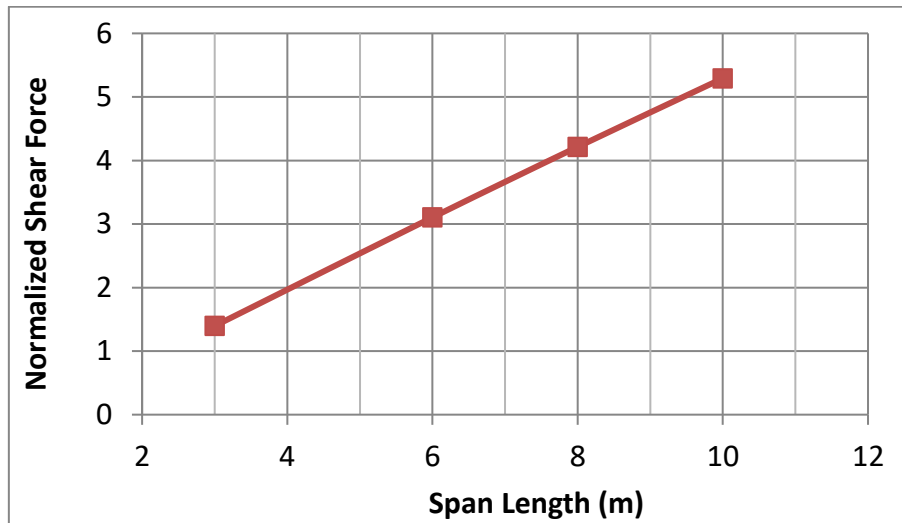


Figure 66: Effect of span length of shear

5.9. Effect of Change in Number of Spans

The effect of changing the number of spans on the design parameters is investigated in Table 18 and Table 19, as well as in Figure 67 to Figure 69. In the analysis, mat having 2, 3, 4, and 5 bays in each of the principal mat directions are addressed. The case of one panel is not considered because it is rarely used in practice. All the cases have 6 m by 6 m panels.

The results of the soil bearing pressure, shown in Figure 67 indicate that the effect of the number of panels is nonexistent for the maximum pressure and very small for the minimum pressure. This is because the maximum soil pressure typically occurs under the four corner columns, a situation which is not affected by the number of panels in all the considered mats.

Table 18: Effect of number of span on design parameters

No. of Spans	Max Soil Pressure (kPa)	Min Soil Pressure (kPa)	Positive Moment (kN-m/m)	Negative Moment (kN-m/m)	Shear (kN/m)
2	23.1	7.93	125	124	208
3	23.4	8.22	148	123	207
4	23.1	9.24	167	124	206
5	23.1	9.22	169	124	206

Table 19: Effect of number of span on normalized design parameters

No. of Spans	Max Soil Pressure	Min Soil Pressure	Positive Moment	Negative Moment	Shear
2	2.08	0.71	0.31	0.31	3.11
3	2.11	0.74	0.37	0.31	3.10
4	2.08	0.83	0.42	0.31	3.10
5	2.08	0.83	0.42	0.31	3.10

The small change in the minimum soil pressure can also be attributed to fact that it occurs at the center of the interior panel(s), which again not affected by the number of panels within a given mat. The results of bending moments are shown in Figure 68, and indicate that the behavior of 2x2 bays mats is significantly different from the other considered mats. In this case, the maximum positive and negative moments are almost equal. The fact that the magnitude of the negative moment stays almost constant irrespective of the number of panels is due to its fixed location, which occurs in the column strip between the corner and adjacent edge panels, as shown in Figure 70. On the other hand, the location of the maximum positive moment changes with the number of panels, again as shown in Figure 70. Generally, the maximum positive occurs at an interior column closest to the mat's center. For 2x2 and 3x3 panels the position of the interior column is close to the edge of the mat, while for 4x4 and 5x5 panels the location of the critical interior column is further away from the edge. Therefore, the maximum positive moment in small mats is highly affected by the edge boundary than in the large mats. As for maximum shear, shown in Figure 69, its location

remains at the face of the edge column adjacent to the corner column, irrespective of the number of panels. Hence, its magnitude remains constant.

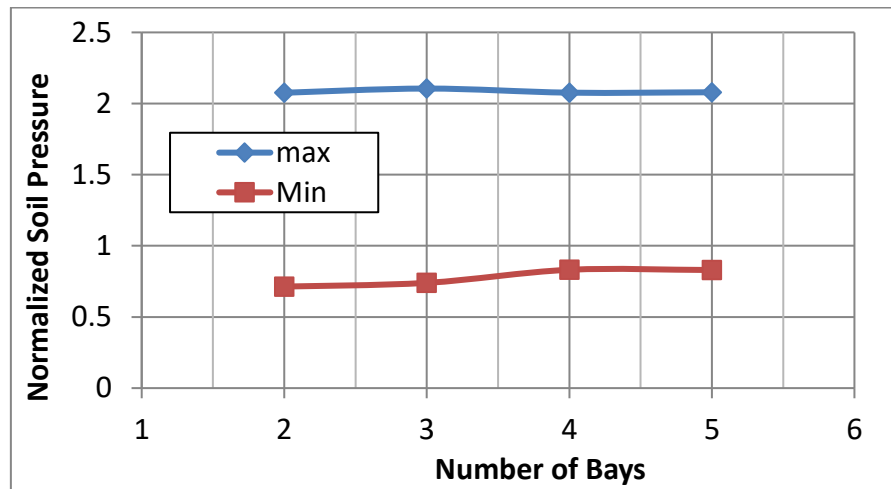


Figure 67: Effect of number of span on soil pressure

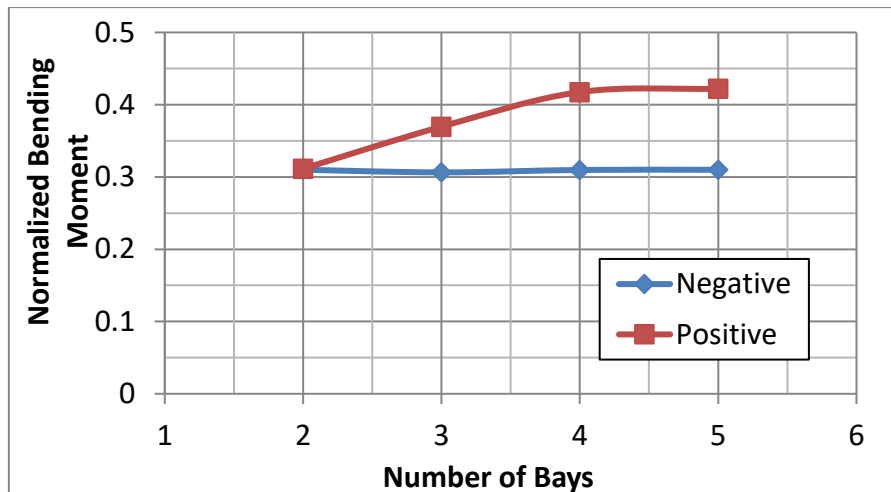


Figure 68: Effect of number of span on bending moment

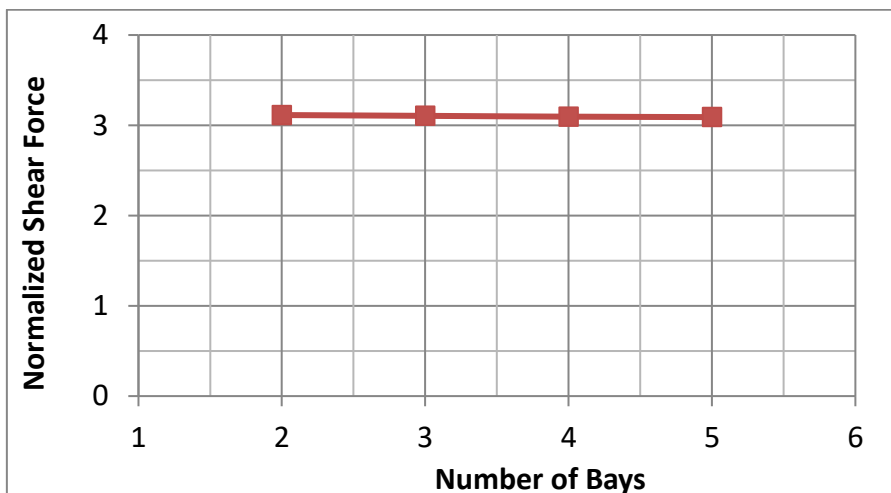


Figure 69: Effect of number of span on shear

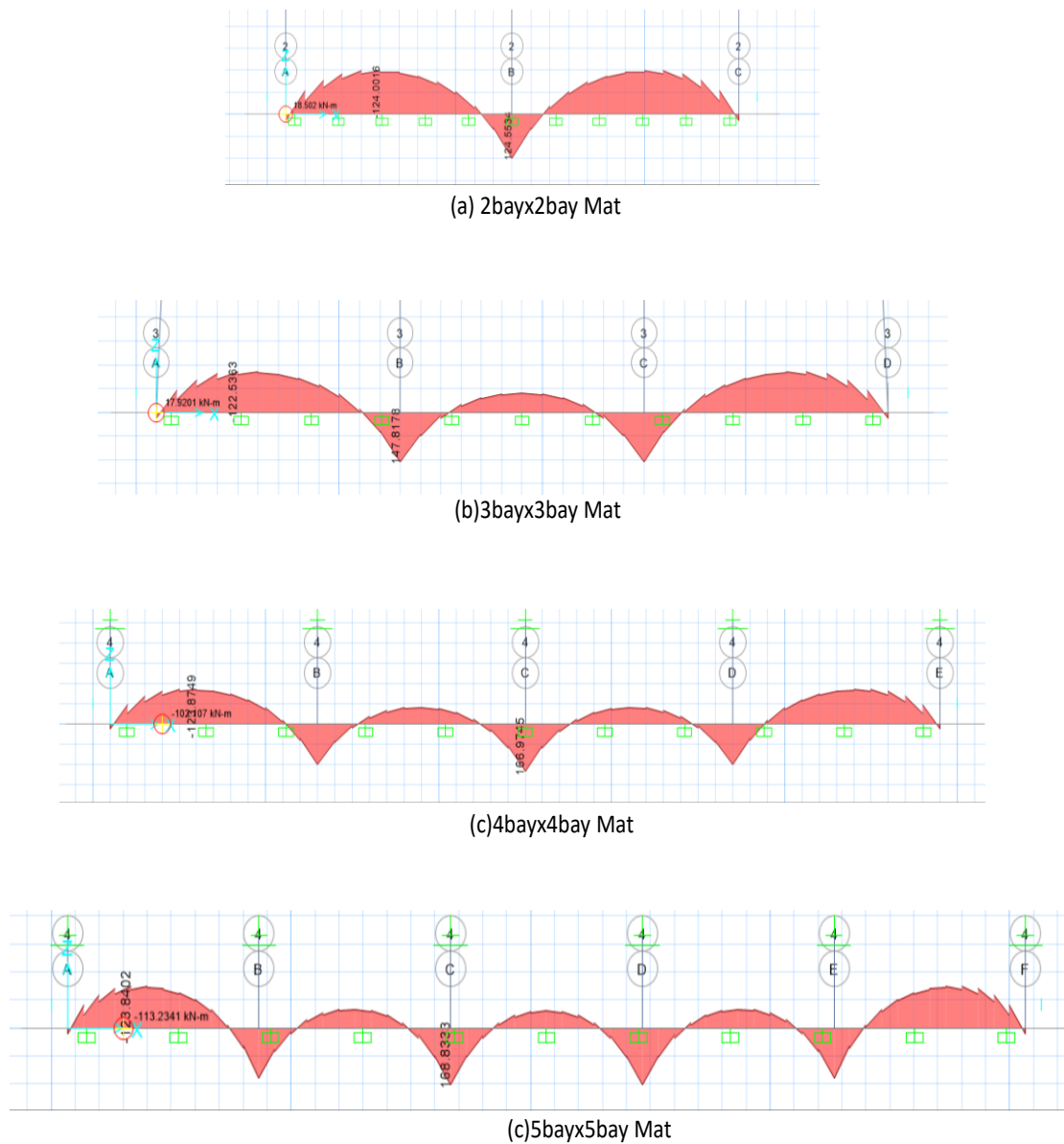


Figure 70: Location of maximum positive and negative moment in mats

5.10. Effect of Aspect Ratio

In this section, the effect of the panel aspect ratio of a mat on the design parameters is investigated. The aspect ratio is defined as the ratio of the width to length of a rectangular panel, in reference to Figure 71. Four different aspect ratios are considered: 0.5, 0.67, 0.83 and 1.0. For each aspect ratio, 3 mats with different panel areas (8 m^2 , 32 m^2 and 72 m^2) are addressed. This results in panels having the following dimensions presented in Table 20. This approach eliminates the effect of the panel area or size (which was investigated earlier) and allows the effect of the aspect ratio to be filtered out.

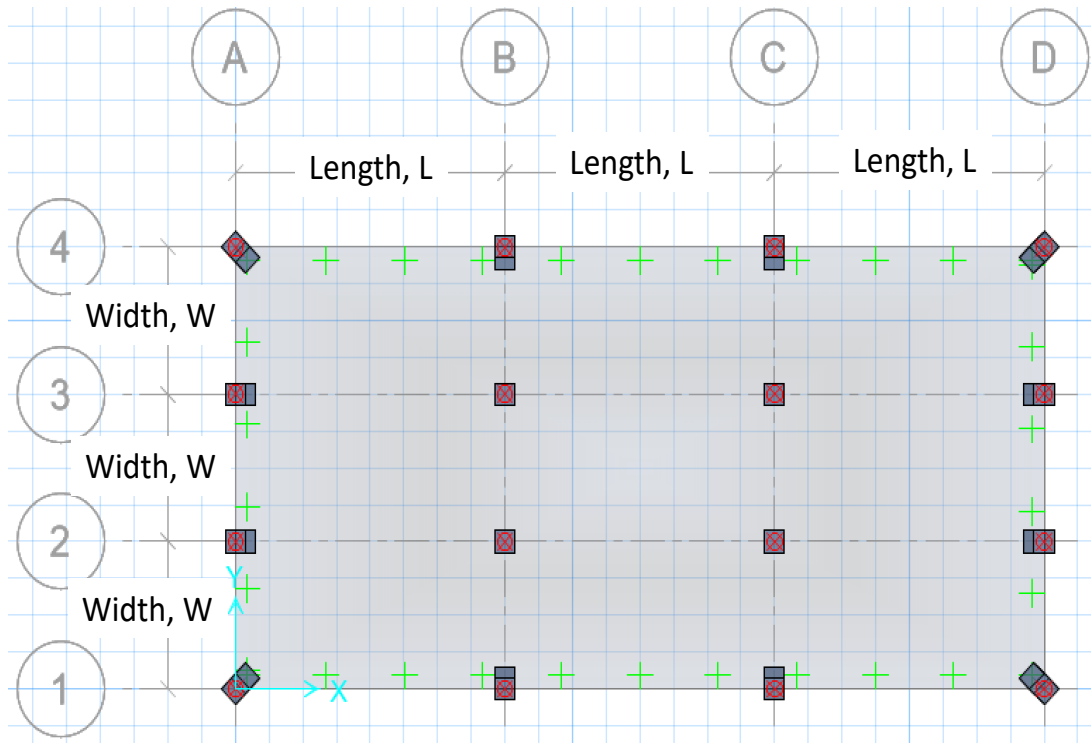


Figure 71: Definition of panel length and width

Effect of the panel aspect ratio on the maximum and minimum soil pressure is shown in Figure 72 and Figure 73, for different panel sizes (i.e. small, medium and large). For small panel size, it can be noted that the maximum and minimum soil pressure are not changed with panel aspect ratio. However, for large size mats, the aspect ratio is affecting both minimum and maximum soil pressures. This is attributed to the mat rigidity which is inversely related to the panel size and thickness. As the panel thickness is the same for all mats tested in this section, therefore, the panel size is the factor that affects rigidity. Mats with small size panel have larger rigidity compared to mats with larger panel sizes. Therefore, it maintains similar soil pressure regardless of its aspect ratio. However, mats with larger panel sizes is expected to express high flexibility, and therefore, its aspect ratio affects the soil pressure the way it shown in Figure 72 and Figure 73. In the meantime, based on configuration shown in Figure 71, the mat rigidity in the width direction is expected to be larger than its rigidity in the length direction, especially for mats with larger panel size. This is may be another reason why the aspect ratio shows an effect on the soil pressure for larger size mats compared to small sizes mats. Rigidity in the width direction approaches the value in length direction as the aspect ratio approaching 1.

Table 20: Effect of aspect ratio on normalized design parameters

Aspect Ratio	Panel Size	Panel Dimensions (mxm)	Normalized Max Soil Pressure	Normalized Minimum Soil Pressure	Normalized Negative Moment Along Panel Length	Normalized Positive Moment Along Panel Length	Normalized Negative Moment Along Panel Width	Normalized Positive Moment Along Panel Width	Normalized Shear Along Panel Length	Normalized Shear Along Panel Width
0.5	Small	2x4	1.23	0.90	0.11	0.07	0.09	0.06	0.93	0.94
	Medium	4x8	2.17	0.66	0.16	0.21	0.15	0.13	1.98	2.09
	Large	6x12	3.98	0.16	0.17	0.30	0.18	0.21	3.09	3.29
0.67	Small	2.32x3.45	1.18	0.93	0.14	0.08	0.12	0.04	1.06	1.12
	Medium	4.63x6.91	2.03	0.75	0.20	0.25	0.19	0.19	2.31	2.43
	Large	6.95x10.4	3.67	0.38	0.23	0.39	0.23	0.32	3.63	3.79
0.83	Small	2.58x3.1	1.16	0.93	0.15	0.09	0.14	0.09	1.21	1.24
	Medium	5.2x6.2	1.99	0.75	0.25	0.30	0.24	0.26	2.67	2.73
	Large	7.7x9.3	3.52	0.48	0.30	0.48	0.27	0.43	4.07	4.18
1	Small	2.83x2.83	1.15	0.94	0.18	0.10	0.18	0.10	1.32	1.32
	Medium	5.66x5.66	1.97	0.75	0.28	0.34	0.28	0.34	2.93	2.93
	Large	8.49x8.49	3.50	0.50	0.36	0.56	0.36	0.56	4.48	4.48

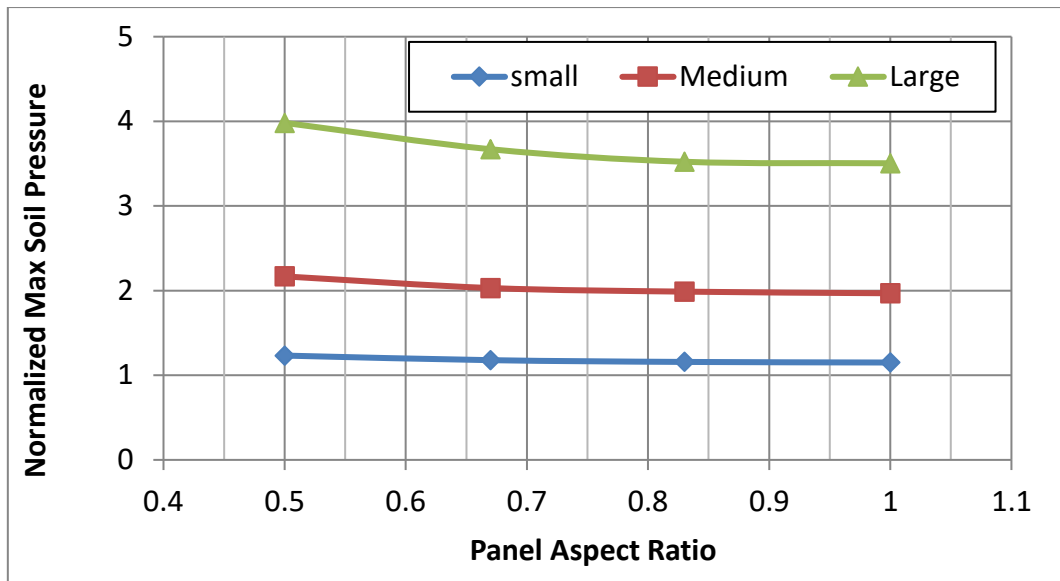


Figure 72: Effect of aspect ratio on maximum soil pressure

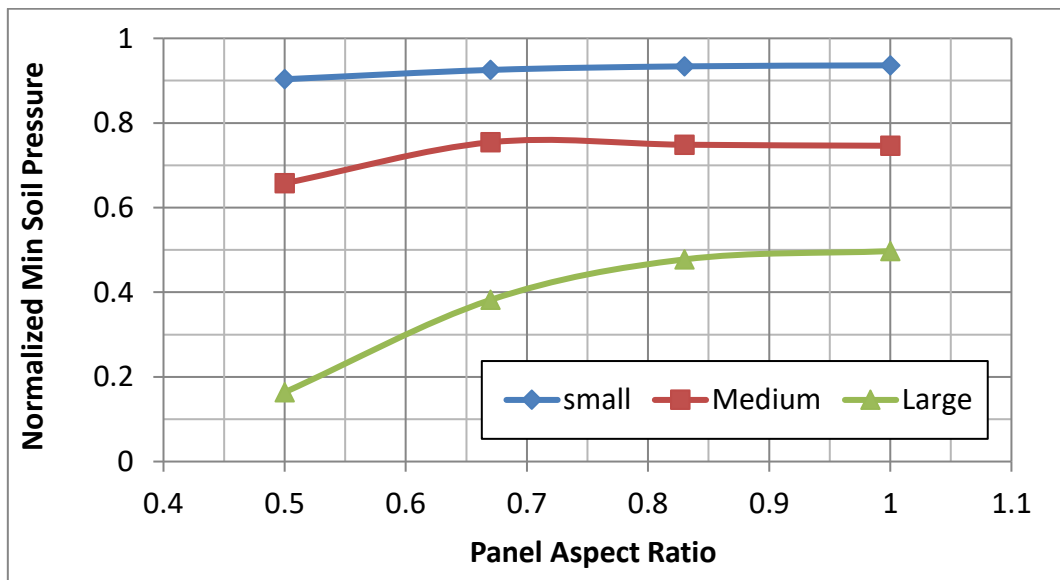


Figure 73: Effect of aspect ratio on minimum soil pressure

Using the same interpretation explained in previous paragraph, the variation of the maximum positive and maximum negative moments in both width and length direction can be interpreted. Figure 74 to Figure 77 shows the maximum and minimum moments for mats with different sizes and different aspect ratios, in both width and length directions. The variation of the maximum moment, both positive and negative could be attributed to the mat rigidity and soil pressure under the mat. Figure 72 and Figure 73 indicates that, for mats with small panel sizes, both maximum and minimum soil pressure are not affected by the aspect ratio. In addition, it is previously explained that, mats with small panel sizes have large rigidity, especially mats with small aspect ratio. Therefore, mats with small aspect ratio, and small sizes show less deflection

which in turns show less moments compared to otherwise mats with larger aspect ratio. As the aspect ratio increased, mat rigidity decreased, leading to larger deflection, and larger moments. It is expected that mats with larger size and larger aspect ratio show larger flexibility and larger deformation compared to other mats. Therefore, these mats show larger maximum moments, both positive and negative. Adding to that the increase in the maximum and minimum soil pressure under mats with large sizes and larger aspect ratio is producing larger moments.

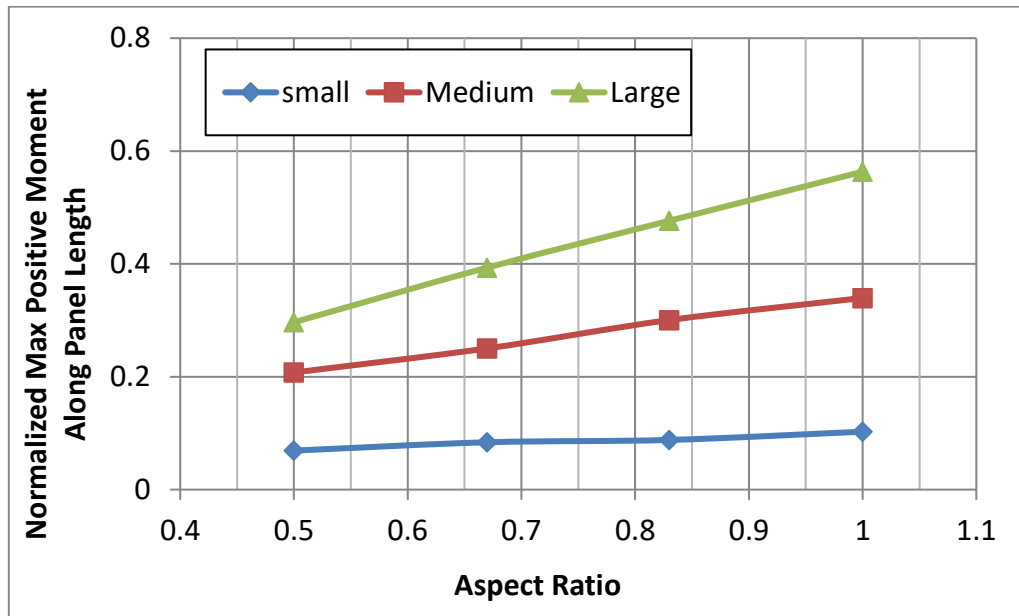


Figure 74: Effect of aspect ratio on positive moment along the panel length

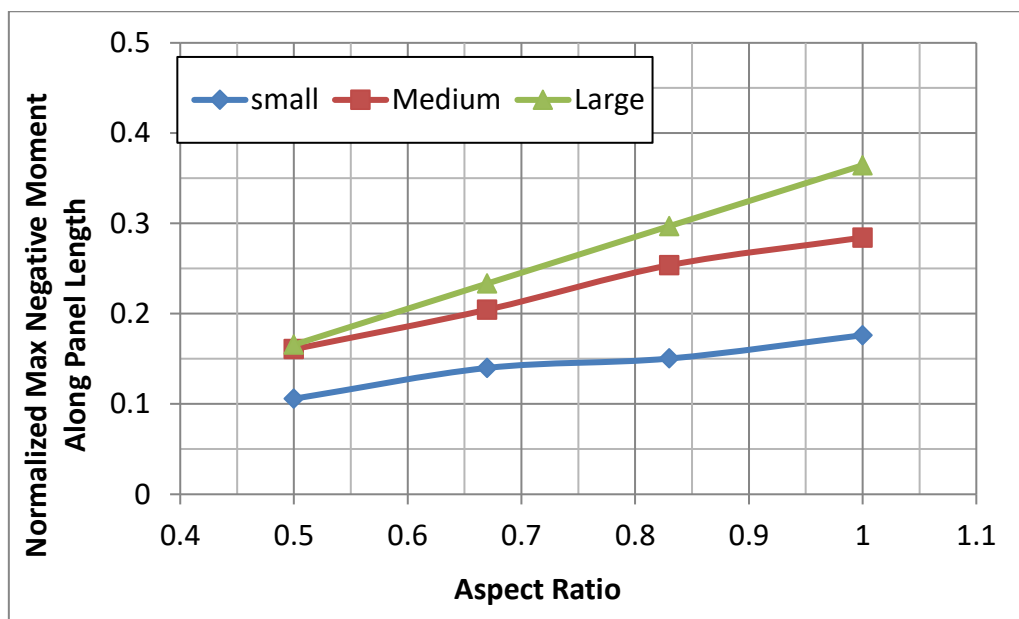


Figure 75: Effect of aspect ratio on negative moment along panel length

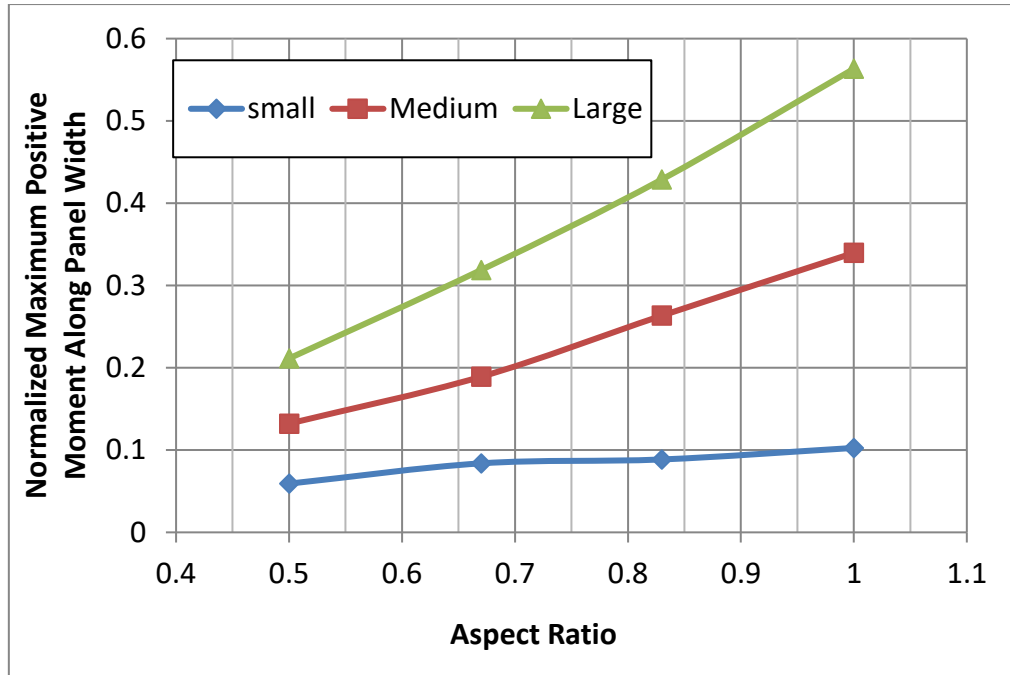


Figure 76: Effect of aspect ratio on positive moment along panel width

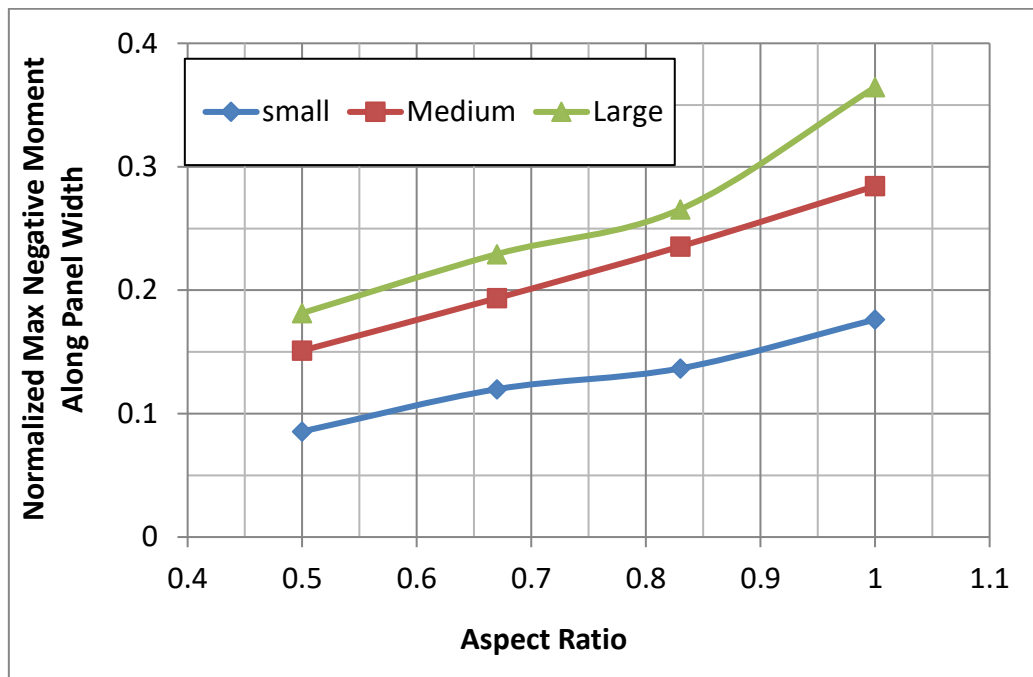


Figure 77: Effect of aspect ratio on negative moment along panel width'

The effect of the mat aspect ratio and panel size on the maximum shear on both length and width direction are shown in Figure 78 and Figure 79, respectively. The maximum shear is related to the soil pressure under the mat foundation. For smaller size mats, the soil pressure, both maximum and minimum, is negligibly affected with the mat aspect ratio, Figure 72 and Figure 73. Therefore, the maximum shear in these mats is slightly increased with the aspect ratio. For larger size mats, the increase in

minimum soil pressure with aspect ratio, shown in Figure 73, results in a significantly increase in the maximum shear of the large size mat.

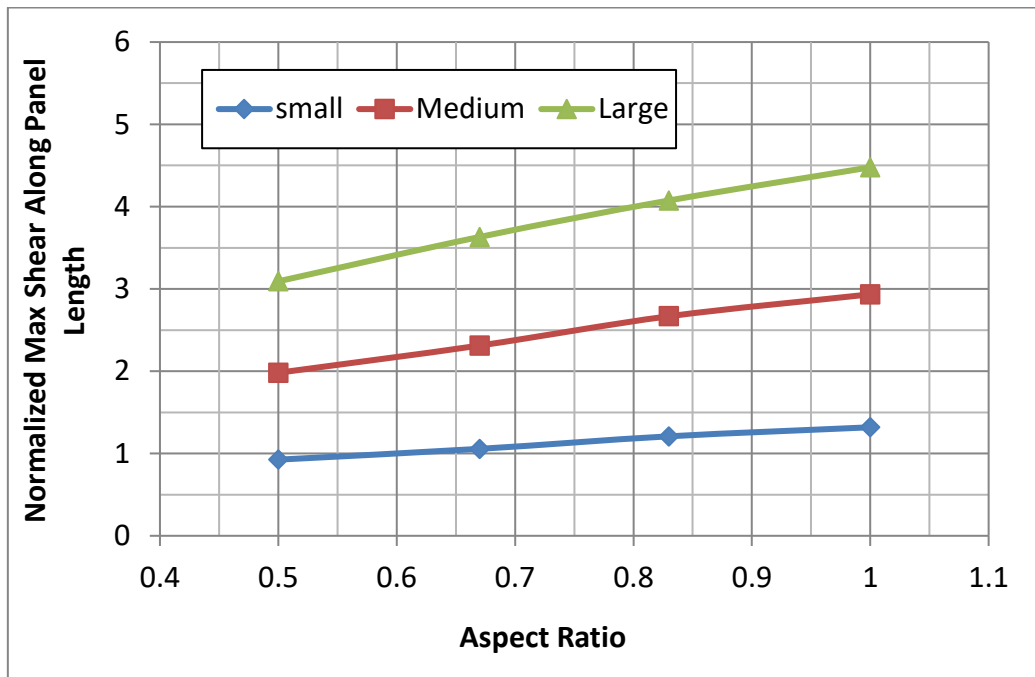


Figure 78: Effect of on aspect ratio on max. shear force along panel length

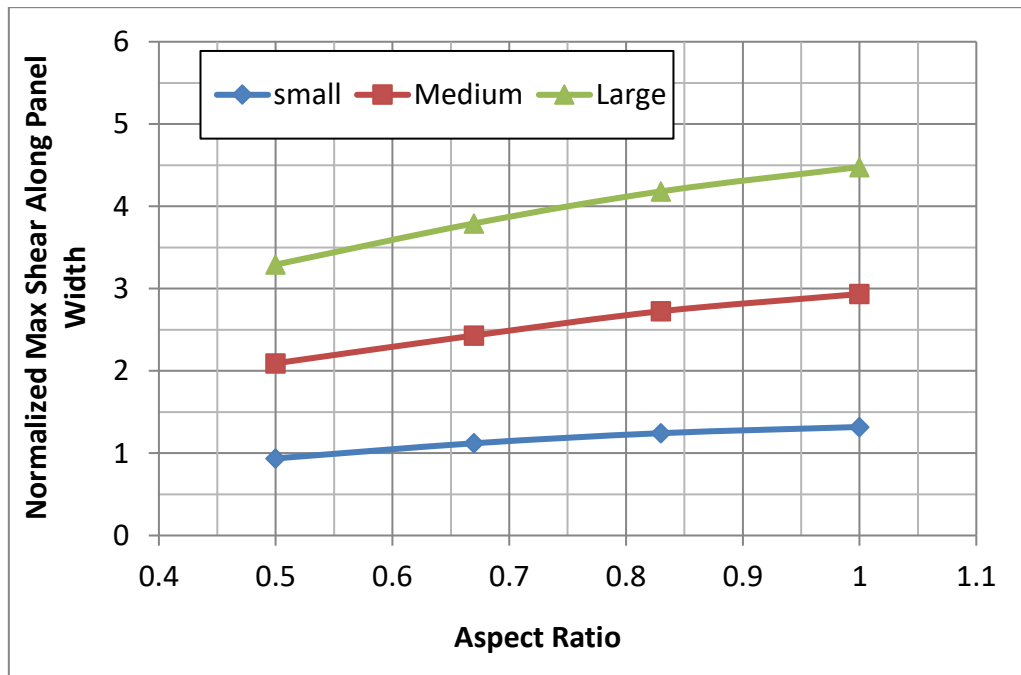


Figure 79: Effect of aspect ratio max. shear force along panel width

5.11. Effect of Eccentrically Loaded Mat

The effect of eccentrically loaded mat is investigated against the reference model to understand the behavior of the mat foundation for soil pressure, shear force and moments. All parameters are the same as the reference model expect the column

loads are distributed in the way that it gives one way eccentricity as shown in Figure 80. The eccentricity value is selected to be $e = 0.5L$ which is larger than $L/6$, and therefore, it classified as large eccentricity loading condition. As expected, the maximum soil pressure is located under the corner column loaded with 400 kN shown in Figure 80, and the minimum soil pressure is located under the opposite corner column which carrying load of 100 kN. The maximum positive moment is located in the vicinity of the interior column carrying 1600 kN, and the maximum positive moment is located in the midway of the column strip connection the edge column with 800 kN load and the interior column with 1600 kN load. Finally, Maximum shear is located under the 800 kN edge column.

Table 21: Effect of eccentrically loaded mat on design parameters

Parameter	Max Soil Pressure (kPa)	Min Soil Pressure (kPa)	Positive Moment (kN-m/m)	Negative Moment (kN-m/m)	Shear (kN/m)
Absolute values	96.4	7.47	694	440	825
Normalized values	3.47	0.27	0.69	0.44	4.95

Figure 81 indicates that the large eccentricity on the mat foundation increases the maximum soil pressure significantly, and reduces the minimum soil pressure, as expected. In other words, it increases the difference between maximum and minimum soil pressure which is considered unfavorable situation from the soil bearing capacity point of view. In addition, overstressing soil in one side of the mat compared to the other side will produce excessive differential settlement, which might cause the full building to tilt, or might exceed the value of settlement allowed by design standards. This large difference in the soil pressure at different points under the mat caused a large difference between maximum positive and maximum negative moments for eccentrically loaded mat compared to centrically loaded mat, Figure 82. In the meantime, the positive and negative maximum moments are significantly larger for the mat with eccentric loads compared to otherwise identical mat with no eccentricity. Finally, the maximum shear for the mat with eccentricity is much larger compared to the mat with zero eccentricity, as indicated in Figure 83.

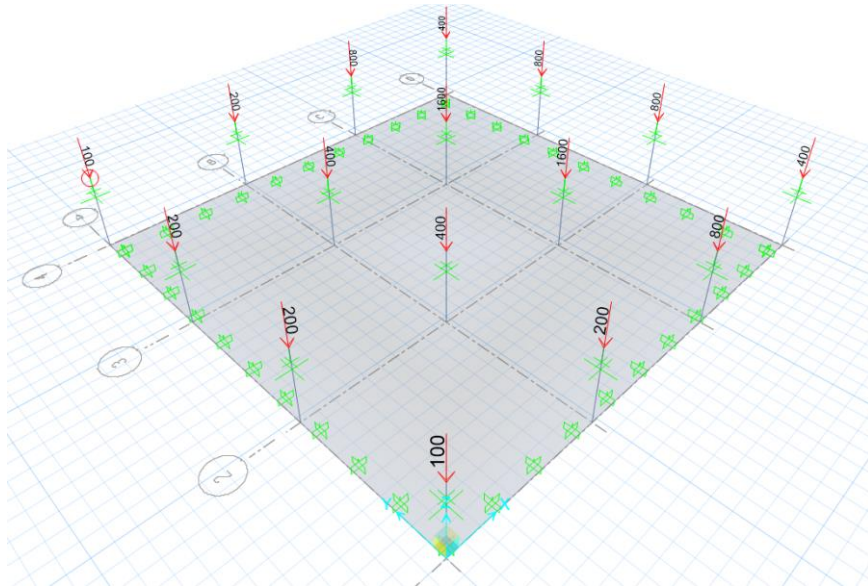


Figure 80: Eccentrically loaded mat

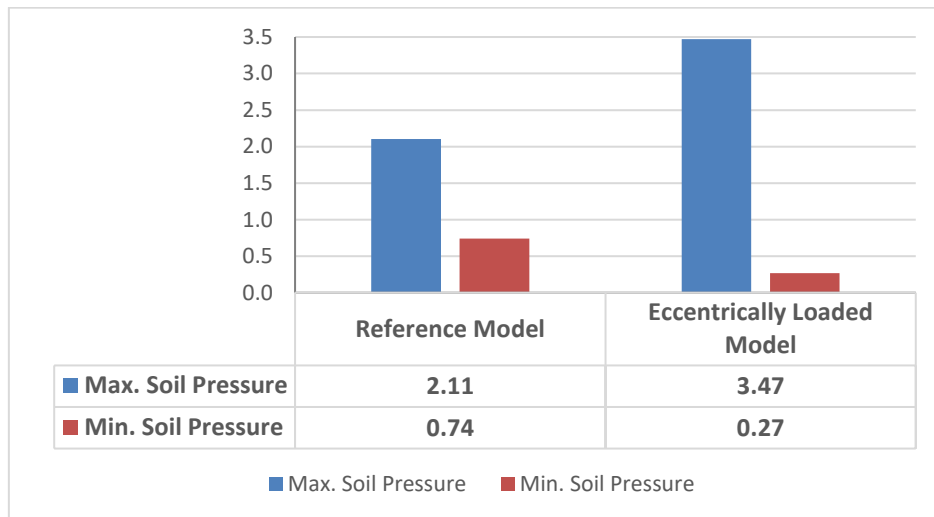


Figure 81: Effect of eccentrically loaded mat on soil pressure

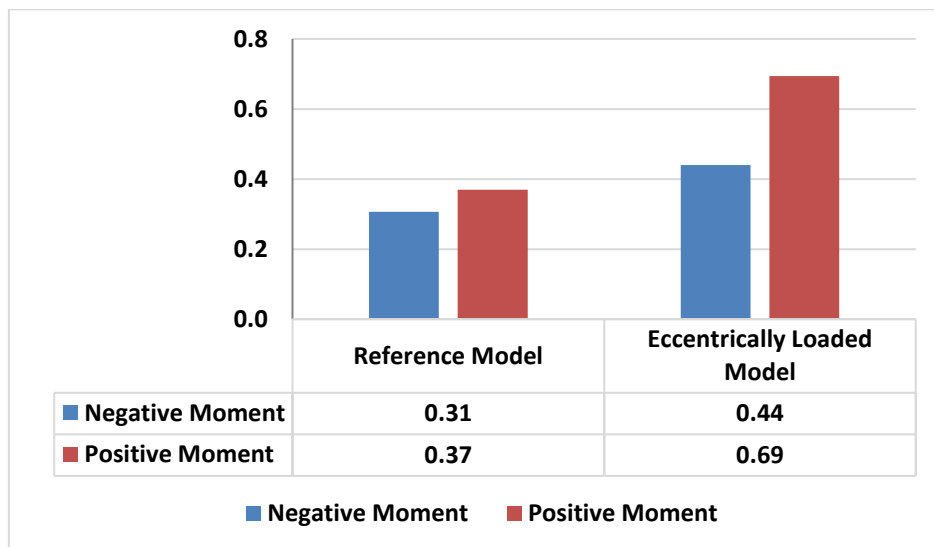


Figure 82: Effect of eccentrically loaded mat on bending moment

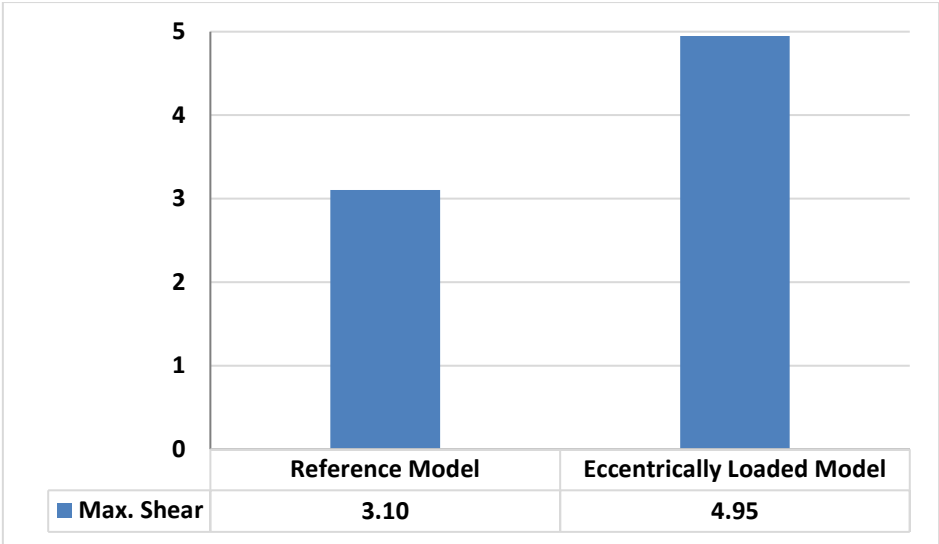


Figure 83: Effect of eccentrically loaded mat on Shear

Chapter 6. Summary and Conclusions

6.1. Summary

Mat foundations are a type of shallow foundation that consists of a continuous concrete slab used to distribute heavy gravity loads from structure over a large area of soil. They are employed in practice when the subsoil is not strong and column loads are so heavy that the spread footings would overlap over the building area. The presence of slab makes the mat foundation useful when the supported building has a basement. A mat can resist large differential settlements beneath columns better than individual. A comprehensive literature review has revealed that there is little theoretical work on the important parameters that affect the structural response of mat foundation. Hence, there is an urgent need to determine the load effect in mat foundation having different geometrical dimensions and subjected to various types of loads with consideration of a range of soil stiffness. The effect of mat geometry, soil elastic properties, concrete material characteristics, and load eccentricity on the soil pressure under the concrete mat and internal shears and bending moments within the mat are investigated in this study. The analysis involves the use of commercially available finite element software. To accomplish the objective, a large number of mats with different geometries (both plan dimensions and thicknesses), number of bays in each direction, panel aspect ratios, load eccentricities, soil types, and concrete properties are investigated.

6.2. Conclusions

All the considered mats, aside from those subjected to eccentric loading, were symmetrically loaded. Columns were positioned at uniform spacing along the two principal directions and subjected to loads in proportion to their tributary areas. Results of this study lead to the following conclusions:

1. The structural behavior of a mat foundation can be best explained by first examining its rigidity and observing the corresponding soil bearing pressure distribution and magnitude under the mat. From the soil pressure distribution one can justify why the bending moment and shear are critical at a certain location.
2. In general, the maximum soil bearing pressure was observed below the corner columns, while the minimum soil pressure occurred at the center of the central panel. The maximum positive bending moment was found below the interior

column closest to the edge, whereas the maximum negative moment was located mid-way between the edge and first interior columns. The location of the maximum shear always happened to be at the face of the edge column nearest to the corner column.

3. As the mat thickness increases, the maximum soil pressure becomes smaller while the minimum soil pressure becomes larger. Likewise, as the mat thickness is increased, the maximum positive moment is decreased and the maximum negative moment is increased, while the shear remains almost constant.
4. The modulus of elasticity of concrete only has a slight effect on the maximum soil pressure, which decreases with an increase in the modulus of elasticity. No effect was observed on the structural behavior due to changes in the concrete Poisson ratio.
5. An increase in the soil modulus of subgrade reaction triggers the maximum soil pressure to increase, while causes the minimum soil pressure to slightly decrease. The effect on the bending moment is more pronounced when the subgrade reaction is small; in that case an increase in the soil stiffness enlarges the positive moment, while reduces the negative moment. The impact on shear is minimal.
6. A reasonable change in the span length greatly affects all the design parameters. As the distance between columns increases, the maximum soil pressure is increased at a much faster rate than the minimum soil pressure is decreased. Larger bay lengths in mats correspond to larger positive moments than negative moments. The shear is linearly correlated with the span length.
7. As the number of bays increases in a mat, only the positive moment under the critical edge columns increases; all other response variables remain unchanged.
8. The effect of the aspect ratio of the panels on the design parameters depends on the size (area) of the panels. Mats with small panel areas behave as rigid; hence, the aspect ratio has little effect on the response. However, mats with large panel areas behave as flexible; thus, the soil pressure distribution, bending moment and shear all vary with a change in the aspect ratio.
9. The difference between the response of concentrically loaded and eccentrically loaded mats is significant. Eccentrically loaded mats are more critical than corresponding symmetrically loaded mats because the larger soil bearing

pressure on the heavily loaded side causes larger bending moments and shears within the panels located in that region.

References

- [1] Bowles J. E., *Foundation Analysis and Design*, N.Y.: McGraw Hill, 1996.
- [2] J. Cernica, *Gecotechnical Engineering*, New York: Wiley, 1995.
- [3] Tabsh S.W., and Al-Shawa A.R., "Effect of spread footing flexibility on structural response," *practice periodical on structural design and construction*, vol. 10, no. ASCE, pp. 109-114, 2005.
- [4] "Buldinghow," [Online]. Available: http://www.buildinghow.com/portals/0/2books/Book-A/3_7-4-RaftFoundation/image010.jpg. [Accessed 28 April 2017].
- [5] "t.yting," [Online]. Available: <https://i.ytimg.com/vi/wXjTDnzFCdo/hqdefault.jpg>. [Accessed 28 April 2017].
- [6] CSI, CSI Analysis Reference manual for SAP200, ETABS, and SAFE, Berkeley, California: Computers and Structures, Inc., 2011.
- [7] Potts D.M., and Zdravkovic L., *Finite Element Analysis in Geotechnical Engineering - Theory and Application*, Thomas Telford Publishing, 2001.
- [8] L. Wood, "The economic analysis of raft foundations," *Numerical and Analytical Methods in Geomechanics*, vol. 1, no. 4, pp. 397-405, 1977.
- [9] Mehrotra B.L., Gupta Y.O. Baska, and Govil A.K., "Approximate Method - Raft Structure Interaction Analysis," in *Annual Conference of the Canadian Society for Civil Engineers*, Manitoba, 1980.
- [10] S. Shukla, "Simplified Method for Design of Mats on Elastic Foundations," *Journal of the American Concrete Institute*, vol. 81, no. 5, pp. 469-475, 1984.
- [11] J. Bowles, "Mat Design," *Journal of the American Concrete Institute*, vol. 83, no. 6, pp. 1010-1017, 1996.
- [12] Liou, G.S. and Lai, S.C., "Structural Analysis Model for Mat Foundation," *Journal of Structural Engineering, ASCE*, vol. 122, no. 9, pp. 1114-1117, 1996.
- [13] G. Meyerhof, "Shallow Foundations," *Geotechnical Special Publication, ASCE*, no. 1181, pp. 1080-1090, 2002.
- [14] Thangaraj D., and Ilamparuthi K., "Influence of relative stiffness of soil-raft-system on the behavior of space frame," *Journal of structural engineering (Madras)*, vol. 34, no. 2, pp. 111-123, 2007.
- [15] B. Das, *Principles of Foundation Engineering*, Pacific Grove, CA: Brooks Cole/Thompson Learning, 2007.

- [16] J. Coduto, *Foundation Design principle and Practice*, Upper Saddle Rive, NJ: Prentice Hall, 2001.
- [17] J. Cemica, *Geotechnical Engineering*, New York: Wiley, 1995.
- [18] R. Peck, *Foundation Engineering*, New York: Wiley, 1974.
- [19] Wang B., Qiu J., Zhao D., Yang X., and Shuai D., "Analysis of raft foundation design based on considering influence of superstructure stiffness," *Global Geology journal*, vol. 12, no. 1, pp. 28-31, 2009.
- [20] Regis J. Colasanti, and John S. Horvath,, "Practical Subgrade Model for Improved Soil-Structure Interaction Analysis: Software Implementation," *Practice Periodical on Structural Design and Construction, ASCE*, vol. 15, no. 4, pp. 1084-1093, 2010.
- [21] I. M. Hasan., "Influence of structural and soil parameters on Mat deflection," *International Journal of Civil and Structural Engineering*, vol. 2, no. 1, pp. 976-987, 2011.
- [22] Nabanita Sharma, Jitendra Deka, Ankita Gogoi, Dipankar Borpuzari, Biki Hussain, "Structural Design Of Raft Foundation Based On Geotechnical Analysis," *Journal of Civil Engineering and Environmental Technology*, vol. 2, no. 11, pp. 31-36, 2015.
- [23] Jha A.K., Utkarsh K., and Kumar R., "Effect of soil-structure Interaction on Multi Storey Buildings on mat Foundation," in *Advances in Structural Engineering*, New Delhi, Springer Nature, 2015, pp. 703-715.
- [24] Ghugal Y., Wankhade R., Prakash M., "Study on Soil-Structure Interaction:," *International Journal of Engineering Research*, vol. 5, no. 3, pp. 737-741, 2016.
- [25] M. Heteneyi, *Beams on elastic foundation*, Michigan: University of Michigan press, 1979.
- [26] American Concrete Institute, *Building Code Requirements for Structural Concrete (318-05) and Commentary (318 R-05)*, Farmington Hills, Michigan: American Concrete Institute, 2005.
- [27] Ferdinand P., Beer E., Russell Johnston, and John T. DeWolf, *Mechanics of Materials*, New York: McGraw Hill, 2002.
- [28] "SGH," [Online]. Available: <http://www.sgh.com/projects/minera-escondida-organic-growth-project-1-tunnel-4>. [Accessed 21 April 2017].
- [29] A. Hernnikoff, "Solution of problems of elasticity by the framework method," *Journal of Applied Mechanics*, vol. 8, no. 4, pp. 169-175, 1941.
- [30] R. Courant, "Variational methods for the solution of problems of equilibrium and vibrations," *Bull. Amer. Math. Soc*, vol. 49, no. 1, pp. 1-23, 1943.

- [31] Clough W., Martin C., Topp J., Turner J., "Stiffness and deflection analysis of complex structures," *Journal of the Aeronautical Sciences (Institute of the Aeronautical Sciences)*, vol. 23, no. 9, pp. 805-824, 1956.
- [32] W. R. Clough, "The Finite element method in plane stress analysis," *2nd Conference on Electronic Computation*, Pittsburgh, 1960.
- [33] H. Falk and C. W. Beardsley, "Finite element packages for personal computers," *Mechanical Engineering*, vol. 107, no. 1, pp. 54-71, 1985.
- [34] R. Clough, "Areas of application of the finite element method," *Computers & Structures*, vol. 4, no. 1, pp. 17-40, 1974.
- [35] "Comsol," [Online]. Available: <https://www.comsol.com/multiphysics/finite-element-method>. [Accessed 23 April 2017].
- [36] Tai-Ran Hsu, "SJSU.EDU," [Online]. Available: http://www.sjsu.edu/me/facultystaff/faculty/tai-ran-hsu/Ch3_Steps_in_FEM.pdf. [Accessed 24 April 2017].
- [37] G. Kirchhoff, "Über das Gleichgewicht and die Bewegung einer elastischen Scheibe," *Journal für reine und angewandte Mathematik*, vol. 40, pp. 51-88, 1850.
- [38] R. Mindlin, "Influence of rotatory inertia and shear on flexural motions of isotropic, elastic plates," *J. Appl. Mech.*, vol. 18, no. 1, pp. 31-38, 1951.
- [39] E. Reissner, "The effect of transverse shear deformation on the bending of elastic plates," *J. Appl. Mech.*, vol. 12, no. 2, pp. 69-77, 1945.
- [40] "Civil Engg World," [Online]. Available: <https://civil-engg-world.blogspot.ae/2012/10/How-Mat-Foundation-Idealized-Software-SAFE.html>. [Accessed 20 April 2017].

Vita

Pouya Partazian was born in 1989, in Shiraz, Islamic Republic of Iran. He received his primary and secondary education in Dubai, UAE. He received his B.Sc. degree in Civil Engineering from the American University of Sharjah in 2012. From 2012 to 2014, he worked as site engineer and senior engineer respectively in Sun Engineering and Contracting and Khansaheb Civil Engineering. Next he joined a BIM management consultancy called iTech as a business development engineer for the first six months and continued with the same firm as a business development manager to present.

In February 2012, he joined the Civil Engineering master's program in the American University of Sharjah as a part time student. His research interests are in finite element, soil-structure interaction, and parametric studies of soil and structure.